Spring 5-7-2016

The Role of CBL Family of E3 Ubiquitin Ligases in Intestinal Epithelial Homeostasis

Neha Zutshi
University of Nebraska Medical Center

THE ROLE OF CBL FAMILY OF E3 UBIQUITIN LIGASES IN INTESTINAL EPITHELIAL HOMEOSTASIS

by

Neha Zutshi

A DISSERTATION

Presented to the Faculty of

the University of Nebraska Graduate College

in Partial Fulfillment of the Requirements

for the Degree of Doctor of Philosophy

Pathology and Microbiology Graduate Program

Under the Supervision of Professor Hamid Band

University of Nebraska Medical Center

Omaha, Nebraska

April 2016

Supervisory Committee

Hamid Band, M.D., Ph.D.

Andrew Dudley, Ph.D.

Rakesh Singh, Ph.D.

Karen Gould, Ph.D.

Vimla Band, Ph.D.

Jennifer Black, Ph.D.

ACKNOWLEDGEMENTS

I would begin by expressing my sincere gratitude to my mentor, Dr. Hamid Band. Not only is he a gifted scientist but a teacher par excellence. His vast knowledge, his encouragement when experiments would fail, his child-like enthusiasm for experiments well done and his immense patience in explaining intricate concepts to me made him a brilliant mentor.

Besides my advisor, I would like to thank the rest of my graduate committee: Dr. Jennifer Black, Dr. Andrew Dudley, Dr. Karen Gould, Dr. Vimla Band and Dr. Rakesh Singh for providing their insightful remarks, which sometimes made me re-analyze the data or dig deep into the literature to find answers to their questions.

My sincere thanks also goes to the Department of Pathology and Microbiology that I was a part of for the past five years. They provided me the opportunity to come to the United States to pursue my dream of getting quality higher education. The journal clubs and annual student's departmental seminars not only increased my repertoire of knowledge but also prepared me to ask pertinent questions. I would also like to thank the support staff that helped me schedule my seminars and committee meetings.

I am grateful to Graduate Studies for providing me with the UNMC Program of Excellence fellowship for two years as well as Dr. Hamid Band's grants that enabled me to complete my studies without any financial roadblocks.

I thank my fellow lab-mates for the innumerable discussions about troubleshooting experiments gone wrong or just about graduate life and for the fun times we shared for the past five years. In particular, I would like to thank Dr. Bhopal Mohapatra, Dr. Wei An and Benjamin Goetz for helping me with my project. Also, I thank my friends Suprit, Abhilasha and Sohinee for providing constant encouragement and advice, for cheering me up when I was upset and for celebrating their and my achievements together.

I thank my childhood friends Bharti and Shriya for their love, friendship and support in the times of need.

I am deeply indebted to my family: my parents, my sister and the lovely little kids Anmol and Anvita for their immense love, support and encouragement throughout my life.

I would like to thank my parents-in-law and my brothers-in-law for their love and support.

Last but not the least; I would like to express my deepest gratitude to my husband, Rahul Sharma. He has been the most amazing companion I could have ever asked for. His love, support and encouragement have provided me the strength to complete my degree. His mere presence has brought a sense of balance and sanity in my life.

THE ROLE OF CBL FAMILY OF E3 UBIQUITIN LIGASES IN INTESTINAL EPITHELIAL HOMEOSTASIS

Neha Zutshi, Ph.D.

Supervisor: Hamid Band, M.D., Ph.D

All adult organs are endowed with a small pool of resident stem cells that must be maintained throughout life to provide for cell turnover during homeostasis and tissue repair following any injury. The unique ability to self-renew as well as to differentiate into functional cells of organs in which they reside makes stem cells essential for the maintenance of organ systems. It is now becoming increasingly evident that aberrant activity of stem cells contributes to diseases such as cancer or tissue/organ atrophy. Thus, it is critical to better understand the mechanisms that regulate adult stem cells. Ligand-activated receptor tyrosine kinases (RTKs) represent an important means to regulate adult stem cells. We and others have established the CBL-family ubiquitin ligases as key negative regulators of RTKs. However, physiological roles of CBL proteins in intestinal epithelial homeostasis are unknown. Recently, we have shown that CBL and CBL-B function as redundant but essential regulators of hematopoietic stem cell (HSC) quiescence and their combined deletion in HSCs of mice leads to a rapidly-fatal myeloproliferative disorder, mimicking a similar leukemic disease associated with mutations of CBL in humans. CBL and CBL-B have also been shown to help maintain asymmetric neural stem cell division. Any role of CBL proteins in the regulation of epithelial stem cells has not been reported. To address such a role, we generated a novel mouse model (Cbl-flox/flox; Cbl-b-null; Lgr5-EGFP-IRES-CreERT2; Rosa26-LacZ) to confer concurrent tamoxifen-inducible loss of CBL and CBL-B in the Lgr5-expressing intestinal epithelial stem cells (IESCs). Tamoxifen injection in this inducible CBL/CBL-B

double knockout (iDKO) mouse model resulted in a rapid and significant reduction in the Lgr5-High IESC pool with a concomitant increase in the Lgr5-Lo transit amplifying cells. Lineage tracing using LacZ-staining revealed an increase in the number of blue progeny in the iDKOs, suggesting an increased IESC commitment to differentiation. Of the progeny, iDKO animals showed a propensity towards enterocyte and goblet cell fate at the expense of Paneth cells. Loss of IESCs in iDKO mice led to slower recovery from intestinal epithelial injury due to X-ray radiation of the abdomen. In vitro deletion of CBL proteins in the crypt culture recapitulated the loss of self renewal phenotype and was associated with hyperactivation of MAPK pathway and downregulation of Wnt pathway effector TCF4. These results demonstrate a novel requirement of CBL/CBL-B in the maintenance of a well-studied epithelial stem cell compartment, the IESC, and suggest that CBL proteins by regulating MAPK pathway protect IESCs from exhaustion.

TABLE OF CONTENTS

LIST OF FIGURES

LIST OF TABLES

LIST OF ABBREVIATIONS

4-OH- 4-hydroxy-tamoxifen

5FU - 5-fluorouracil

APC - adenomatous polyposis coli

Bmi1 - B lymphoma Mo-MLV insertion region 1

BrdU - 2-Bromo 5'-deoxyuridine

CBC- Crypt base columnar cell

CBL- Casitas B-Lineage Lymphoma

°C - degrees centigrade

CKI - Casein kinase I

ChgA- ChromograninA

DCAMKL1 – Doublecortin and CAM kinase-like 1

Dkk1 - Dickkopf related protein 1

Dll - Delta-like ligand

DNA - Deoxyribonucleic acid

Dsh - Disheveled

E - Embryonic day

EDTA - Ethylene diamine tetraacetic acid

EGF - Epidermal growth factor

FZD - Frizzled receptor

GAPDH - Glyceraldehye phosphate dehydrogenase

GFP - Green fluorescent protein

GSK3β - Glycogen synthase kinase 3β

HBSS- Hank's Balanced Salt Solution

HSC - Hematopoeitic stem cell

IESC- Intestinal epithelial stem cell

Lgr5 - Leucine-rich repeat-containing G-protein coupled receptor 5

Lyz- Lysozyme

Muc2- Mucin2

Ngn3 - Neurogenin 3

NICD - Notch intracellular domain

nM- nanomolar

Olfm4 - Olfactomedin 4

P- Postnatal day

PBS - Phosphate buffered saline

PI3K - PtdIns (3, 4, 5) kinase

PTEN - phosphatase and tensin homologue

q-PCR - quantitative polymerase chain reaction

RNA - Ribonucleic acid

RPM - Revolutions per minute

RTK- Receptor tyrosine kinase

TA - transit amplifying cells

TAM- Tamoxifen

Tcf – T-cell factor

μM - micromolar

μg - microgram

1 Introduction

1.1 Development and architecture of the small intestine

Gastrointestinal (GI) tract development doesn't begin until gastrulation is complete and the three germ layers come together in the form of hollow tube in which the innermost endoderm (which later becomes mucosal epithelium) gets surrounded by mesoderm (derivatives of which become loose connective tissue, vascular structure and muscularis) and ectoderm (that forms enteric nervous system) that then undergo complex patterning along the three axes of symmetry of the embryo (anterior-posterior, dorsal-ventral, left-right) (1, 2). While the anterior-posterior axis divides the GI tract into foregut (forming pharynx, esophagus, and stomach), midgut (small intestine, cecum and ascending colon) and hindgut (fated to become rest of the colon, rectum and anus), the dorso-ventral and left-right axes guide counterclockwise turning and looping of the gut keeping the stomach on the left (2, 3). The innermost endoderm layer of the tube retains its stratified structure until mid-late gestation (E15 in mice) when it begins to undergo cytodifferentiation into to columnar epithelial cells upon receiving inductive signals from the surrounding mesoderm (1, 4). These signals also enable the endoderm derived epithelium to model into luminal projections called "villi" and proliferative "intervillus" epithelium. This process is complete by E19 in mice (**figure1.1**). Crypts begin to organize from intervillus epithelium between postnatal day 1 (P1) to postnatal day 14 (P14). Epithelial cell proliferation in the intestine rapidly increases as crypts multiply in number by a process called crypt fission and villi lengthen as rate of proliferation exceeds the rate of cell death. Development of murine gut is complete by P28 (1).

The adult GI tract comprises of four layers (**figure1.2**). The luminal-most layer is called mucosa. It comprises of the columnar epithelium and supporting loose connective tissue called lamina propria that sit on top of a smooth muscle layer called "muscularis

mucosae". Mucosal layer rests on top of the submucosa which is made up of connective tissue rich in blood and lymph vessels, nerve fibers, and cells of the immune system. Submucosa is placed on top of muscularis propria that is made up of inner circular smooth muscle fibers and outer longitudinal smooth muscle layer. In between these two layers of muscularis propria are autonomic nerve fibers and ganglionic clusters of the myenteric plexus. This enables neural control of the peristaltic movement initiated in the muscularis propria that allows passage of the food along the gut. Outermost layer of the intestine is called serosa which is a mesothelium lining that protects the gut from frictional damage in the peritoneum (5).

1.2 The Intestinal Epithelium

The major functions of the intestine include digestion and absorption of nutrients entering the gut lumen and forming a barrier against pathogens. These functions are carried out by the specialized columnar epithelial cells of the mucosal layer of the intestine. The intestinal epithelium is organized into luminal finger-like protrusions called "villi" (to increase the surface area for absorption) and invaginations into the underlying submucosa called the "Crypts of Lieberkühn". The epithelial lining of the intestine is a unique tissue that undergoes rapid turnover most likely propelled due to exposure to constant mechanical, chemical and biological insults. The entire lining is replaced every 3-5 days in mammals. To balance the loss of cells, intestinal epithelial stem cells (IESCs) and their transit amplifying progeny residing within the crypt carry out extensive proliferation (6, 7). While the IESCs divide every 24 hours to form the transit amplifying compartment, the latter divides every 12 hours for 4 cell divisions until it terminally differentiate into cells of absorptive or secretory lineage that move on to the villi connected to the crypt (8).

Figure 1-1 Development of the gastrointestinal tract.

Formation of the endoderm as a part of gastrulation occurs first around E5-E7.5 in mice. The hollow endodermal gut tube forms when two ventral invaginations, one at the anterior (anterior intestinal portal, AIP) and the other at the posterior (caudal intestinal portal, CIP) end of the embryo elongate and fuse together. At this time lateral plate-derived splanchnic mesoderm comes to surrounds the endoderm and connects the tube to the dorsal body wall. At a later time point neural crest cells from the dorsal neural tube migrate and colonize the gut to establish the (ENS). The endoderm at E10.5 is a stratified epithelium that undergoes morphogenesis into columnar epithelium that moulds into luminal projections called villi separated by intervillus proliferative zones by E15.

Figure 1.1

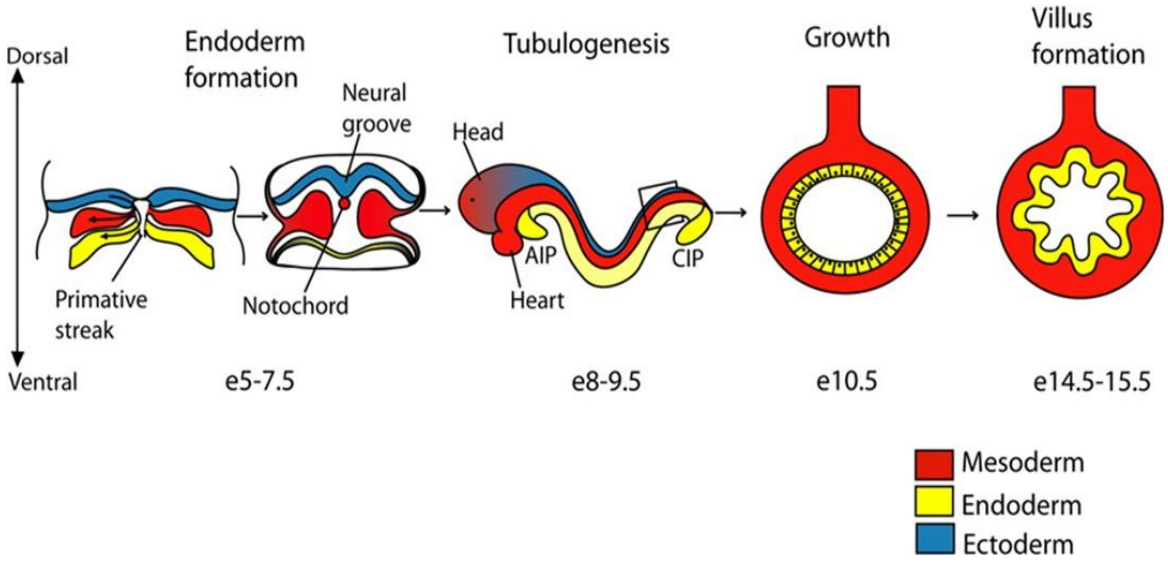

Noah et al., Experimental Cell Research 317 (2011) 2702-2710.

Figure 1-2 Architecture of mammalian intestine.

The schematic shows the organization of different layers of the intestine namely outhermost Serosa, followed by Muscularis which encircles Submucosa and the innermost layer of Mucosa.

Figure 1.2

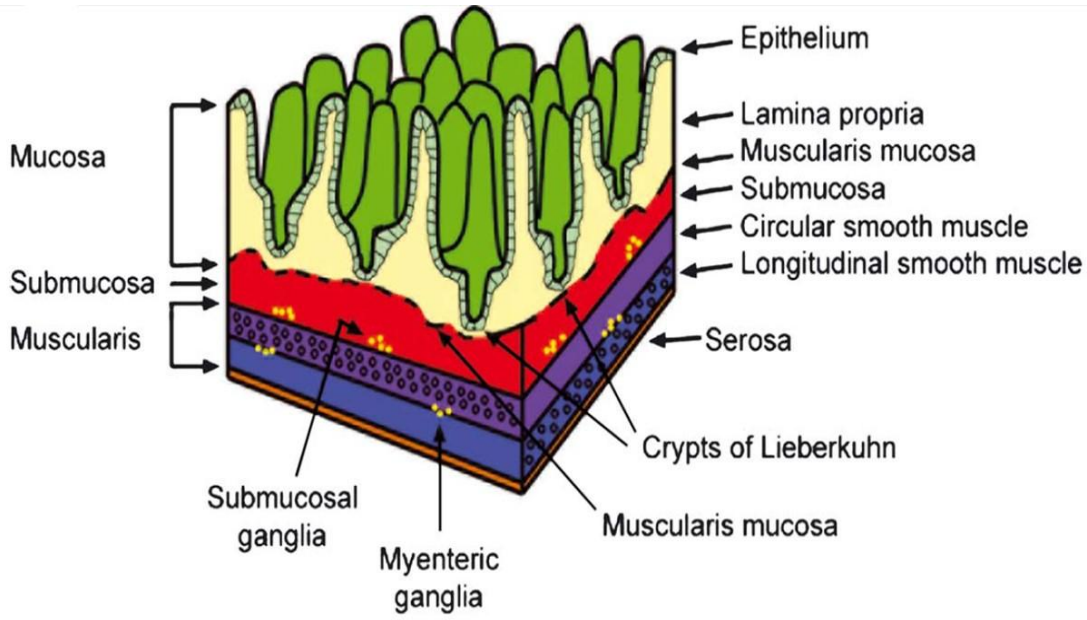

Wallace et al., Mechanisms of Development 122 (2005) 157–173.

The differentiated cells further migrate along the villus for the next 2-3 days post which they undergo cell death and fall off into the intestinal lumen. These differentiated functional cells are well defined by their morphology, location, function and marker expression (**figure 1.3**). These include the enterocytes, goblet cells, Paneth cells, enteroendocrine cells, tuft cells and M cells. The absorptive enterocytes are the most abundant progeny lining the GI tract. They are columnar with brush border epithelium on their apical surface. These cells are also a storehouse of various hydrolytic enzymes which they secrete into the lumen to allow breakdown of partially digested chyme. These enzymes such as sucrase isomaltase, lactase and alkaline phosphatase also help identify enterocytes in the gut. Goblet cells produce and secrete mucous to lubricate and protect the epithelial lining. The mucous layer in the small intestine can be divided into two: a firm, sterile inner layer and a more pervious outer layer that harbors IgAs and anti-mircrobial peptides to block the pathogens. Goblet cells increase in number from proximal to distal end of the intestine. They are mostly present on the villus but can be found in the crypts as well. They can be recognized by their “goblet shape”, by staining the tissues with Periodic acid-Schiff (PAS) stain that labels mucopolysaccharides and by expression of proteins such as Mucin2. Paneth cells are the only post-mitotic cells present at the crypt base intercalated between CBC intestinal stem cells. They thus serve niche signals to the stem cells. Paneth cells also secrete antimicrobial compounds such as defensins and lysozyme into the gut lumen. They are also unique as they are the only differentiated cell type that lives for as long as 6-8 weeks. They can be recognized by their characteristic eosinophilic granules, staining with PAS and expression of Lysozyme. Neuroendocrine hormone secreting enteroendocrine cells and opioid secreting tuft cells are rare populations of epithelial cells that can be present on the villi or the crypt. They are recognized by markers such as ChromograninA and DCaMKL1 respectively. Lastly, Microfold or M cells present on lymphoid Peyer’s patches

present antigens from the gut lumen to the underlying immune cells. Glycoprotein 2 is a marker for mature M cells (6, 7, 9).

Because of the clearly defined hierarchy of cells, well-understood architecture of the tissue and ease of in vitro manipulation due to established markers and protocols, the intestinal epithelium serves as an attractive model system to study proliferation, self-renewal, differentiation, apoptosis and migration.

1.3 Intestinal Epithelial Stem Cell

Stem cells are present in most adult tissues and are defined as the cells that can maintain tissue homeostasis by harboring the capacity to generate all mature cell types of a given organ, as well as renew their own pool. They were also proposed to be rare, quiescent and dividing asymmetrically to maintain one of their own while creating one progenitor to differentiate further. After a long-standing debate about the identity of stem cells, it has now been established that the true stem cells of the intestinal epithelium are the crypt base columnar cells (CBCs) present at the base of the crypt intermingled with Paneth cells. CBCs were first identified by Cheng and Leblond in 1974 (10-12). Using electron microscopy, they identified that crypt base was not just made of differentiated Paneth cells but also comprised of slender, wedge shaped CBCs (**figure 1.4**). They also provided evidence for “stemness” of this population by employing a crude method of lineage trace, where they analyzed radiolabeled phagosomes in CBCs that had survived the exposure to 3H-Thymidine and phagocytosed other CBCs that did not. They showed that the radioactivity could later on be located in more mature cells.

Figure 1-3 Organization of cells along the crypt-villus axis.

The schematic shows stem and transit-amplifying (TA) compartment of the intestine within the crypt and arrangement of more differentiated cells along the villus.

Figure 1.3

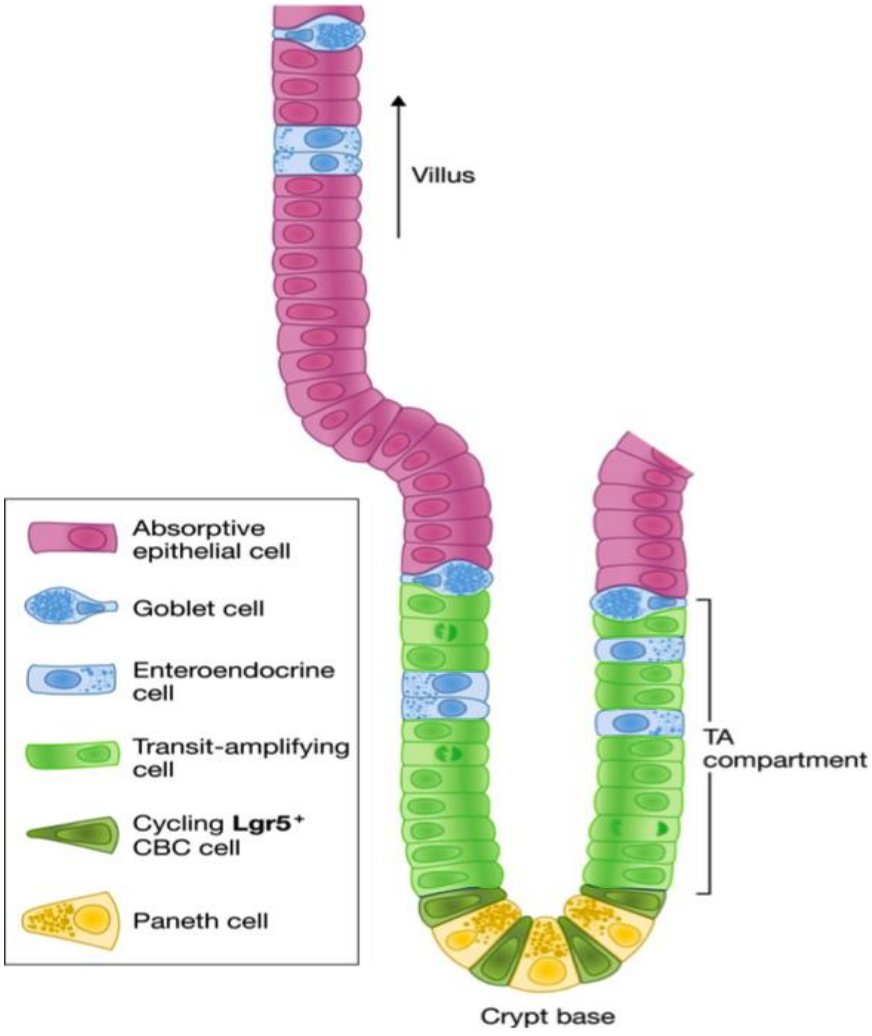

Modified from Schuijers and Clevers. The EMBO Journal 31 (2012), 2685–2696

Figure 1-4 Electron micrograph of a small intestine crypt base.

It shows CBC stem cells (black arrows) identified by their slender shape, basal nuclei and luminal microvilli, tightly intermingled with Paneth cells (red arrows).

Figure 1.4

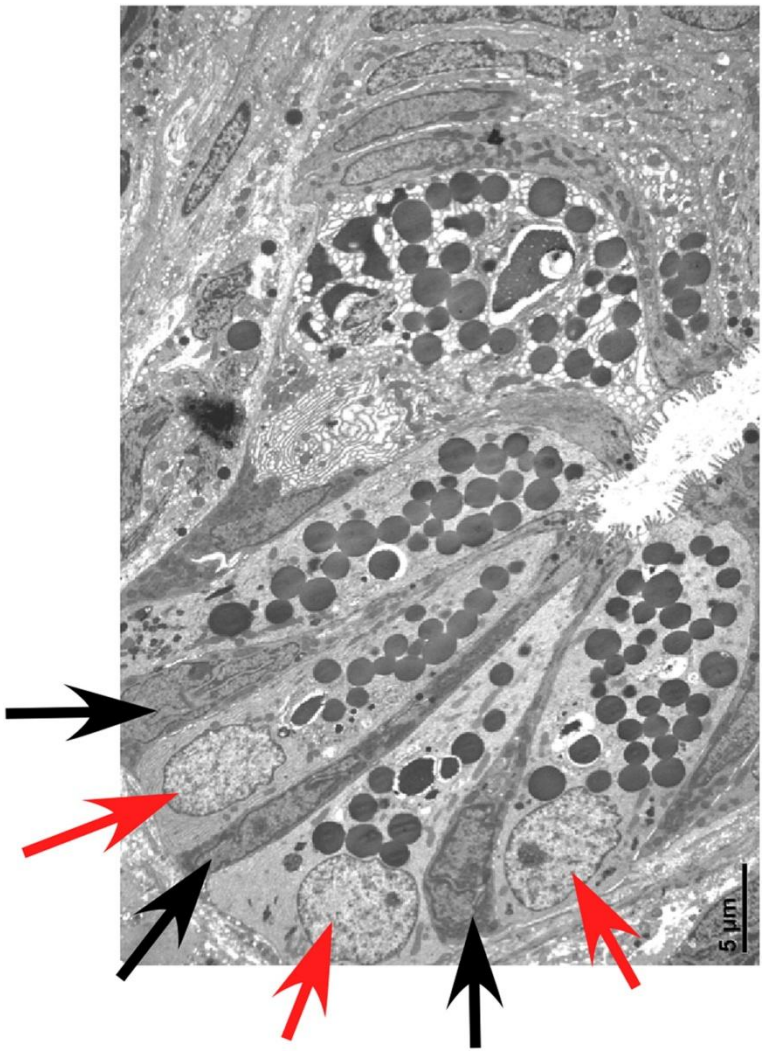

Nick Barker et al., Cell Stem Cell 11(2012) 452-460.

Recently, the cause of CBCs as a stem cell candidate was championed by Clevers group (13). They identified a Wnt target gene, Lgr5 that was exclusively expressed in the CBCs. They used Lgr5 promoter driven tamoxifen inducible-Cre recombinase fusion protein, Cre-ERT2 and transgenic Cre reporter allele R26-Lox-Stop-Lox-LacZ expression to unambiguously establish CBCs as multipotent, long-lived stem cells of the intestine (13). It was, however, not easy to establish Lgr5+ CBCs as true stem cells of the intestine because they challenged the accepted paradigm for stemness. They were neither rare (14-15 per crypt) nor quiescent (divided every 24 hours) (13, 14, 15). They were relatively resistant to radiation injury and divided symmetrically (13, 14). Since then, however, Lgr5+ cells have been identified as having self-renewal potential in several epithelial organs such as hair follicle (16), mammary gland (17, 18), stomach (19), kidney (20), inner ear (21), pancreas (22)(23) and liver (23).

Another population of stem cells called +4 stem cells fitted the traditional definition of stemness and was originally proposed as the label retaining putative stem cell of the intestine by Potten and colleagues (24, 25). Since then several groups have reported the presence of a rare, quiescent stem cell around the +4 position relative to the base of the crypt identified by expression of various markers such as Bmi1(26, 27, 29), Lrig1 (30), HopX (31), mTert (32), pPTEN (33, 34), and so on. Although most of these studies have relied on the rarity, quiescent nature (DNA label retention) and the ability to regenerate epithelium upon injury, only a handful of them have used the gold-standard of lineage tracing to establish the multipotency of these candidates (27, 30, 31). Nonetheless, the quiescent nature and low abundance of these stem cells in the gut can't justify these cells as the sole bona fide stem cells that could meet the homeostatic needs of the organ. Indeed, several studies have now established that CBCs are the actual work-horses that meet the daily requirements of proliferation and differentiation while

quiescent +4 cells are the reserve stem cell population called in during the times of stress(13, 26, 30).

More recently this reconciliation and agreement about the separate roles of Lgr5+ and +4 stem cells has been put to further test. It was shown that the expression of all the +4 stem cell markers was highly enriched in the Lgr5+ stem cells (32). Plus, when the entire Lgr5 expressing population was wiped out using Lgr5-DTR mice (a model in which human diphtheria toxin receptor was knocked-into the Lgr5 locus to selectively ablate Lgr5+ cells following exposure to Diphtheria toxin) mice could not recover from radiation induced epithelial injury (35). These experiments hinted that quiescent stem cells were not a separate compartment but a sub-population of Lgr5+ CBCs. Takeda et al., in a landmark paper showed a bi-directional interconversion between these two populations of stem cells (31).

A further twist in the tale came about when Buczaki et al., showed that Lgr5 expressing label retaining cells (expressing all the +4 stem cell markers) are actually secretory progenitors (36). These cells under normal homeostasis are destined to become Paneth and other secretory cells but under radiation injury conditions can be re-wired to become stem cells that then contribute to regeneration. Similarly another study identified that DLL1 expressing secretory progenitor regained stemness under conditions of *in vivo* stress or *in vitro* culture (37). In the same vein, Stamataki et al., in 2011, showed that strong expression of DLL1 and exit from cell cycle were linked together in the intestinal crypts (38). More recently, the Clevers group has shown that enterocyte progenitors could also contribute to epithelial homeostasis in the absence of Lgr5+ stem cells (39). Thus, keeping these multiple studies of plasticity within the crypt cells in mind, at present it seems that stemness may not be hard-wired in the intestinal crypt cells and may be a function of exposure to the right cues from the niche (40).

1.4 Lgr5+ Stem Cells

During development, Lgr5+ cells are first observed at P1 as cluster of cells in the intervillus epithelium. P5 onwards as crypts begin to form, they settle down to the bottom of the crypt and it is after P15 that they start to mingle with the Paneth cells. Lineage tracing as early P5 has established that Lgr5+ cells possess stem cell characteristics (42). Paneth cells and surrounding mesenchymal tissue form a niche that tightly regulates the strength of signals needed to maintain these stem cells in a narrow zone of the crypt base. A number of studies have investigated the role the Paneth cells as providers of niche signals to the CBCs (42-47). While some have suggested that Paneth cells are dispensable for maintenance of stem cells (42, 44) possibly due to the overlapping signals by the sub-epithelial myofibroblasts (43, 48), others have shown that loss of Paneth cells results in loss of stem cell compartment (45-47). Also co-culture of stem cells with Paneth cells significantly increases the survival of stem cells *in vitro*. Among the several factors secreted by Paneth cells, Wnt3a, TGF-α/EGF and Jag1/DLL4 seem to be the most potent at providing stemness cues to the CBCs (49). These factors have thus been used extensively now to culture Lgr5+stem cell and their progeny as 3 dimensional organoids.

Functionally, Lgr5 is a seven pass transmembrane protein that is a receptor for the Rspondin family of ligands (RSPO1-4) and potentiates Wnt/β-catenin signaling (50-53). Mechanistic dissection of this agonistic function of Lgr5 in the Wnt pathway was made possible after the discovery of RNF43 and ZNRF3, the E3 Ubiquitin ligases that downregulate Frizzled receptors by ubiquitinating and targeting the receptors for lysosomal degradation (52, 53). Lgr5-bound to RSPO1 was shown to engage RNF43 and ZNRF4 in a complex that was eventually cleared from the membrane and allowed stabilization of Wnt signaling complex at the plasma membrane (53). Whole body

knockout of Lg5 leads to neonatal lethality possibly due to swallowing air because of ankyloglossia (defects in tongue and jaw) resulting in gastrointestinal distention and no milk in the stomach of these pups (54). Lgr stands for leucine-rich repeat containing G-protein-coupled receptor. Lgr5 has two other homologues, Lgr4 and Lgr6. The three members harbor multiple leucine rich repeats (16-18) in their extracellular domain flanked by cysteine-rich sequences on both sides of these repeats, followed by a 7 transmembrane region and a cytoplasmic tail that unlike other GPCRs does not interact with heterotrimeric G proteins or β-arrestin (50, 55, 56) (**figure1.5**). Thus, their ability to modulate Wnt pathway is independent of GPCR function (50, 55). While Lgr5 expression in the intestine is restricted to CBCs, its homologue Lgr4 is expressed throughout the crypt (55). Lgr4 knockouts/ hypomorphs were shown to have multiple developmental defects including neonatal lethality, growth retardation, reproductive and ophthalmic deficits depending upon the background strain of mice or the extent of loss of Lgr4 (57). It is interesting to note that while conditional deletion of Lgr5 in the adult intestinal epithelium did not affect normal homeostasis, loss of Lgr4 caused a marked reduction in proliferation within the crypts and combined loss of both the family members was fatal within 4 to 5 days of induction of deletion (55). Lgr6 is not expressed in the gut and is mostly thought not be involved in canonical Wnt signaling, however, Lgr6+ stem cells have been found in the isthmus region of the hair follicle (15). Lgr6 Knockout mice have no obvious phenotype (15).

In an effort to better understand how mutation carrying crypts out grow normal crypts, scientists have studied the kinetics of self-renewal of Lgr5+ cells, because in addition to maintaining normal intestinal epithelium, these cells have also been implicated to be the cells-of-origin of mutation in colon cancer (58). Multi-color lineage tracing was carried out by Snippert et al., using R26-Confetti mice crossed to Lgr5-

CreERT2 to follow the clonal behavior of individual Lgr5+ cell in multiple crypts at the same time (14). It was found that all the Lgr5+ cells labeled within the first 24 hours of tamoxifen induction and divided symmetrically to yield equally potent stem cells but over time any one clone stochastically predominated evicting others from the crypt base in a neutral competition for niche and thereby driving a crypt to monoclonality (14). This neutral kinetics and symmetrical cell division by Lgr5+ cells was independently demonstrated by Winton and colleagues as well (59) and has now also been accepted to occur in humans (60-63). Ritsma et al. looked further at how the niche signals dictated the spatiotemporal assignment of the winner stem cell clone during the neutral drift phenomenon using in vivo live imaging of lineage tracing through abdominal imaging window implanted in mice (64). They showed that most often the central CBCs would "win" by out-competing the rest of them creating a monoclonal crypt. This was observed to be due to passive displacement of the border stem cells out of the niche following division of the central stem cells to allow positioning and better adjustment of the newly formed stem cells within the limited niche space even though all the stem cells were equipotent to begin with, thus, forcing the evicted stem cells to undergo differentiation (64).

Figure 1-5 Predicted structure of Lgr5.

The schematic shows the domain structure of Lgr5 comprising of an extracellular domain with multiple leucine-rich repeats, a 7 pass trans-membrane domain, followed by an intracellular domain.

Figure 1.5

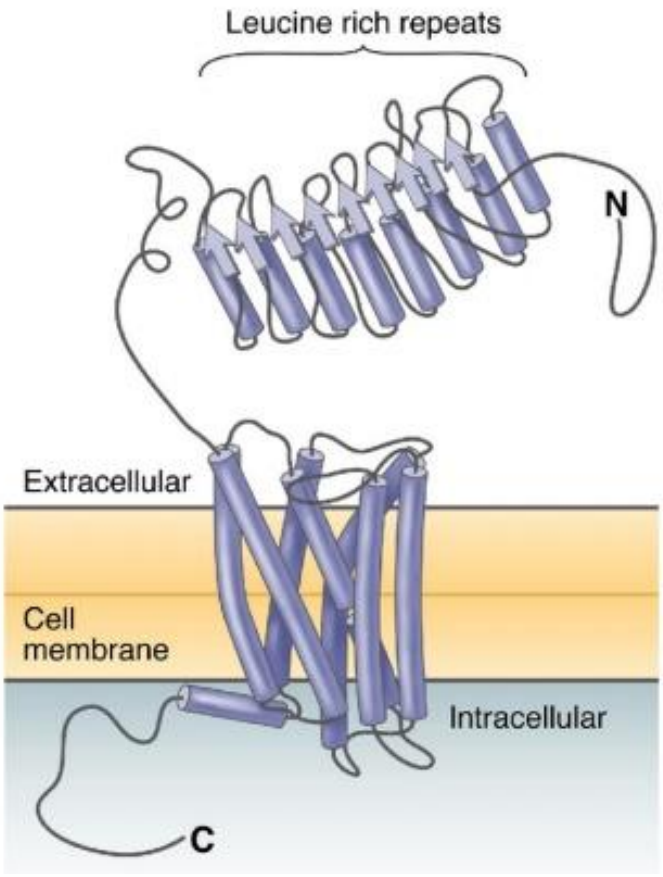

Barker and Clevers. Gastroenterology 138 (2010) 1681-1696.

Because of their cycling nature, Lgr5+ cells are considered to be more susceptible to mucosal insults such as irradiation and cytotoxic drugs like doxorubicin and 5-FU. It has been shown that under these conditions, quiescent/ label retaining stem/progenitor population can take over homeostasis. In a mouse model carrying, Lgr5-DTR, Bmi1-CreERT2 and Rosa26-LacZ alleles it was shown that diphtheria toxin exposure did not affect the normal epithelial integrity of the intestine while the same treatment along with tamoxifen (to activate Bmi1 Cre) increased LacZ+ lineage tracing ribbon of cells from the Bmi1 locus. These findings were confirmed independently by another group (26). Lineage tracings from HopX and Lrig1 loci were found to increase as well upon exposure to radiation (30, 31). More recently, secretory progenitors marked by DLL1 and LRC have also been shown to contribute to epithelial homeostasis when subjected to mucosal injury (36, 37). It has been proposed that these more mature cells, upon falling back into the “stem cell zone” can regain stemness and de-differentiate. What is also interesting is that for these progenitors to form organoids *in vitro*, Wnt3a is necessary (a true niche signal provided by Paneth and other non-epithelial cells). The LRC reported in the literature is relatively short-lived (up to 4 weeks after labeling) and may not be a true stem cell. However, new LRCs keep forming from the Lgr5 compartment on a regular basis that can be called into action in case of damage to the cycling stem cell compartment (66). These multiple studies demonstrating exquisite plasticity of several crypt progenitor/ LRCs could be indicative of the fact that stemness is not a function of expression of a particular marker in the intestinal epithelium but is defined by the positioning of a cell within the niche. Thus, it is critical to look at the key signaling networks in action within and surrounding the crypts.

1.5 Signaling pathways in the maintenance of intestinal epithelium

The location of CBCs deep in the crypt pocket intermingled with Paneth cells puts them in an environment which is conducive for short range interactions as is required in case of pathways such as Wnt and Notch. Below is the description of different signaling pathways operational in the crypt milieu that maintain stem cell number and function.

1.5.1 Wnt

Wnt signaling regulates several aspects of maintenance of intestinal epithelial homeostasis. It is critical for keeping proliferation intact within the stem/transit amplifying compartment intact, inhibiting differentiation (other than Paneth cells), and regulating localization of cells along the crypt-villus axis.

Wnts are the ligands that act within a short range to trigger this signaling cascade by binding to their cognate receptors Frizzled (Fzd) and co-receptors Lrp5/6 present on nearby cells via their palmitate group. This binding event introduces a conformational change in these receptors that allows associated kinase, CK1γ to phosphorylate the cytoplasmic tail of Lrp. This phosphorylated complex sequesters scaffold proteins Disheveled (Dsh) and Axin (which are a part of a complex including casein kinase1 (CK1), adenomatous polyposis coli (Apc) and Glycogen synthase kinase 3β (GSK3β) that in the absence of Wnt activation binds to β-catenin to phosphorylate its amino-terminus to target it for proteosomal degradation), to allow stabilization of β-catenin, that then translocates to the nucleus and interacts with TCF/LEF family of transcription factors to induce transcription of Wnt-target genes (67).

In the intestine, Wnt3, Wnt6 and Wnt9b are the main epithelial secreted Wnts, mostly by Paneth cells and Wnt2b, Wnt4, and Wnt5a are the mesenchymal Wnts (43).

Although, Fzd 2, 4, 5, 6 and 8 are all expressed in the epithelium, Fzd 7 is most abundantly expressed in the Lgr5+ CBCs along with LRP5 and 6 (68). It is also known that the mesenchyme surrounding the crypts secretes Wnt antagonists such as Frizzled related proteins 1 and 5 (the soluble proteins that compete for Wnts) and Dickkopfs (Dkks, inhibitors of LRP function) (69-71). The main effector of Wnt signaling in the adult small intestine, TCF4, is expressed all along the crypt-villus axis (69).

The evidence for the vital role of Wnt pathway in intestinal epithelial self-renewal came from two major observations. One, along with the studies of loss of function mutations of Apc as a cause for familial adenomatous polyposis, several studies pointed to development of intestinal tumors with dysregulation of other Wnt pathway components (72-80). Two, abrogation of Wnt signaling through knockout of Tcf4 or overexpression of DKK1 resulted in complete loss of proliferation within the crypts (81-83).

In association with other signaling pathways, Wnt also participates in fate determination of progenitors. Dysregulated Wnt signaling by the loss of Apc was shown to decrease differentiation towards all mature cell types except for Paneth cells and this phenotype was successfully rescued by c-Myc deletion (77, 78, 84). Similarly, overexpression of c-Myc caused loss of goblet cells (85). Paneth cells seem to depend extensively on the Wnt pathway for their maturation and positioning. Several Wnt-target genes regulate the function of Paneth cells such as cryptdins, defensin and Sox9 (47, 78, 84, 86). Hyperactive Wnt doesn't affect the number of Paneth cells but impacts their localization (84). On the other hand, disruption of β-catenin within a secretory progenitor compartment (marked by Neurogenin3) leads to reduced differentiation towards Paneth cells (87).

Differentiation within the intestinal epithelium is closely connected to migration of cells out of the crypts and Wnt signaling regulates both migration and positioning of cells

along the crypt-villus axis. EphB receptors are receptor tyrosine kinases that regulate the migration of cells along the epithelial lining by remodeling the actin cytoskeleton (88-90). Interaction of EphB receptors with their transmembrane ligands (EphrinBs) generates repulsive forces that segregate cells expressing either of them into opposing gradients (88, 91). The Wnt pathway has been shown to positively regulate the expression of EphB receptors, Eph2 and Eph3, within the crypt while suppressing the expression of their ligands EphrinB1 and B2 which are highly expressed at the crypt-villus junction (92-95). Loss of EphB2 causes mislocalization of progenitor cells while loss of EphB3 results mispositioning of Paneth cells along the crypt-villus axis (95, 92).

1.5.2 Notch

In the intestine, Notch signaling plays an important role in maintenance of stem cells as well as in the binary fate decision of secretory vs. absorptive cells (97-103).

In mammals, the Notch family is comprised of 4 single transmembrane Notch receptors (Notch1–4) and 5 single transmembrane ligands, Delta-like1 (DLL1), Delta-like 3 (DLL3), Delta-like 4 (DLL4), Jagged1 (Jag1) and Jagged 2 (Jag 2). Expression analysis of rodent gut has revealed that Notch 1 and Notch 2 are the main Notch receptors that are expressed in the gut (104). In situ hybridization, LacZ knock-in alleles for Dll1 and Dll4 and immunofluorescence staining has showed that Jag1, Dll1, and Dll4 are the potential ligands for Notch receptors in the intestine (97, 104-106).

The pathway initiates when ligand and receptor present on neighboring cells interact with each other leading to proteolytic cleavage and release of the intracellular domain (NICD) of the receptor. NICD, upon release, translocates to the nucleus and forms a complex with the transcription factor CSL (RBP-J in mouse), inducing transcription of downstream target genes (107). Notch is able to regulate stem-cell proliferation and differentiation in the intestine through its target genes such as Ascl2, Olfm4 and Hes1

(101, 108). Block in Notch pathway causes loss of expression of stem cell specific genes such as Olfm4, Ascl2 and Lgr5 and reduction in proliferating crypt progenitors (101, 103). Notch regulates differentiation decisions through its target gene Hes1 which represses the expression of the basic helix-loop-helix transcription factor Atoh1 (also called Math1) (108). Atoh1 is the main regulator of secretory cell fate as its loss in the intestinal epithelium leads to complete absence of secretory cells. On the other hand, Hes-1 null mice have increased proportion of all the secretory cells at the cost of enterocytes (109, 110). Notch signaling also inhibits enteroendocrine fate specification by directly inhibiting the expression of Neurogenin3 (Ngn3). It is interesting to note that ectopic expression of Notch in the Ngn3+ enteroendocrine progenitor cells drives differentiation towards enterocytic and goblet cell fate (111, 112).

The nature of interaction between Notch receptors and their ligands is that of lateral inhibition. Ligand expressing Paneth cells are located right next to the receptor expressing stem cells. This keeps the stem cells in an active Notch environment, maintaining proliferation and suppression of differentiation by downregulation of Atoh1 and at the same time inhibits activation of Notch in its neighboring cells. In accordance with this thought, it has been observed that a transient increase in the expression of DLL1 within a cell overlaps with its exit from the cell cycle and these cells then become the “quiescent” secretory fate precursors (37, 38).

Overall, genetic depletion of Notch pathway components (Notch1/Notch2) (41, 103) or DLL1/DLL4 (97) or pharmacological block through γ-secretase inhibitors (which prevent cleavage of NICD) (102) or receptor neutralizing antibodies (41, 101, 102) results in loss of proliferating cells and increased differentiation towards secretory cell fate. Thus, Notch signaling maintains proliferating crypt progenitors and balances between secretory and absorptive cell differentiation.

1.5.3 BMP

In the context of intestine, BMP signaling is a potent inhibitor of proliferation and inducer of differentiation. This pathway includes the ligands, bone morphogenetic proteins (BMPs) that bind to a Ser/Thr receptor type I/II heterodimers to cause phosphorylation of the receptor type I and activation of downstream effectors of SMAD family of proteins which translocate to the nucleus to carry out transcription of BMP target genes. The receptors, ligands as well as the intracellular effectors are expressed in epithelium as well as in the surrounding stroma. Also, the soluble BMP inhibitors of the follistatin, chordin and gremlin family are expressed mostly within the mesenchyme (113). Studies have demonstrated that abrogating BMP signaling by knockout of Bmpr1A or overexpression of BMP inhibitor Noggin resulted in enhanced proliferation, increased crypt fission, ectopic formation of crypts along the crypt-villus axis and eventual development of intestinal polyposis (114, 115). Loss of BMP signaling results in impaired secretory cell differentiation and no effect on enterocytes (116).

The anti-proliferative effect of BMP signaling has been attributed to its ability to antagonize Wnt signaling and partly by directly stabilizing p21CIP/WAF, the cell cycle inhibitor (117, 34). It is for this reason that the stroma around the crypt is enriched in BMP inhibitors gremlin and noggin (119).

1.5.4 RTK/MAPK/PI3K Pathway

Ample evidence supports an indispensable role of receptor tyrosine kinases (RTKs) and their ligands in intestinal development and maintenance, although the details of how the intracellular players further impact self-renewal, differentiation and migration are not as well documented as that for Wnt and Notch pathways.

Humans have 58 known RTKs that can be subdivided into 20 families. They all have similar domain architecture: an N-terminal extracellular ligand binding domain, a transmembrane region, followed by a C-terminal cytoplasmic tail that comprises of juxtamembrane regulatory regions and a tyrosine kinase domain. In an inactive state, these receptors can be found on the plasma membrane as sitting alone or in homo or hetero dimers with their family members. Ligand binding can induce dimerization of individual receptors or bring together already formed dimers into a conformation that allows activation of the tyrosine kinase domain in the C-terminus of these receptors. This activation leads to trans-phosphorylation of key tyrosine residues on these tails. These phospho-tyrosine residues then become signal transduction hubs through activation of downstream MAPK cascade or PI3K pathway. Receptor phosphorylation can also recruit Src homology-2 (SH2) or phosphotyrosine-binding domain (PTB) containing negative regulators of this signaling such as CBL or SHP1 that can instigate ubiquitination and targeting of the receptor for lysosomal degradation or dephosphorylation of signaling tyrosine residues respectively. This negative regulation is of extreme importance in keeping the signaling downstream of RTKs under check (120, 121).

Specific roles for RTKs have been identified in the gut. It has been shown that, epidermal growth factor (EGF), the ligand for EGFR RTK, drives the mucosal maturation in utero, regulates expression of adult enterocytic enzymes (122-124), and promotes proliferation in neonatal and adult mammalian intestinal epithelium (125-127). Mice with compound deletion of EGFR ligands, TGF-α, EGF and amphiregulin (AR), show spontaneous duodenal lesions, stubbier villi, and increased susceptibility to Dextran sulfate-induced injury along with growth retardation (128). EGFR-dependent epithelial cell migration is required for epithelial renewal and wound healing (129-131). When mouse strain background permits live EGFR-/- births, pups display gross defects in the

intestinal mucosa along with reduced proliferation (132-134). The ISC niche function of Paneth cells requires them to secrete ErbB ligands (49). RTKs of the EphB-family, FGFR and IGFRs have also been shown to play crucial roles during gut morphogenesis, mucosal proliferation and crypt survival, differentiation and positioning of cells along the crypt-villus axis (88, 134-139). In addition, Lrig1, a negative regulator of ErbB family of RTKs was recently shown to be enriched within the crypt compartment and its loss led to formation of duodenal adenomas (30, 140). RTKs are also key players in oncogenesis and other pathologies of the gut (141-149).

With respect to self-renewal and fate determination two sets of studies have elegantly demonstrated how RTKs can modulate the epithelial architecture. Heuberger et al., recently demonstrated that loss of Shp2, a positive regulator of RTK signaling, leads to expansion of Paneth cells at the cost of goblet cells along with an increase in the Lgr5+ stem cells. They attributed this phenotype to loss of Mek-Erk signaling, that potentiated Wnt signaling through de-stabilization of a shorter non-functional isoform of TCF4 (150). RTK signaling can also activate the PI3K/Akt pathway, which is a potent inducer of cell proliferation and inhibitor of apoptosis (151, 152). In the context of intestinal epithelium, PI3K/Akt pathway has been assessed through the impact of BMP signaling on PTEN, a negative regulator of the PI3K/Akt pathway (33, 34). It was shown that within the Label retaining +4 compartment, BMP signaling enhanced PTEN activity and inhibited nuclear accumulation of β-catenin (33, 34). Similarly, loss of PTEN resulted in de novo crypt formation and increased crypt fission and even intestinal polyp formation (33, 34, 154). This work showed how activated Akt, could induce phosphorylation of β-catenin and ultimately activation of Wnt (115, 34).

These divergent ways by which RTK signaling interacts with Wnt and other pathways makes it a unique signaling system that requires more detailed analysis especially of the context under which flux through these two different routes takes place.

Through understanding of these different molecular networks that regulate stem cell function within its niche (**figure1.6**), scientists have developed in vitro culture conditions (including RSPO1, EGF, Noggin along with laminin based extracellular matrix) to grow crypts as three dimensional organoids (**figure1.7**) (49). This ability to grow organoids in vitro not only allows us to manipulate these crypt cultures to answer scientific questions but could also have potential applications in regenerative medicine and in testing efficacy of pharmacological agents against cancer and other diseases (155).

Figure 1-6 Cell signaling at the base of the intestinal crypt.

The schematic shows how growth factors such as Wnt, Notch and EGF supplied by the surrounding niche support the maintenance, proliferation and differentiation within the stem cell compartment.

Figure 1.6

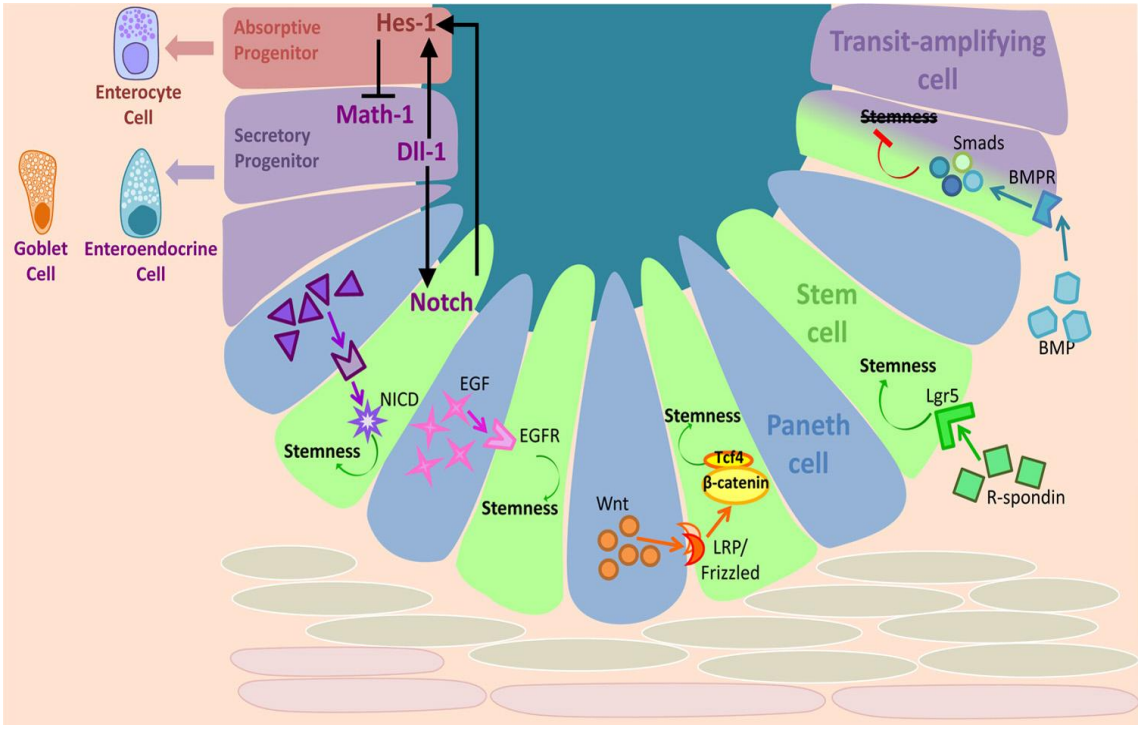

Tan and Barker Seminars in Cancer Biology 32 (2015) 40–53

Figure 1-7 Structural organization of in vitro cultures crypt derived organoids.

Schematic shows the arrangement of crypt and villus domains within in vitro cultured organoids. Stem cells are shown as green colored wedge shaped cells at the bottom of crypt domains.

Figure 1.7

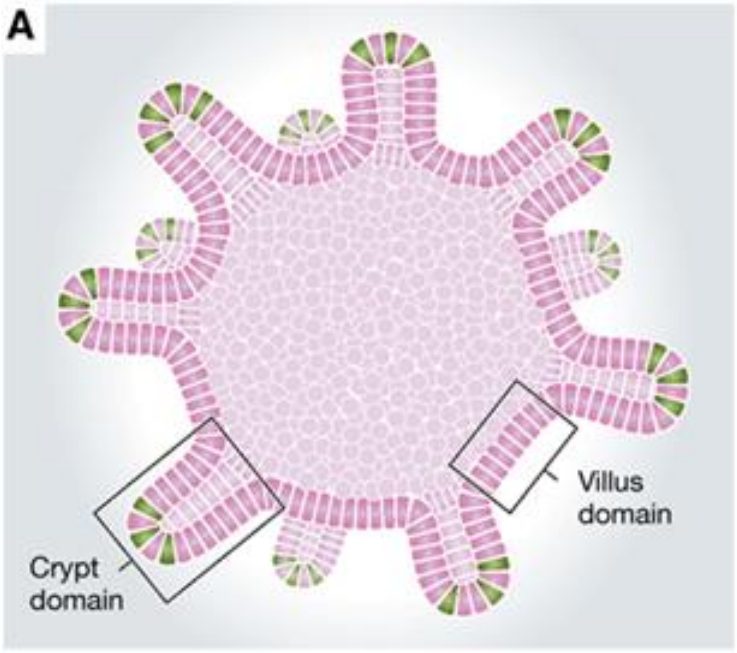

Schuijers and Clevers. The EMBO Journal 31 (2012), 2685–2696

1.6 Why study intestinal stem cells

Their ability to continuously self-renew while generating progeny makes IESCs excellent candidates for use in regenerative medicine but this also makes them susceptible to accumulating cancer causing mutations. Thus, targeting self-renewal of this cancer causing stem like cell can serve as an effective therapeutic strategy (156).

Progression of cancer from benign adenomatous polyps to highly aggressive carcinomas has been shown to be a function of continuous accumulation of mutations (157). From stem cell Cre based deletion of tumor suppressors or cancer stem cell xenograft transplantation experiments; substantial evidence has accumulated over the years to believe that normal stem cells can serve as the “cell of origin” within which accumulation of mutations can potentially result in colorectal cancer (58, 159-165). This is called the “bottom-up” model (155). Other observations that support this model include: the architecture of adenomas is very similar to normal crypts with the ability to differentiate into all the mature cell types being retained (166). Using lineage tracing, assessment of clonality upon activation of oncogenic $Kras^{G12D}$ revealed that much like their normal counterparts, mutated crypts moved towards fixation of a clone albeit the size of individual clones and drift towards monoclonality was much quicker, possibly due to increased cell cycle rates of the mutated cells. What was even more interesting to note was that because the stochastic dynamics of neutral drift remained intact, quite often WT clones were seen to replace mutant ones, demonstrating a mechanism by which the normal intestinal architecture attempted to thwart fixation of mutations. Also, similar to normal crypts, once fixed, mutated clones were seen to expand within the tissue through crypt fission (159, 160). Thus, it will be crucial to find ways to target these cancer stem cells without affecting normal stem cells.

1.7 CBL Family Ubiquitin E3 Ligase

1.7.1 Evolutionary history and domain architecture of CBL proteins

CBL (Casitas B-Lineage Lymphoma) was first identified as an oncoprotein, v-CBL, a Cas NS-1 retroviral Gag-fusion protein of 357 amino acids long that caused pre- and pro-B cell lymphomas in mice (167). Subsequent discovery of the full length cellular version, c-CBL (913 a.a. in mice) revealed that v-CBL was C-terminal truncated form of the protein fused to viral Gag protein (168). Mammalian CBL family includes two other members namely CBL-B and CBL-C. While c-CBL and CBL-B are full length proteins, CBL-C is a shorter form lacking some of the key C-terminal domains (**figure1.8**) (169).

The N-terminal region in all the three members comprises of a Tyrosine Kinase Binding (TKB) domain that recognizes a specific phospho-tyrosine (pY) motifs on activated receptor and non-receptor tyrosine kinases. The TKB domain is made up of a unique assortment of domains found only in CBL proteins. These include a four-helical bundle (4H), an EF hand and an SH2 domain (170). A highly conserved helical linker and RING (Really Interesting New Gene) finger domain follow the TKB region of CBL. Linker and RING finger domains bestow the E3 ligase function on to CBL proteins as they together serve as a scaffold for binding of E2, ubiquitin conjugating enzyme (**figure 1.9**) (171). These three regions (TKB, Linker and RING finger) together comprise the N-terminal domain of CBL proteins. In addition to the N-terminal domain, CBL and CBL-B also are comprised of a C-terminal tail made up of proline-rich (PR) and leucine-zipper (LZ)/Ubiquitin-Associated (UBA) domains. While the PR domain enables CBL and CBL-B to interact with SH3 domain containing proteins like Src-family kinases, Grb2 and CIN85, the LZ/UBA domain allows ubiquitination and dimerization of CBL proteins although its exact functional significance remains unclear (169). CBL and CBL-B also

harbor several key pY residues, which upon phosphorylation bind to SH2 domain containing proteins such as Vav, p85 subunit of PI3K and Crk family proteins (169).

Evolutionarily, orthologs of CBL proteins have been found in all metazoan species with fairly similar domain structure. The most primitive organism to have a version of CBL has been traced back to a slime mold, *Dictyostelium discoideum*. Dicty-CBL has a conserved N-terminal domain architecture minus the linker region. Interestingly, this version of the TKB domain interacts with a protein tyrosine phosphatase, PTP3, and downregulates it to potentiate STAT signaling (172). While worms (Sli-1 of *C.elegans*) have a single CBL protein, insects (D-CBL (short) and D-CBL (long) of *D. melanogaster*), fish, amphibians and birds have two forms. All mammals on the other hand have three CBL proteins (169).

Figure 1-8 Evolutionary conservation of the primary structure and domain organization of CBL proteins.

Comparison includes: the three human (*Homo sapiens*) CBL proteins (CBL; CBL-B; and CBL-C); Chicken (*Gallus gallus*) CBL; Zebra fish (*Danio rerio*) CBL; Frog (*Xenopus tropicalis*) CBL; Fly (*Drosophila melanogaster*) long and short CBL; Worm (*Caenorhabditis elegans*) CBL (SLI-1); and Dicty (*Dictyostelium discoideum*) CBL (Cbl-A).

Figure 1.8

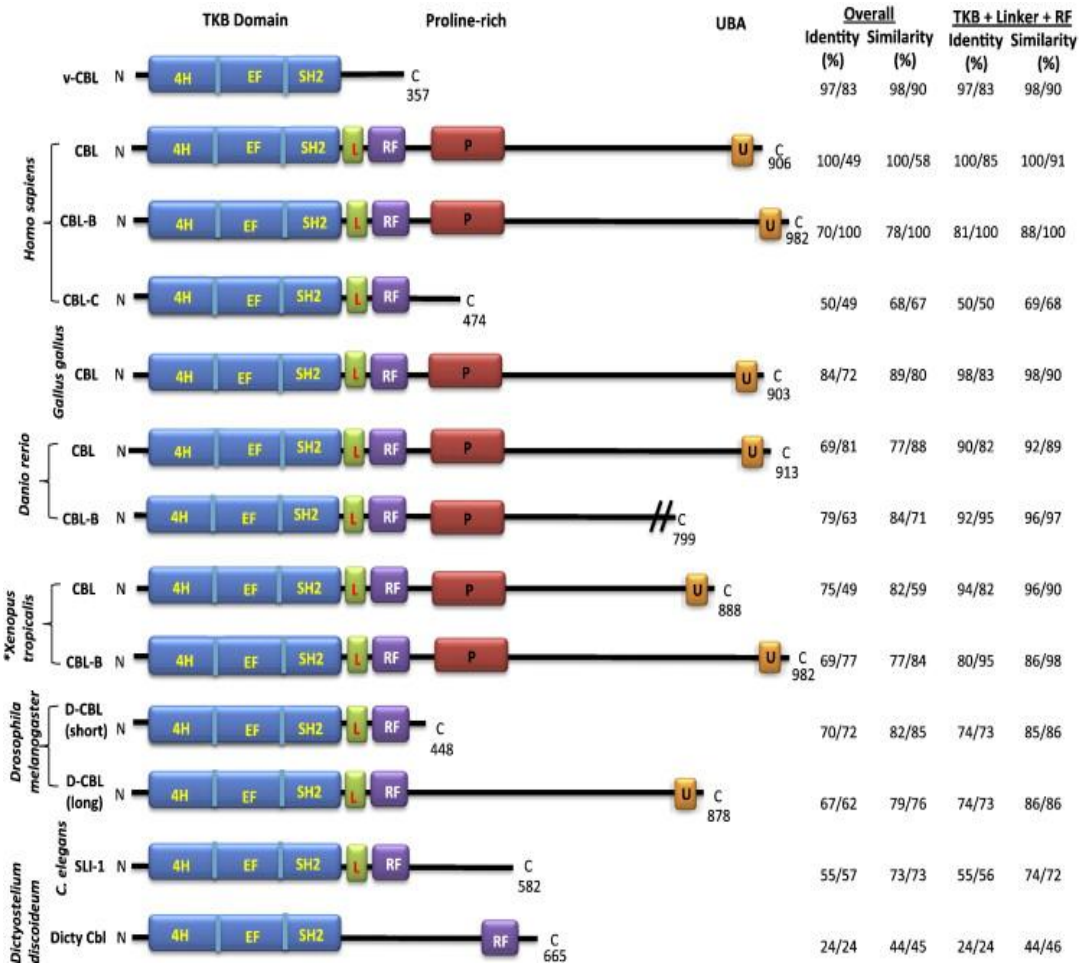

Mohapatra et al., Biochimica et Biophysica Acta 1833 (2013) 122–139

Figure 1-9 Domain architecture of CBL proteins and major interacting partners.

The N-terminal Tyrosine Kinase-Binding (TKB) domain binds to phospho-tyrosine (pY)-containing target proteins, including activated receptor and non-receptor tyrosine kinases. The Linker (L) and the RING finger (RF) regions bind to ubiquitin conjugating enzymes (E2). The proline-rich motifs (Pro-rich) bind to SH3 domain containing proteins such as Src family kinases (SFK). Recruitment of CBL to its targets often induces phosphorylation at tyrosine residues in the C-terminal region of the protein that further engages SH2 domain-containing signaling proteins. The Ubiquitin-associated (UBA) domain/leucine zipper near the C-terminus is involved in ubiquitin binding and dimerization.

Figure 1.9

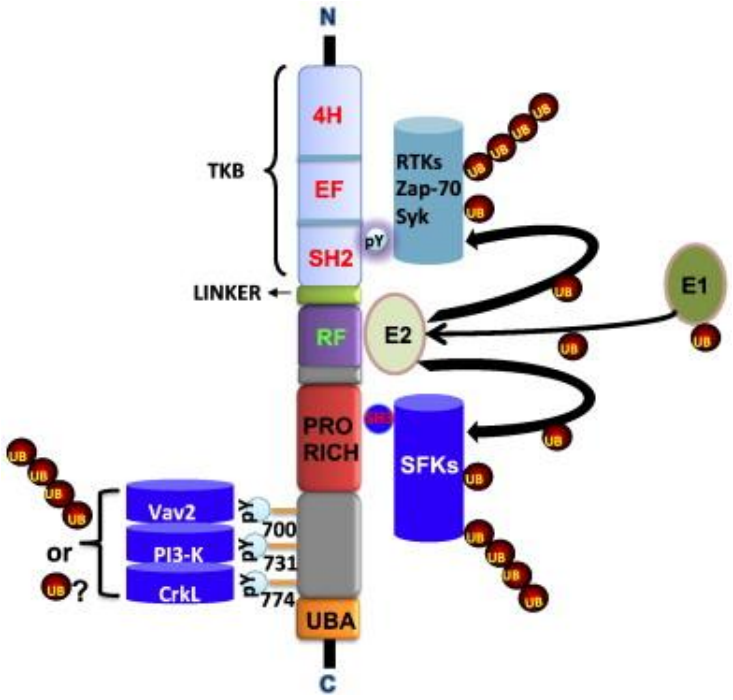

Mohapatra et al., Biochimica et Biophysica Acta 1833 (2013) 122–139

1.7.2 Function & localization of CBL proteins

Numerous studies provided indirect evidence for the role of CBL in negative regulation of activated protein tyrosine kinases (PTKs); however, it was in 1997 that using oriented phosphopeptide libraries and mutagenesis we showed for the first time that the N-terminal domain of CBL bound to the negative regulatory pY motifs of ZAP70 and Syk (173). Similar studies of TKB domain interaction of CBL were further extended to RTKs such as PDGFR and EGFR (174-176). Biochemical studies later established that CBL induced downregulation of activated RTKs by ubiquitination and lysosomal degradation of the internalized receptor (175, 177) could be attributed to the E3 ligase function of the RING finger domain (178). The generality of this ubiquitination related negative regulatory function of CBL was quickly extended to other RTKs such as c-MET and M-CSFR, and non-receptor PTKs such as Fyn, Lck, Src, ZAP-70 and Syk (179-185).

Structural and mutational studies have elucidated that while CBL attaches to its targets via the TKB or the proline-rich domains and the C-terminal pY residues; binding of E2 ubiquitin conjugating enzyme requires both Linker and RING finger regions. Particularly, phosphorylation of a critical tyrosine residue (Y371) in the linker region of CBL alters its conformation in a way that not only increases its binding to E2 but also brings E2 closer to the CBL targets (186). This association renders the PTK targets (multi) mono-ubiquitinated or polyubiquitinated, which are further sorted to lysosomal or proteosomal degradation (169).

Localization studies mainly focused on c-CBL have shown that it is localized to the cytosol but can also be found on membrane due to its association with membrane receptors and membrane adaptor proteins (187).

Few studies have gauged the physiological function of CBL proteins in a cell. In T cells, it was shown that CBL proteins regulated actin cytoskeleton needed for

stabilization of immunological synapse such that loss of CBL proteins led to prolonged synapses, resistance to induction of anergy, hyperactivation of the T-cell receptor (independent of co-stimulation from CD28), enhanced proliferation and cytokine secretion (169). CBL/CBL-B deficient mammary epithelial cells on the other hand were shown have increased migration upon being exposed to growth factors such as EGF or HGF, with no effect on proliferation (188). In contrast, Cbl-/- or Cbl/Cbl-b double knockout (DKO) hematopoietic stem and progenitor cells showed marked increase in proliferation upon cytokine stimulation (189-191).

In order to understand the physiological roles of CBL proteins, gene knockout mouse models have been helpful. It has been shown that while CBL and CBL-B are ubiquitously expressed in all tissues, expression of Cbl-c is restricted to epithelial tissues (169, 192). Cbl null mice, otherwise viable, show some hyper-cellularity in the lymphoid organs especially spleen, thymus and bone-marrow (190, 193, 194). Also, they display lean muscle mass due to elevated insulin action (195-196). In addition, males are hypofertile (196). Deletion of Cbl-b makes mice autoimmune when challenged by antigen due to hyperactivation of T and B cells (197, 198). Under pathogen-free laboratory conditions though, Cbl-b-/- have no apparent developmental abnormality (169). In addition, an interesting role of CBL-B (and possible of Cbl as well) as an inducer of muscle atrophy associated with its ability to downregulate insulin receptor signaling has emerged from the literature (199-202). Knockout of Cbl-c has not been associated with any anatomic observable phenotype (192, 203). In contrast, combined germ-line deletion of Cbl and Cbl-b results in embryonic lethality (203). Mice with germ-line double deletion of Cbl with Cbl-c and Cbl-b with Cbl-c have been recently generated in our lab and are viable. From unpublished observations in our lab, conditional whole body deletion of floxed Cbl and Cbl-b alleles using R26-CreERT in adult animals is also incompatible with life as mice

die within 5 days of tamoxifen induction due to complete breakdown of intestinal epithelial barrier. This suggests that CBL and CBL-B, the two full length proteins of the CBL family, play essential but possibly redundant roles during embryonic development as well as adulthood.

Because of the functional redundancy of CBL and CBL-B, mice with conditional (floxed) Cbl alleles on a Cbl-b null background have been generated to study pertinent tissue-specific roles of CBL and CBL-B (189, 203). Using Lck-Cre to generate CBL/CBL-B DKO T cells heightened the autoimmune phenotype and hyper-responsiveness of T cells to antigen stimulation as seen in CBL-B null mice (203). Loss of CBL/CBL-B in the B cells of mice led to a loss of peripheral tolerance (205). Even more remarkable results were seen in the case of hematopoietic stem cells where combined loss of CBL and CBL-B led to the development of myeloproliferative disorder (MPD) in mice which was fatal within 8 weeks of birth (189). A RING finger domain missense mutant knocked-into one allele and a complete loss of the other allele of Cbl phenocopied the DKO phenotype of MPD but at a significantly slower pace (191), illustrating that MPD resulted from the loss of E3 ligase activity of CBL.

All together, these studies point to selective and redundant functions of CBL and CBL-B possibly linked to their relative expression within a tissue type. However, more studies are needed to better understand their roles especially in non-immune organ systems.

1.7.3 CBL in Stem Cells and Cancer

As mentioned before, CBL was first identified as a retroviral fusion oncoprotein (v-CBL) capable of inducing T- and B-cell lymphomas, erythroleukemia, and myeloid leukemia with a latency period of 5-6 months (167, 169). Two other oncogenic variants of CBL have since been identified in murine cell lines derived from carcinogen-induced

lymphomas (187) namely 70Z CBL (Linker-RING finger mutant incapable of binding to E2) and p95 CBL (hyper-phosphorylated form of CBL found near the membrane).

In humans, mutations in the helical linker and RING finger domain have been reported in myelodysplastic syndromes such as juvenile myelomonocytic leukemia (JMML), chronic myelomonocytic leukemia (CMML) and atypical chronic myeloid leukemia (aCML) (206-210). Cbl mutations have so far not been reported for any epithelial cancers, although a recent report on Noonan Syndrome, a developmental disorder characterized by stunted growth, malformations of heart and facies, showed germ-line heterozygous deletion of Cbl as the cause (211).

Over the last few years, published as well as unpublished data from our lab as well as from other studies have been pointing towards a very interesting role played by the CBL family of proteins in the regulation of stem/ progenitor compartments. In the hematopoietic system, we recently demonstrated that the earlier reported fatal MPD was a result of combined loss of CBL/ CBL-B within the hematopoietic stem cells (HSCs) and not the progenitors. In addition, we showed that CBL proteins were essential for maintenance of quiescence of HSCs such that DKO HSCs lost repopulation ability over time due to exhaustion (212). In the neural system, one study showed the upregulation of CBL protein in response to oxidative stress in neural progenitor cells (213) while another study demonstrated that double deletion of Cbl and Cbl-b in the neural stem cells led to loss of asymmetric distribution of EGFR into daughter cells and increase in the number of neurospheres formed (214). With respect to osteoblast differentiation, it was shown that knock-down of Cbl in the mesenchymal stromal cells led to hyperactivation of STAT5 and thereupon increased differentiation to osteoblast cell fate (215).

Even though several epithelia relevant RTKs and non-receptor PTKs are targets of CBL proteins, no study has looked at their role in maintaining epithelial tissue. With this in mind, we generated conditional deletion of Cbl in the Cbl-b null background in the mammary gland using MMTV-Cre as well as WAP-Cre. DKO resulted in considerably reduced ductal branching. An in-depth investigation of this phenotype has revealed a significant reduction in the mammary stem cell population ($CD24^{+}/CD29^{hi}$) and a concomitant increase in the luminal epithelial population. This phenotype was confirmed with Lgr5-Cre based deletion of Cbl and Cbl-b in the mammary stem cells which showed shrinkage of the basal population (reported to harbor mammary stem cells) and expansion of luminal fate. With respect to the expectations of CBL's role as a negative regulator of PTK signaling, the observed phenotype of delayed development of the mammary gland seemed counterintuitive especially keeping the hyper-proliferative HSC phenotype in mind. Thus, in order to investigate these tissue type specific differences in the role of CBL proteins in the epithelial stem/progenitor compartment, we proposed to study CBL proteins by employing the well characterized stem to mature epithelial cell hierarchy of the intestinal epithelium using the well-established Cbl fl/fl; Cbl-b-/- genetic system created by our lab. Not only would this study enhance our knowledge about the function of CBL proteins in the intestine but also provide mechanistic details to reconcile the divergent phenotypes of hematopoietic and mammary stem cells.

2 Materials and Methods

2.1 Mouse Strains

All mice used for experiments were approximately of 6-8 weeks of age. Lgr5GFP-CreERT2 and Rosa26-LacZ reporter mice were purchased from Jackson Laboratories and interbred. This genotype served as a control. These mice were further bred with Cbl floxed; Cbl-b null mice (189) to obtain Cbl fl/fl; Cbl-b null; Lgr5-CreERT2; R26-LacZ experimental mice so that tamoxifen inducible stem cell specific deletion of Cbl and Cbl-b could be achieved. Cbl knockout (194)(198) and Cbl-b knockout (198) mice have been used to study the function of individual genes in the intestine with WT littermate C57BL/6J mice serving as controls. Cbl f/f; Cbl-b f/f; R-26-CreERT mouse model recently generated in our lab was used to perform organoid assay to by deleting Cbl/Cbl-b *in vitro*.

All mouse strains were maintained on C57BL/6J background under specific pathogen-free conditions and handled in accordance with protocols approved by the Institutional Animal Care and Use Committee (IACUC) of UNMC. Mice were genotyped using tail DNA (primer sequences in Table-2.1).

2.2 Induction of Gene Deletion

Tamoxifen free base (MP Biomedicals, Catalog no. ICN15673880) was resuspended in sunflower oil (Catalog no. Sigma Aldrich, S5007) at a concentration of 10 mg/ml. 1ml Aliquots were made and frozen at -20°C.

At 6 weeks of age, gender matched Lgr5-CreERT2; R26-LacZ and Cbl f/f; Cbl-b-/-; Lgr5-CreERT2; R26-LacZ mice were given intra-peritoneal injection of 2 mg of tamoxifen for 3 consecutive days to activate inducible Cre recombinase. Animals were analyzed 3

days after the last injection (or 5 days after the first), 8 days after the last injection (or 10 days after the first) or 4 months after the last injection.

2.3 Animal Euthanasia

All mice used in this study were sacrificed by first anesthetizing using isoflurane (Piramal Healthcare, Catalog no. NDC66794-017-25) followed by cervical dislocation to confirm death.

2.4 Tissue Harvest and Histological Analysis

Mouse small intestine was excised carefully from the peritoneal cavity by first snipping at the ileo-cecal junction and pulling away to disentangle the intestine from the mesh of mesentery and finally cutting at the pyloric end of stomach. The intestine was immediately placed in a Petri dish, and gently flushed with cold phosphate buffered saline (PBS) to remove fecal matter using a 30 ml syringe and a blunt ended needle. Once cleaned, intestine was kept on a blotting sheet, cut open longitudinally, swiss-rolled and placed in formalin (Sigma Aldrich, Catalog No.HT501128) for overnight fixation at room temperature. Fixed tissue was processed, embedded in paraffin and sectioned to 5 uM thickness.

2.5 Immunofluorescence (IF)

Tissue sections were de-paraffinized and rehydrated followed by antigen retrieval in sodium citrate antigen unmasking solution (Vector Laboratories) using microwaving for 20 min. Slides were then washed in PBS and blocked for 1 hr in TBS-T (Tris Buffered Saline with 0.1% Tween-20) containing 5% goat serum (Sigma Aldrich, G9023) followed by overnight incubation at 4°C with optimized concentrations of primary antibodies {(BrdU, Developmental Studies Hybridoma Bank, Iowa, G3G4,1:25) , Chromogranin A

(1:200, Abcam, Catalog No.15160), Cleaved Caspase 3 (Cell Signaling, Catalog No.9664, 1:200), GFP (Cell Signaling Rabbit monoclonal, 2956, 1:200), GFP (Chicken, Catalog No.1020, Aves Laboratories, 1:2000)}. Tissue sections were then washed thrice in PBS for 5 minutes each, followed by incubation with fluorescently-tagged secondary antibodies (Molecular Probes Alexa series, all 1:400 in blocking buffer) for 1 hr at room temperature, washed 3X with PBS and mounted with Vectashield with DAPI to stain nuclei (Vector Laboratories).

2.6 Immunohistochemistry (IHC)

Tissue sections were de-paraffinized and rehydrated followed by antigen retrieval in sodium citrate antigen unmasking solution (Vector Laboratories) using microwaving for 20 min. Slides were then washed in PBS and kept in 5% H2O2 for blocking endogenous peroxidase for 1 hour at room temperature. Slides were washed with PBS and blocked using Mouse Ig Blocking Reagent from Mouse on Mouse (MOM) kit of Vector Laboratories for Cbl (mouse monoclonal, anti-Cbl, BD Bioscience, 1:400) and Cblb (mouse monoclonal, anti-Cblb, Abcam, 1:100) or using 5% goat serum (Sigma Aldrich, G9023) for ChromograninA (1:200, Abcam) and Ki67 (Rat eBioscience, 145698-82, 1:200) for 1 hour at room temperature. Slides were washed twice with PBS and incubated with primary antibodies mentioned above for overnight at 4°C. The next day, slides were washed thrice with PBS for 5 min each and incubated with biotinylated secondary antibodies. ABC amplification IHC kit (Vector Laboratories) was used as per vendor's instructions to amplify the signal. Slides were washed twice and peroxidase staining was developed using DAB (3,3'-diaminobenzidine, Vector Laboratories) as HRP substrate. The slides were counterstained with hematoxylin, dehydrated and mounted in automated counter-stainer (Sakura Tissue-tek Prisma) at the UNMC Tissue Science

Core Facility. In all cases, a species matched isotype IgG or genetic knockouts were used as a negative control.

2.7 β-Galactosidase (LacZ) Staining

Protocol published by Barker and Clevers was used to perform lineage tracing using LacZ staining (216). Briefly, freshly dissected intestinal tissue was flushed clean with cold PBS and fixed in Gluteraldehyde fixative (1% formaldehyde, 0.2% gluteraldehyde, 0.02%NP-40 in PBS) for 2 hours at 4°C. Tissue was washed twice with PBS and incubated in equilibration buffer (2mM MgCl2, 0.02% NP-40, 0.01% sodium deoxycholate in PBS) for 30 minutes at room temperature. After this, equilibration buffer was replaced by LacZ substrate {5mM K3Fe(CN)6 , 5mM K4Fe(CN)6, 2mM MgCl2, 0.02% NP-40, 0.1% sodium deoxycholate, 1mg/ml X-gal in PBS} and incubated for 4 hours at 37°C away from light. After blue color developed, tissue was washed twice with PBS, swiss rolled and incubated in 4% paraformaldehyde at 4°C overnight. Next morning, fixative was removed and tissue was washed with PBS and dehydrated in alcohol gradient (70%, 96% and 100% for 1 hour each) and paraffin embedded. 5uM tissue sections were cut, paraffin cleared and rehydrated, followed by counterstaining with nuclear fast red (Vector Labs).

2.8 Intestinal stem cell isolation and flow cytometric analysis

A modification of the Intestinal stem cell consortium protocol was used for making stem cell enriched single cell suspension of intestinal epithelium (217). Briefly, freshly dissected intestinal tissue was flushed clean with ice cold washing buffer (100 µg/ml penicillin/streptomycin, 10mM HEPES, 2mM Glutamax in HBSS) and cut open longitudinally to expose the lumen. A glass coverslip was used to scrape off the villi and the tissue chopped into 5 mm long pieces. The chopped pieces were then washed

several times with cold washing buffer by vigorously pipetting until the supernatant was almost clear. After this, the tissue was placed in dissociation reagent #1 {15mM EDTA, 1.5 mM DTT, 10µM ROCK inhibitor (Y27632, TOCRIS), 100 µg/ml penicillin/streptomycin, 10mM HEPES, 2mM Glutamax in HBSS} and rocked slowly at 4°C for 30 minutes. Supernatant was removed and replaced with fresh cold washing buffer and the tube was shaken vigorously. Tissue pieces were allowed to settle down and supernatant was passed through 70µM cell strainers and centrifuged at 1200 rpm for 5 minutes at 4°C. The pellet was resuspended in 10 ml washing buffer and centrifuged at 600 rpm for 2 minutes at 4°C. The cell pellet obtained was incubated in dissociation reagent # 2 {TrypLE Express (thermo scientific) 1:2 dilution, 10µM ROCK inhibitor (Y27632, TOCRIS), 0.5 mM N-acetylcysteine (Sigma), 200 µg/ml DNAaseI in Intestinal Epithelial Stem Cell Media (IESC Media) (Advanced DMEM/F12 supplemented with 1X N2 (invitrogen), 1X B27 without vitamin A (invitrogen), 10 mM HEPES, 2mM Glutamax (invitrogen),100 µg/ml penicillin/streptomycin} for 8 minutes at 37°C, pipetting intermittently to reduced cell clumping. Equal volume of neutralization buffer (10% FBS in IESC Media) was added to the tubes and the cell suspension was passes through 20µM cell strainers. Followed by this, cells were centrifuged at 1000 rpm for 5 minutes at 4°C. Supernatant was discarded and cells were resuspended in 1 ml of cold IESC media and counted under a microscope. After assessing the yield, cells were stained by incubating with Alexa 700 conjugated anti-CD45 antibody (BioLegend, Catalog No. 103128, 0.25 µg per 10^6 cells) at 4°C for 30 min. Cells were washed twice after that and propidium iodide was added to the cells before analyzing using BD LSR2 instrument. Post data collection, further analysis was done using BD FACS DIVA software.

In another analysis, single intestinal epithelial cells were stained with fixable-Blue LIVE/DEAD stain (invitrogen) using manufacturer's protocol. Cells were then washed

and stained for DLL1 using DLL1-PE (ebioscience, Caalog No. 12-5767-80, 0.25 µg per 10^6 cells) antibody by incubating at 4°C for 30 min. Cells were washed twice after that and analyzed using BD LSR2 instrument.

2.9 RNA Isolation, cDNA synthesis and quantitative PCR analysis

Flow analyzed cells were directly sorted into 500 µl of RNA lysis buffer of RNAqueous®-Micro Total RNA Isolation Kit from Thermo Scientific (Catalog No. AM1931). Instructions from the kit were followed to isolate RNA. Yield of RNA was assessed using nanodrop instrument and cDNA synthesis kit from QIAGEN was used to make cDNA (catalog No. 205311). QuantiTect SYBR® Green PCR Kit was used to perform real-time PCR analysis on a Bio-Rad CFX-96 Thermo Cycler. Primer sequences (obtained from Sigma-Aldrich) are listed in Table 2.2. Relative gene expression was calculated according to the ΔCt method, and normalized to GAPDH reference gene expression.

2.10 Lysate preparation and Western Blot

Freshly-excised, cleaned and chopped fragments intestine were incubated in 2mM EDTA in cold PBS at 4°C for 30 minutes to isolate intestinal epithelium from the remaining tissue. Once epithelial layer was separated (by shaking vigorously and taking the supernatant), it was pelleted and homogenized using a Pro-Sientific homogenizer in RIPA lysis buffer 50mM Tris Chloride (pH 7.5), 100 mM NaF, 0.1% SDS, 1 mM EDTA, 1 mM PMSF, 10 µg/ml Aprotinin, 10 µg/ml Leupeptin, 1 mM Na3VO4, and NP-40 0.02%). Intestinal organoid lysates were prepared in the same lysis buffer. Further lysates were quantified using BCA kit from Thermo Scientific. 40 µg of lysates were resolved on 8% SDS–PAGE and transferred to PVDF membranes, which were then blocked with 2% BSA in TBS-T and incubated overnight at 4°C with specific antibodies diluted in TBS-T.

The following antibodies were procured from commercial sources: Mouse monoclonal antibody (mAb) anti-Cbl (Clone 17/c-Cbl, BD Bioscience); Rabbit monoclonal antibody (mAb) anti-Cbl-b (Clone D3C12, Cell Signaling Technology); Mouse monoclonal antibody (mAb) anti-HSC70 from Santa Cruz Biotechnology Inc. (Clone B6, Santa Cruz, CA). Membranes were washed 3X in TBS-T, incubated with HRP-conjugated species specific secondary antibodies (Zymed Laboratories, South San Francisco, CA) and signals were detected with Pierce ECL substrate (Thermo scientific).

2.11 Abdominal Radiation

Mouse irradiation was accomplished on the TrueBeam linear accelerator in the Radiation Oncology Department at UNMC. Mice were first sedated with Ketamine/Xyalzine, restrained to prevent movement to ensure reproducible positioning for radiation and imaged using the simulation CT scanner. The radiation target abdominal region was contoured and mice were exposed to a dose of 14Gy X-ray radiation.

2.12 Organoid Culture

A modification of the organoid protocol from Sato et al. was used for making organoids from crypts of R-26 CreERT; Cblf/f; Cblbf/f mice (49). Freshly dissected, cleaned and chopped fragments of ileum were incubated in 2mM EDTA in cold PBS at 4°C for 30 minutes in a 15ml Falcon tube. Tissue fragments were allowed to settle, supernatant was replaced with washing buffer (recipe mentioned under section 2.8) and the tube was shaken by hand for 3 minutes to release epithelial layer from the remaining tissue. Supernatant was passed through 70μM cell strainer and rinsed with fresh washing buffer. Crypts were counted under the microscope and volume containing 500 crypts/ well was pelleted. Supernatant was removed and crypts were resuspended in Matrigel

(BD Bioscience, Catalog No. 356237) mixed with growth factors (EGF 5ng/ml; Noggin 100ng/ml; R-spondin 500 ng/ml) and plated in a 24 well plate (Costar) which was then kept at 37°C to polymerize for 15 minutes. Wells were filled with 500µl of IESC media (recipe mentioned under section 2.8). Spent medium was replaced on the 4th day after plating with IESC containing EGF, Noggin, R-spondin 1 conditioned medium (1:10) and Wnt-3a conditioned medium (1:10). HEK293 cells, which overexpressed recombinant R-spondin1 were a gift from Dr. Mark R. Frey and Wnt-3a overexpressing L cells were purchased from ATCC.

After the first passage, organoids from Cre positive and Cre negative control mice were split in a 1:4 ratio and grown for another 4 days at which point media containing 400 nM 4-hydroxitamoxifen (4-OHT) (Sigma) was added and organoids remained in it for the next 72 hours before they were re-passaged or used for experiments.

2.13 Statistical Analysis

Statistical analysis was performed using Paired two-tailed student's t-test to compare the results between control and knock-out mice. Data are presented as average values $\pm$ SEM. The results were considered significant if $P < 0.05$.

Table 2.1 Genotype Primers		
Gene	**Forward 5'-3'**	**Reverse 5'-3'**
Cbl WT	AAGTTCCAAGCCTAGCCAGATATGTGTGTG	TCCCCTCCCCTTCCCATGTTTTTAATAGACTC
Cbl Del	TGGCTGGACGTAAACTCCTCTTCAGACCAATAAC	TCCCCTCCCCTTCCCATGTTTTTAATAGACTC
Cbl floxed	GTGGTGGCTTGCAATTATAATCCTACCACTTAGG	GTTTGAGATGTCTGGCTGTGTACACGCG
Cbl-b del	CCCAGCAAAAGTAGCCAATG	CTTGCAAAAAGGACTAAGATTC
Cblb floxed	GGCAGAACCACTGAGACACATTTA	GGCTGCCAAACTGCTACCCAGGAG
Lgr5 - CRE ERT2(WT)	CTGCTCTCTGCTCCCAGTCT	ATACCCCATCCCTTTTGAGC
Lgr5- CRE ERT2 (Mutant)	CTGCTCTCTGCTCCCAGTCT	GAACTTCAGGGTCAGCTTGC
Cre	GCGGTCTGGCAGTAAAAACTATC	GTGAAACAGCATTGCTGTCACTT
R26-LacZ (WT)	AAA GTC GCT CTG AGT TGT TAT	GGA GCG GGA GAA ATG GAT ATG
R26-LacZ (Mutant)	AAA GTC GCT CTG AGT TGT TAT	GCG AAG AGT TTG TCC TCA ACC

Table 2.2 Primers used for quantitative real-time PCR		
Gene	**Forward 5'-3'**	**Reverse 5'-3'**
Cbl	AGCTGATGCTGCCGAATTT	TTGCAGGTCAGATCAATAGTGG
Cbl-b	GGAGCTTTTTGCACGGACTA	TGCATCCTGAATAGCATCAA
GAPDH	CCTGGAGAAACCTGCCAAGTATG	AGAGTGGGAGTTGCTGTTGAAGT
DLL1	CCCATCCGATTCCCCTTCG	GGTTTTCTGTTGCGAGGTCATC
Nurog3	GAGTCGGGAGAACTAGGATG	CAGTCCCTAGGTATGAGAGT
Alpi	ATCCATCTGTCCTTTGGTATC	TGATGAGGTTCTTAGCTGAT
Lgr5	AACGGTCCTGTGAGTCAACC	ATGGGGTAAGCTGGTGATGC

3 Results

3.1 CBL proteins are expressed in a gradient along the crypt-villus axis

In order to study the role of CBL proteins in the maintenance of intestinal epithelium it was imperative to understand their expression pattern. Thus, in the absence of any previously reported study on CBL proteins in the intestine we began by analyzing the expression of CBL and CBL-B through immunohistochemistry, immunoblotting and quantitative real-time PCR. Due to the lack of reagents to study CBL-C at the protein level, we made use of the Cbl-c knockout mouse model (192), which has a knock-in of LacZ into the Cbl-c locus. These mice were crossed to Lgr5-GFP-CreERT2 mice and this model was used to study the expression of Cbl-c at mRNA level. Lastly, by employing Cbl, Cbl-b and Cbl-c single knockout mice we sought to learn about the possible compensation at the transcript level between Cbl family members.

Immunohistochemical (IHC) staining for Cbl on tissue sections from 6 week old WT and Cbl-/- mice revealed that CBL was expressed in an increasing gradient from villus to crypt. Cbl null animal was used as a negative control for the staining (**figure3.1a, b**). Using the same technique to study the expression of CBL-B, we found a similar pattern of increasing gradient of expression for CBL-B from villus to crypt, although it was less obvious in this case (**figure3.1c, d**). To confirm our findings of IHC, we prepared mucosal whole tissue lysates from different regions of the intestinal epithelium, with one fraction being enriched in crypts and the other in villi (**figure3.1e, f**). We found both the proteins to be substantially enriched in the crypts vs. villi and much like the IHC, Cblb was more highly expressed in the villi than CBL. Phospho-histone3 (pH3) and CyclinD1 are markers of proliferation to be found only within the crypt while Villin is ubiquitously expressed although more enriched in villus vs. crypt. These three proteins were probed

to validate the fractions prepared. HSC70, a housekeeping protein was used as a loading control. To study the expression of Cbl-c, LacZ and GFP co-stainings were performed on 6 weeks old Cbl-c-LacZ/LacZ; Lgr5-GFP-CreERT2 mice (Fig3.1g). While GFP antibody marked the Lgr5 expressing CBCs and their progeny (still retaining residual GFP protein) in the crypts, Lac Z (Cbl-c) was mostly localized to the differentiated cells on the villi. This pattern was in agreement with the previously published report on Cbl-c (192). In **figure 3.1h-i** and we scraped mucosal tissue from the luminal surface of the intestine to perform real-time PCR for Cbl and Cbl-b on the samples from WT, Cbl-/-, Cbl-b-/- and Cbl-c-/- mice. GAPDH was used as a normalization control. Cbl expression increased by more than 5 fold in Cbl-b-/- while it increased by about 2 fold in Cbl-c-/- mice as compared to the WT. Cbl-b expression was increased by about 2 fold in both Cbl-/- and Cbl-c-/- mice as compared to WT. This trend of compensation of expression in single null animals could be suggestive of functional redundancy between Cbl family members.

Figure 3-1 Expression analyses of CBL family members.

Immunohistochemical (IHC) staining for CBL on tissue sections from 6 week old WT and Cbl-/- mice reveals that CBL expresses in an increasing gradient from villus to crypt (**a, b**). A similar expression gradient is seen for CBL-B (**c, d**). Crypt-villus fractionation confirmed enrichment of CBL and CBL-B within the crypts by immunobloting (**e, f**)**.** Cbl-c expression analysis using LacZ-knock-in mice showed predominant expression within the villi, IHC for Lgr5-GFP in these mice marked the crypt compartment and showed no overlap between the two staining (**g**)**.** Relative expression levels of Cbl, and Cbl-b mRNA in WT, Cbl-/-, Cbl-b-/- and Cbl-c-/- murine mucosal epithelium was assessed **(h, i**). GAPDH was used as a normalization control. Compensation of expression in single null animals is suggestive of functional redundancy between Cbl family members. Figures 3.1 a-g were repeated three times on three different samples. Figure 3.1 h-i were performed twice on two different samples.

Figure 3.1a

WT Small Intestine

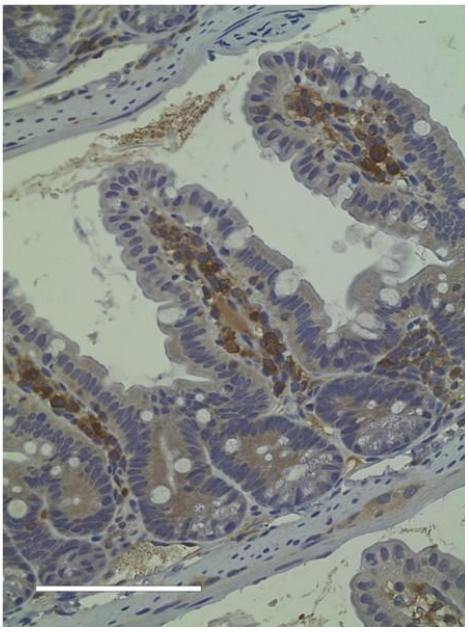

Figure 3.1b

Cbl-/- Small Intestine

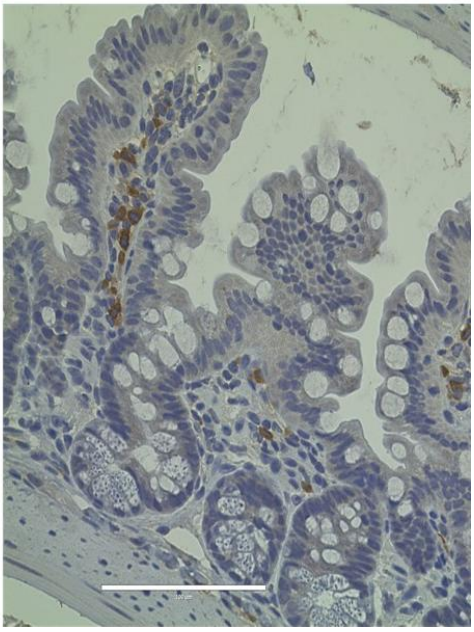

Figure 3.1c

WT Small Intestine

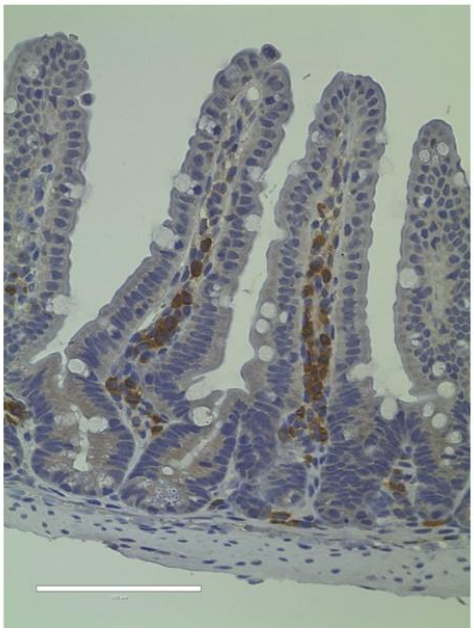

Figure 3.1d

Cblb-/- Small Intestine

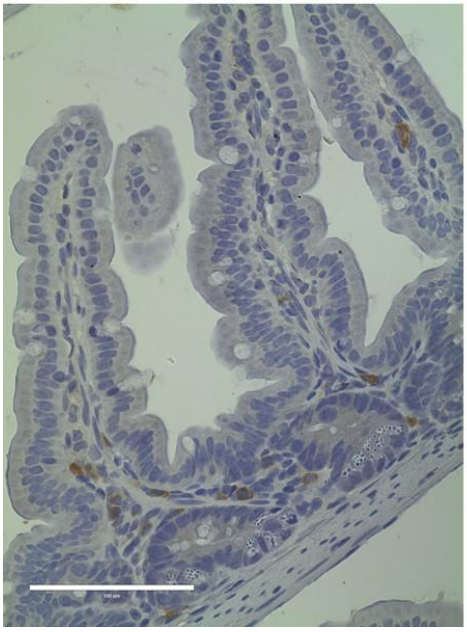

Figure 3.1e

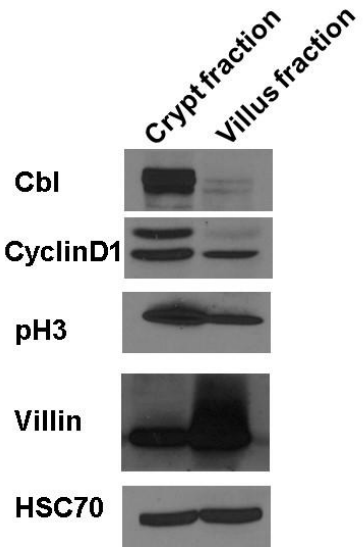

Figure 3.1f

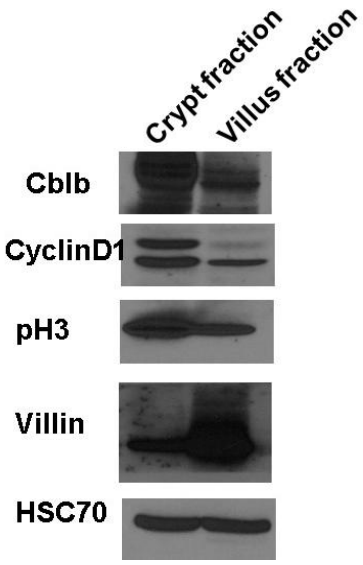

Figure 3.1g

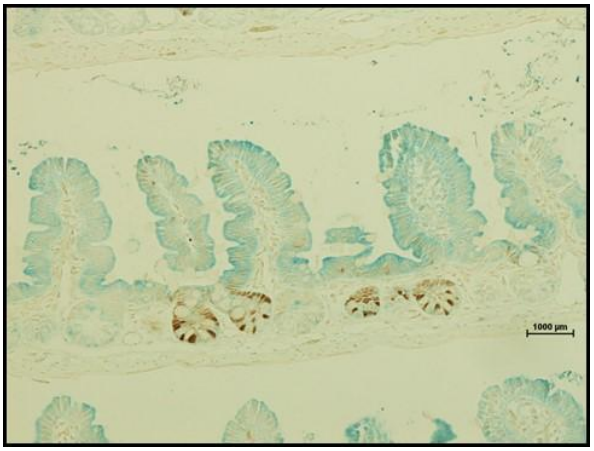

Figure 3.1h

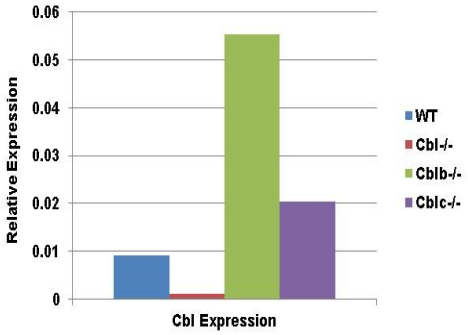

Figure 3.1i

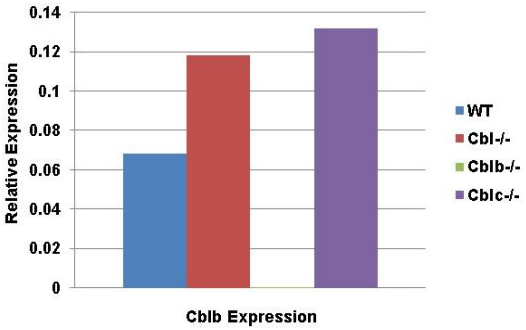

3.2 Cbl null mice show increased proliferation and differentiation to goblet cell fate

Since Cbl-c expression was localized mostly to differentiated cells, and the main focus of our work was to determine the role CBL proteins in the mechanism of maintenance of intestinal epithelium, we decided to focus on the two full length proteins CBL and CBL-B that were enriched in the crypts, the epicenter of regenerating epithelium in the intestine. To begin our investigation, we looked at the gastrointestinal tissue from 6 weeks old Cbl-/- and Cbl-b-/- mice. While Cbl-b-/- looked indistinguishable from the WT, Cbl-/- showed goblet cell hyperplasia as revealed by PAS staining (**figure3.2 a-e**).

Short term BrdU (bromodeoxyuridine) pulse of 4 hours was used to analyze the number of proliferating stem and progenitor cells in the crypts of WT and Cbl-/- mice (**figure 3.2f-h**). We found that in the absence of CBL there was a modest increase in the BrdU+ cells as compared to the WT.

3.3 Construction and validation of Lgr5+ stem cell specific knockout model of Cbl/Cbl-b

As mentioned before, combined complete genetic knockout Cbl and Cbl-b is not viable (203); thus, we decided to make an inducible DKO of these two genes in the Lgr5+ stem cell compartment by crossing together Cbl f/f; Cbl-/- mice (previously generated in our lab to probe the role of these proteins in hematopoietic stem cells and mammary stem cells) (189, 212) (Mohapatra et al., unpublished) with Lgr5-GFP-CreERT2 mice (13) that had already been mated with R26-LSL-LacZ reporter mice. Lgr5-GFP-CreERT2 mice are an ingenious genetic model used widely in intestinal epithelial biology to study Lgr5+ stem cells as they express GFP as well as a tamoxifen inducible Cre recombinase under the Lgr5 promoter.

Figure 3-2 Histological analyses of Cbl-/- and Cblb-/- mice.

PAS staining on tissue sections from age matched WT, Cbl-/- , Cblb-/- mice revealed a significant increase in the number of goblet cells with no change in Paneth cell number in the Cbl null mice (**a-e**). WT and Cbl-/- mice subjected to a short pulse (4 hour) of BrdU showed increased commitment to S phase of the cell cycle in the Cbl null mice (**f-h**). The experiments were repeated four times.

Figure 3.2a **WT**

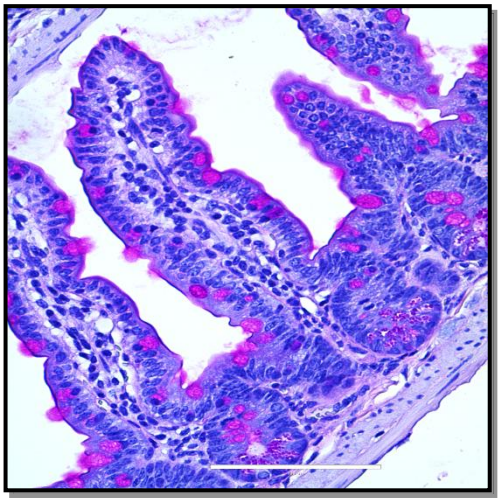

Figure 3.2b **Cbl-/-**

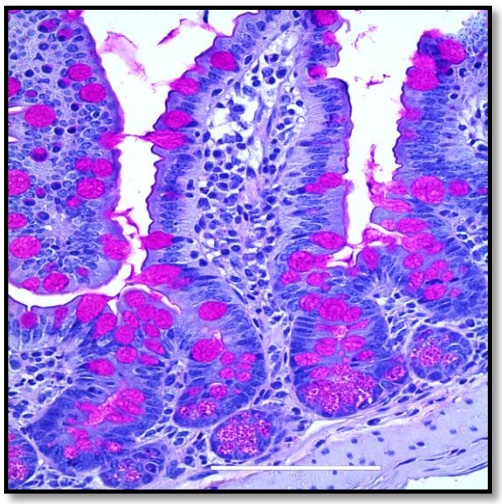

Figure 3.2c
Cblb -/-

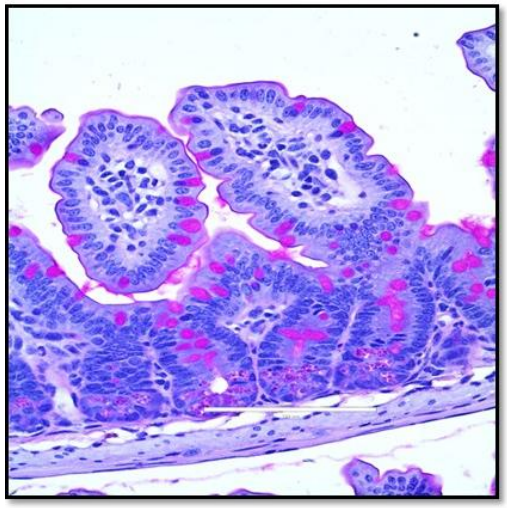

Figure 3.2d

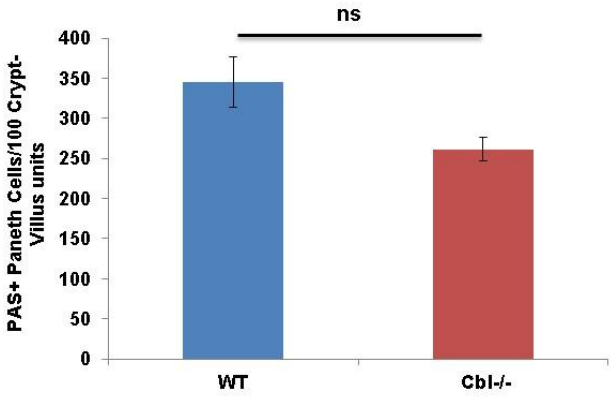

Figure 3.2e

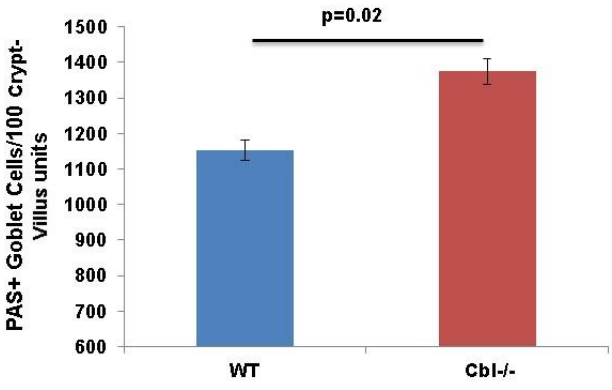

Figure 3.2f

Figure 3.2g

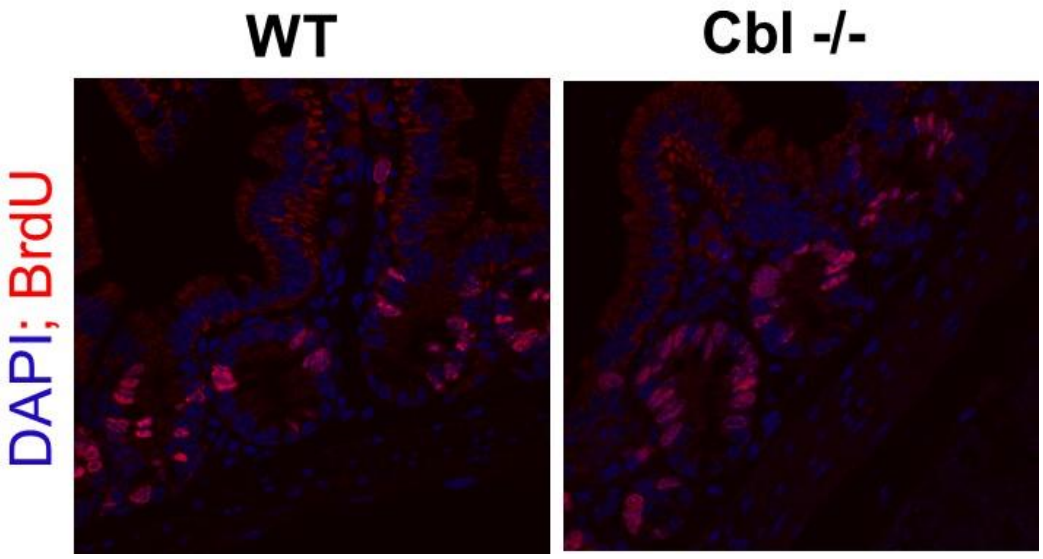

Figure 3.2h

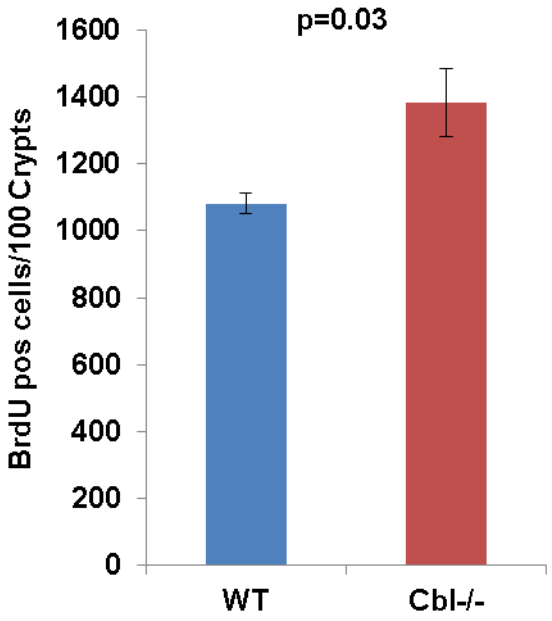

Based on the relative expression of GFP researchers can study not just stem cells (GFP high expressors) but also their early progeny in which GFP has not yet completely decayed (GFP low expressors). Introduction of floxed Cbl and null Cbl-b alleles into Lgr5-GFP-CreERT2 mice allowed us to monitor self-renewal of Lgr5+ stem cells by tracking GFP expressing cells. In addition, inserting R26-Lox-Stop-Lox-LacZ reporter allele into these mice allowed us to not only track deletion of Cbl but also perform lineage tracing of Lgr5+ stem cells in which activation of Cre had taken place. **Figure 3.3a** shows the all the alleles introduced into our experimental mouse model. To perform experiments on these mice, we injected them with 2 mg of tamoxifen (TAM) mixed in sunflower oil intraperitoneally for three consecutive days and analyzed them at various time points indicated in **Figure 3.3b**. Also mentioned in **figure 3.3b** are the genotypes used in the following experiments. In order to validate correct workings of our mouse model, 72 hours after the last injection, we sorted live epithelial cells into two fractions based on their relative expression of GFP namely Hi (GFP-high) and Lo (GFP-low) in addition to sorting GFP negative (GFP^{-ve}) fraction which could potentially represent differentiated progeny that had lost GFP expression and performed qPCR for Cbl and Cbl-b in WT and inducible DKO (iDKO) mice (**figure3.3. c-d**). This experiment showed that relative to GFP^{-ve} cells in the WT mice, Cbl and Cbl-b were both most highly expressed in the GFP-Hi cells and tamoxifen treatment was successful in deleting Cbl within the Lgr5 compartment. Deletion of Cbl was also confirmed by performing IHC for the same proteins (**figure3.3 e**). As was seen in the qPCR analysis, expression of Cbl was not completely gone and this was because while half of the crypts showed loss of CBL, the expression remained intact in the other half of the crypts. This is in accordance with the published reports of the CreERT2 construct of Lgr5 being epigenetically silenced in about half of the crypts (13).

Figure 3-3 Generation and validation of stem cell specific Cbl/Cbl-b iDKO mouse model.

Schematic shows targeted alleles used to generate conditional DKO animals (**a**). Conditional deletion of floxed Cbl alleles on a Cbl-b null background in Lgr5+ cells is carried out by using TAM inducible Lrg5-CreERT2. R26-LSL- LacZ is used as a reporter. Schematic of experimental plan followed and genotypes used (**b**). Tamoxifen induced mosaic deletion of Cbl demonstrated by IHC and real time PCR while Cblb is constitutively knocked out (**c-e**). Experiments shown in figure 3.3 c-e were repeated three times.

Figure 3.3a

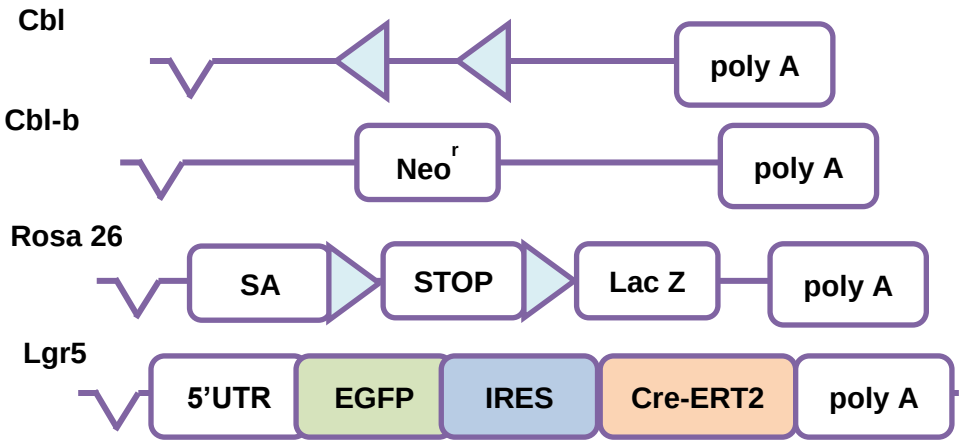

Figure 3.3b

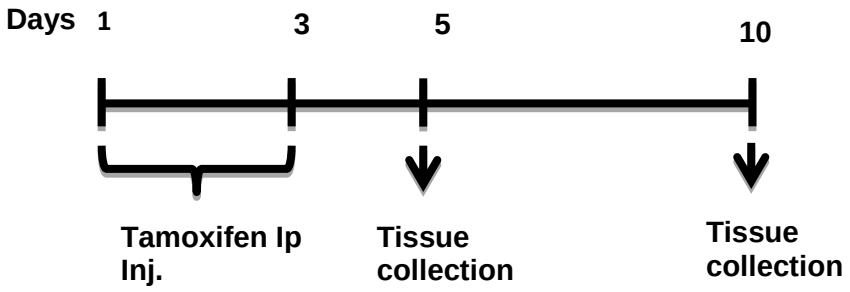

Control Genotype/ WT: Cbl+/+; Cblb+/+; Lgr5Cre+ve; R26-LSL-LacZ+

Experimental/DKO Genotype: Cbl f/f; Cblb-/-; Lgr5Cre+ve; R26-LSL-LacZ+

Figure 3.3c

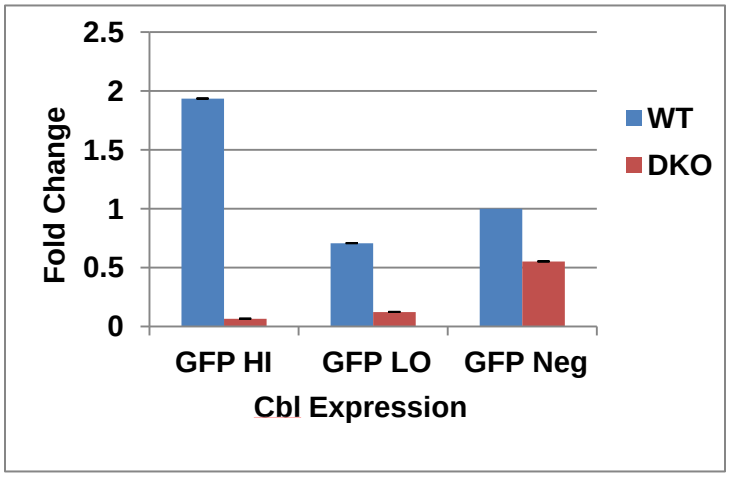

Figure 3.3d

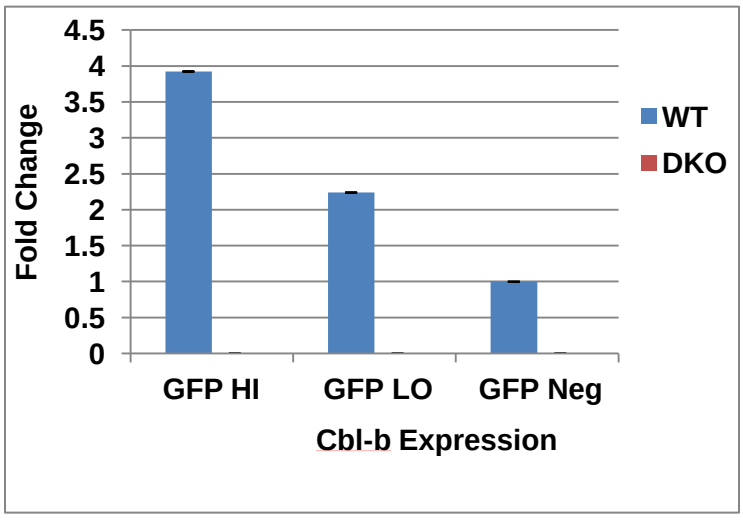

Figure 3.3e

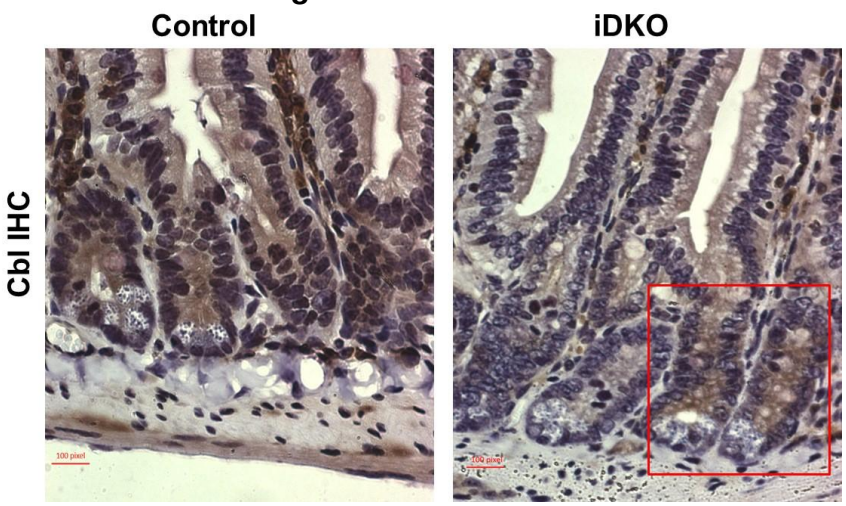

3.4 iDKO mice show increased proliferation with no alteration in apoptosis

WT and iDKO animals were subjected to TAM injection as mentioned above. On 5th and 10th day after treatment mice were injected with 2mg of BrdU and analyzed for proliferation changes. There was a significant increase in proliferating cells in iDKO vs WT after 5d of Cbl/Cbl-b loss and the trend looked similar at 10d after TAM (**figure3.4 a-f**). In order to assess any changes in cell death, tissue sections from mice of both genotypes were stained with cleaved caspase 3 antibody. No significant difference was observed in the number of apoptotic cells in WT vs iDKO (**figure3.4 g-k**).

3.5 iDKO mice show expansion of progenitor population at the expense of Lgr5+ stem cells

To study the function of CBL proteins in the maintenance of stem cells we analyzed the impact of their loss on the percentage of GFP expressing Lgr5+ cells. For this experiment, crypts were isolated and dissociated into single cells from WT and iDKO mice after 5 and 10 days of induction. Single cells were subjected to flow cytometric analysis according to gating strategy delineated in **figure 3.5 a-h**. We found that at 5 days after TAM induction there was a significant reduction in the number of GFP Hi stem cells and a concomitant increase in the number of GFP Lo progenitor cells (**figure3.5 a-d**). **Figure 3.5 e-h** shows unstained and single stained controls for one representative experiment done at 5 days after TAM. A similar trend of reduction of GFP Hi cells and increment in GFP Lo cells was observed at day 10 after TAM treatment (**figure3.5 i-j**). Combining experiments from 4 independent experiments we found that there was a significant reduction in the percent GFP Hi Cells and an increase in GFP Lo cells at both the time points (**figure3.5 k-n**). Together with the proliferation analysis, this interesting observation pointed towards increased commitment towards differentiation in the iDKO

Lgr5+ stem cells. This loss of stem cells was however temporary, as progenitor population de-differentiated to give rise to GFP+ stem cells when analyzed at 2 months after TAM (**figure 3.5 o**).

Figure 3-4 iDKO animals show increased proliferation with no change in apoptosis.

BrdU staining after short pulse showed significant increase in commitment to S phase of cell cycle after 5 days and 10days of TAM treatment (**a-f**). Cleaved caspase 3 immunostaining revealed no change in number of dead cells in WT vs iDKO at 10d time point. Each experimental time point was repeated three times.

5d Time Point

Figure 3.4a **Figure 3.4b**

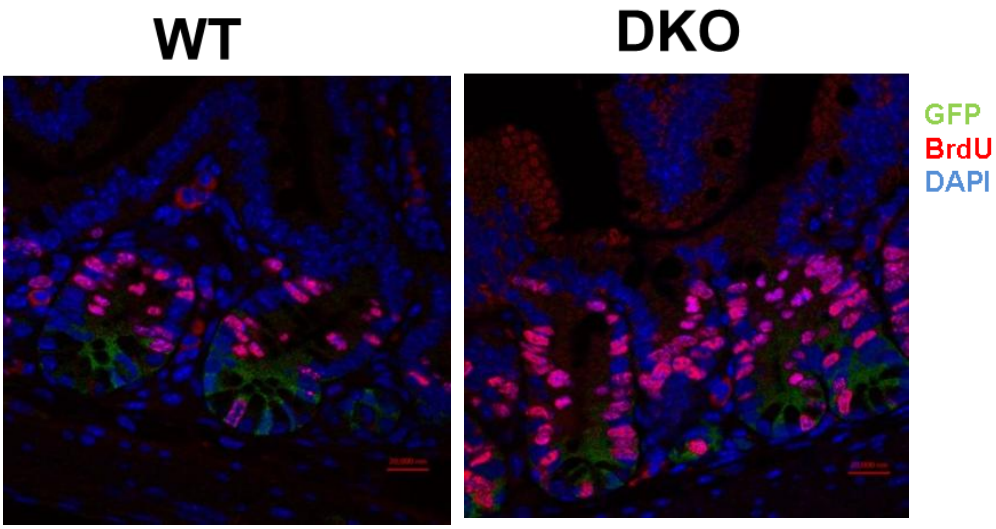

Figure 3.4c

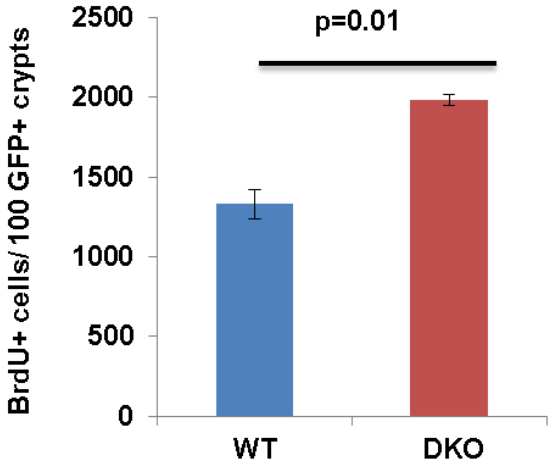

10d Time Point

Figure 3.4d **Figure 3.4e**

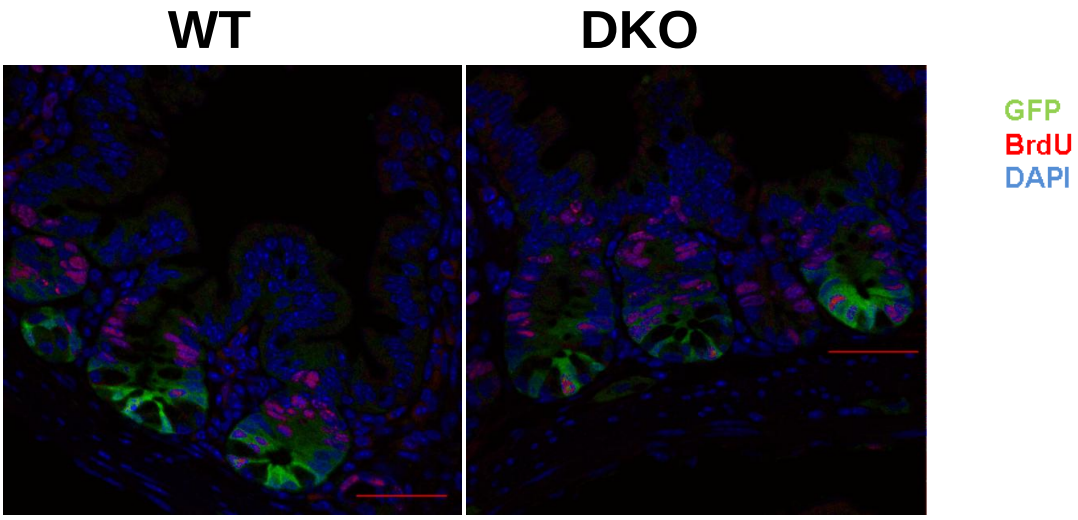

Figure 3.4f

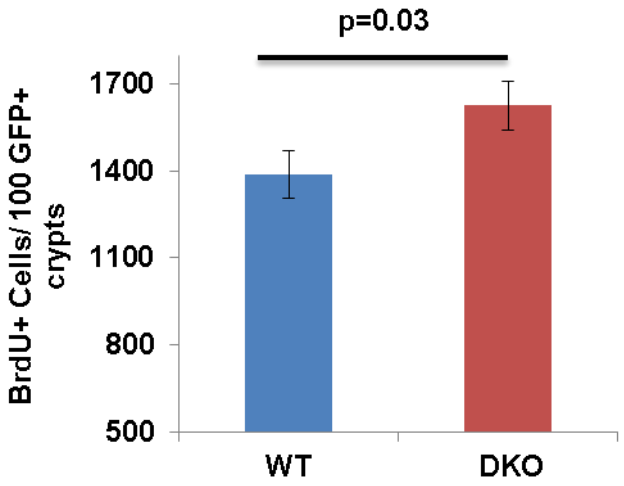

Figure 3.4g

Figure 3.4h

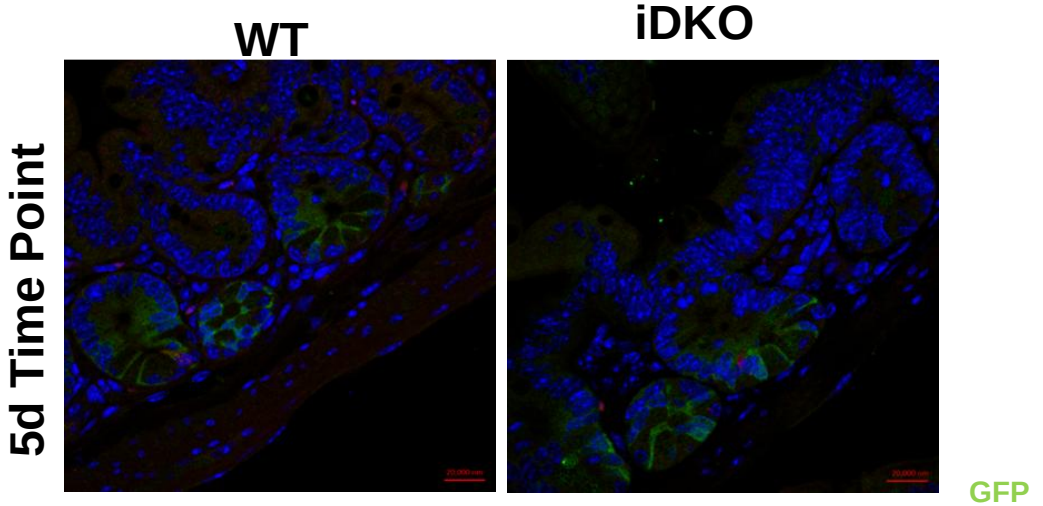

Figure 3.4i

Figure 3.4j

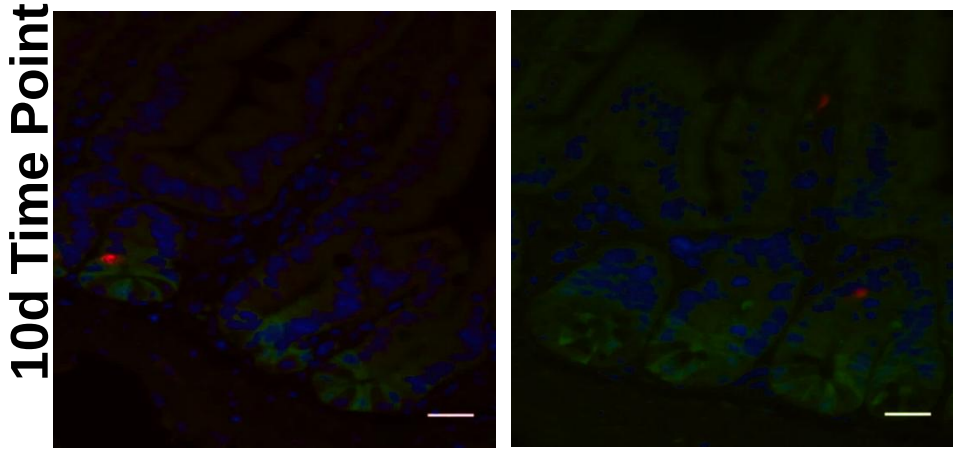

Figure 3.4k

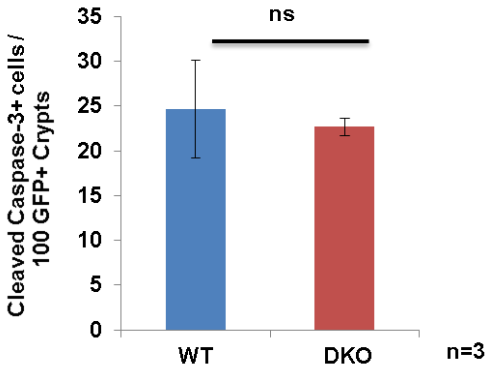

Figure 3-5 Loss of Cbl/Cbl-b coerces stems cell to undergo exhaustion.

Flow cytometric analysis of live epithelial cells showed a significant expansion of Lgr5-GFP Lo (progenitor) cells and a concomitant decrease in Lgr5-GFP Hi (stem cells) at 5 days (**a-d; k-l**) and 10 days (**i-j; m-n**) after TAM induction in iDKO mice vs. WT. Unstained and single stained controls are shown to delineate the gating strategy followed (**e-h**). This loss of stem cells is overcome once the effect of TAM subsides as analyzed here at 60d after treatment (**o**) exemplifying the plasticity within the crypt. Each time point was repeated four times.

Figure 3.5a

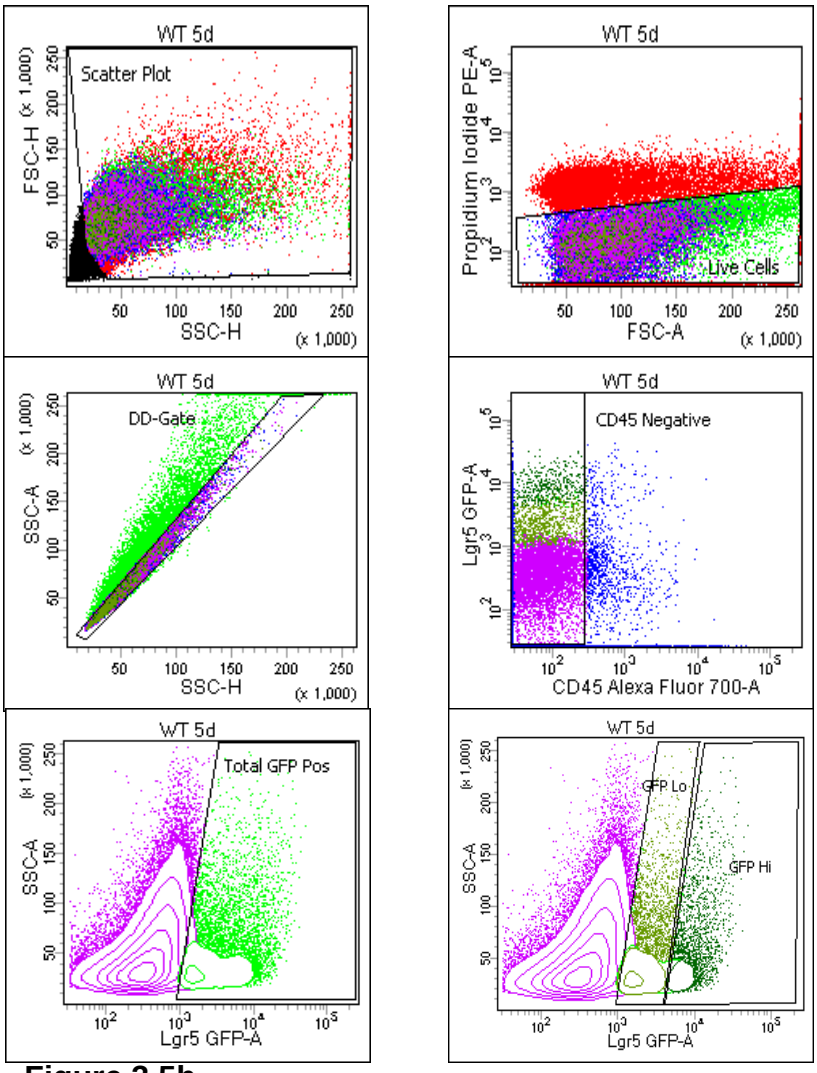

Figure 3.5b

Tube: WT 5d

Population	#Events	%Parent	%Total
All Events	361,345	###	100.0
Scatter Plot	240,442	66.5	66.5
Live Cells	119,610	49.7	33.1
DD-Gate	83,809	70.1	23.2
CD45 Negative	34,964	41.7	9.7
Total GFP Pos	5,717	16.4	1.6
GFP Hi	1,960	34.3	0.5
GFP Lo	3,538	61.9	1.0

Figure 3.5c

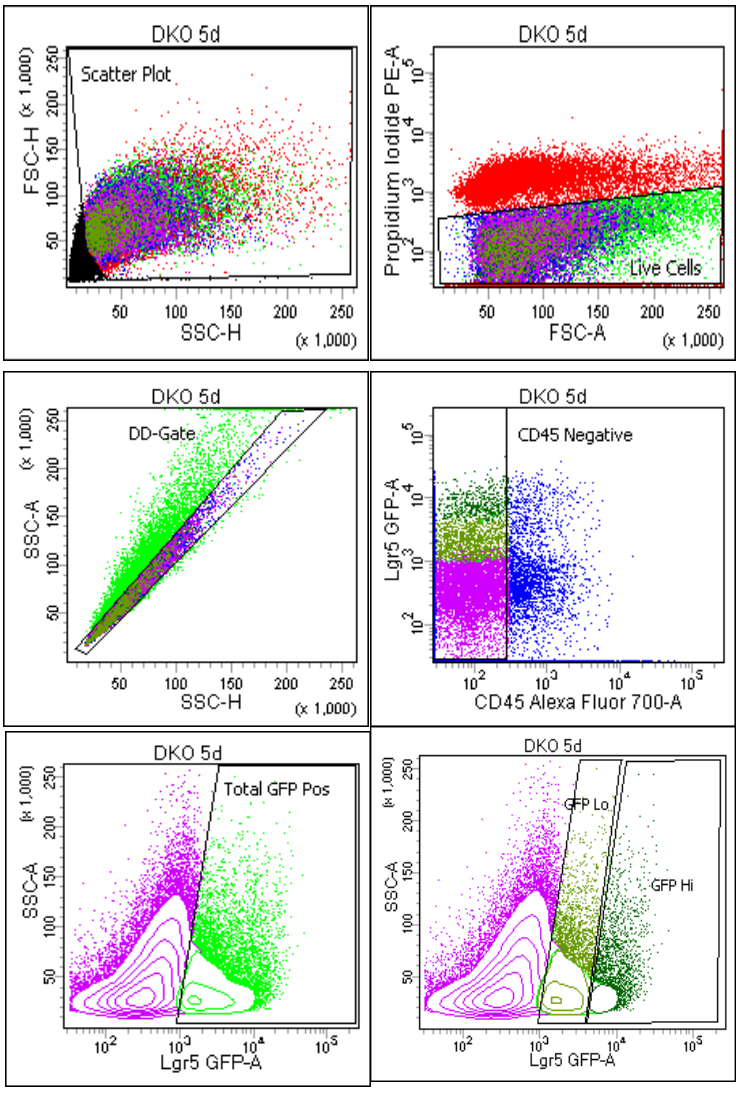

Figure 3.5d

Tube: DKO 5d

Population	#Events	%Parent	%Total
All Events	383,807	####	100.0
Scatter Plot	286,453	74.6	74.6
Live Cells	131,516	45.9	34.3
DD-Gate	95,167	72.4	24.8
CD45 Negative	43,235	45.4	11.3
Total GFP Pos	9,084	21.0	2.4
GFP Hi	2,430	26.8	0.6
GFP Lo	6,279	69.1	1.6

Figure 3.5e-h

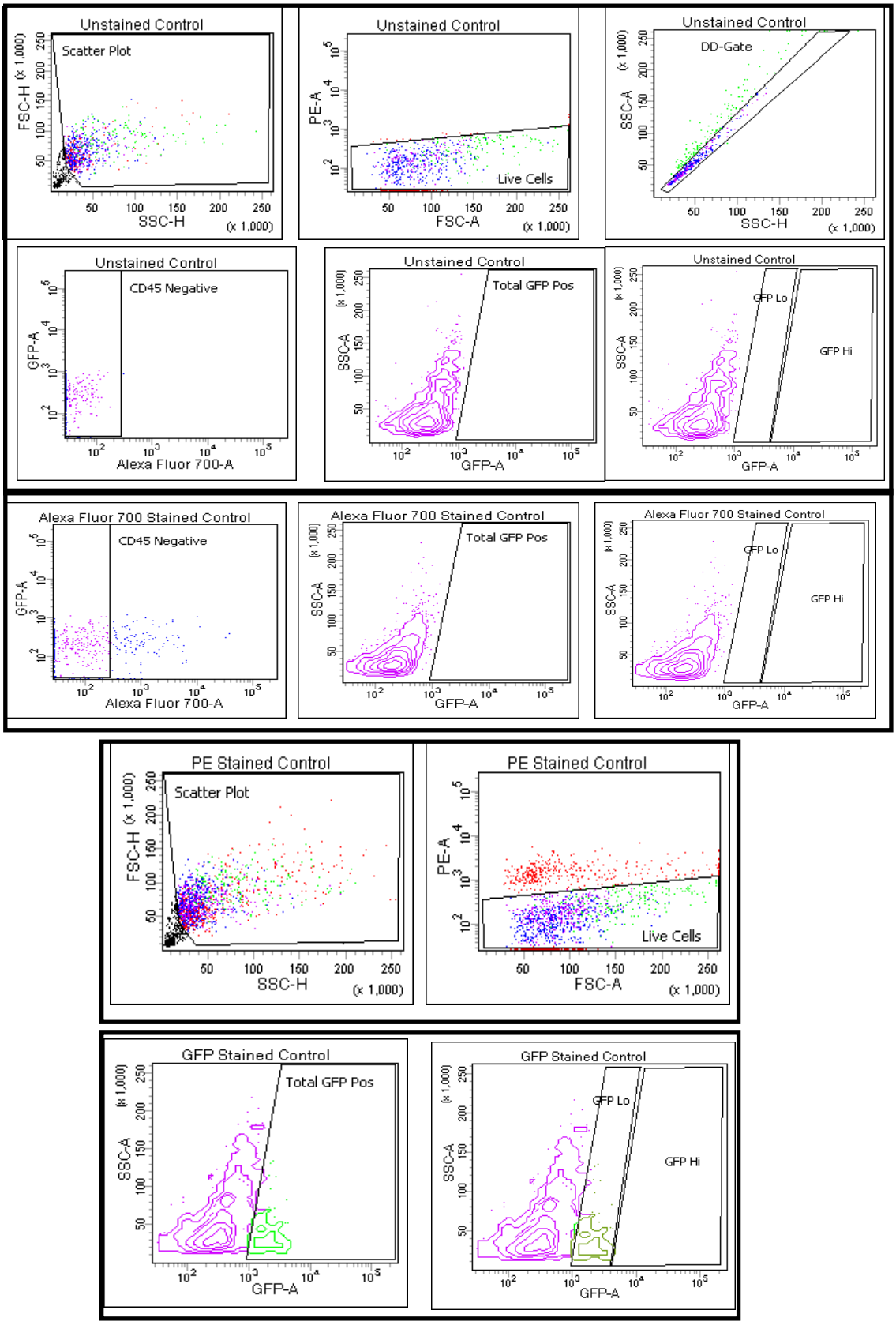
Unstained Control
Scatter Plot
FSC-H (x 1,000)
SSC-H (x 1,000)
Unstained Control
Live Cells
PE-A
FSC-A (x 1,000)
Unstained Control
DD-Gate
SSC-A
SSC-H (x 1,000)
Unstained Control
CD45 Negative
GFP-A
Alexa Fluor 700-A
Unstained Control
Total GFP Pos
SSC-A (x 1,000)
GFP-A
Unstained Control
GFP Lo
GFP Hi
SSC-A (x 1,000)
GFP-A
Alexa Fluor 700 Stained Control
CD45 Negative
GFP-A
Alexa Fluor 700-A
Alexa Fluor 700 Stained Control
Total GFP Pos
SSC-A (x 1,000)
GFP-A
Alexa Fluor 700 Stained Control
GFP Lo
GFP Hi
SSC-A (x 1,000)
GFP-A
PE Stained Control
Scatter Plot
FSC-H (x 1,000)
SSC-H (x 1,000)
PE Stained Control
Live Cells
PE-A
FSC-A (x 1,000)
GFP Stained Control
Total GFP Pos
SSC-A (x 1,000)
GFP-A
GFP Stained Control
GFP Lo
GFP Hi
SSC-A (x 1,000)
GFP-A

Figure 3.5i

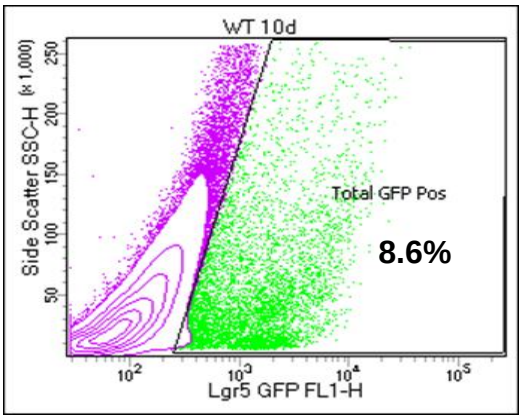

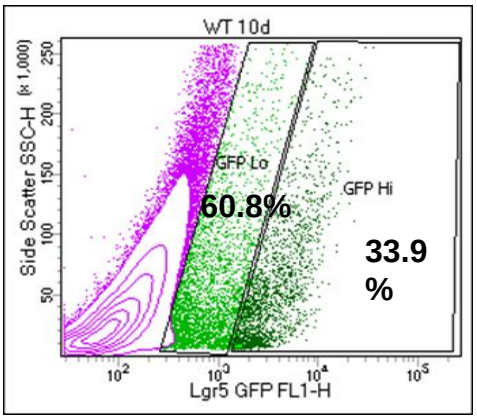

Figure 3.5j

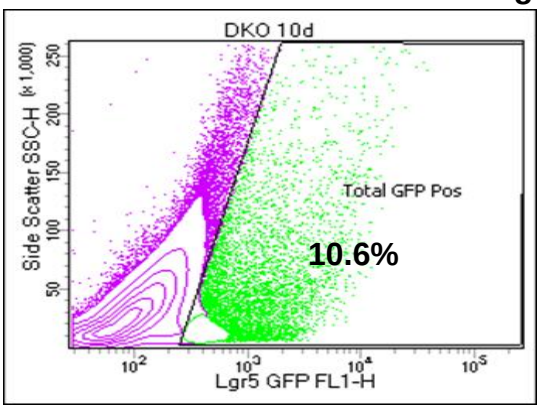

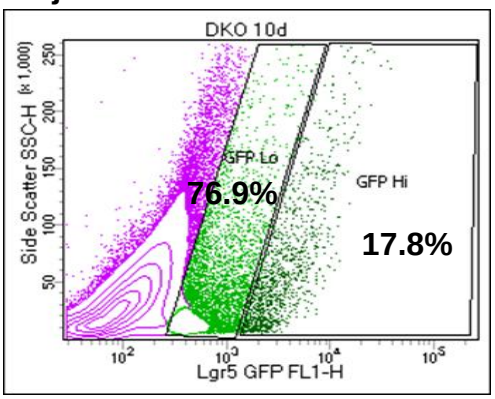

5d Time Point

Total GFP positive cells

Figure 3.5k

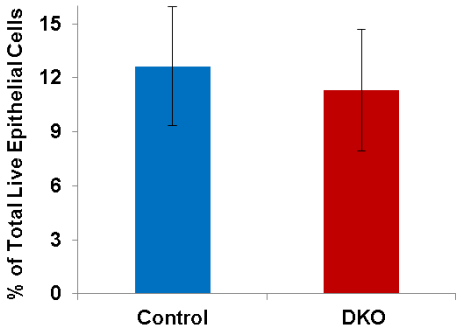

Figure 3.5l

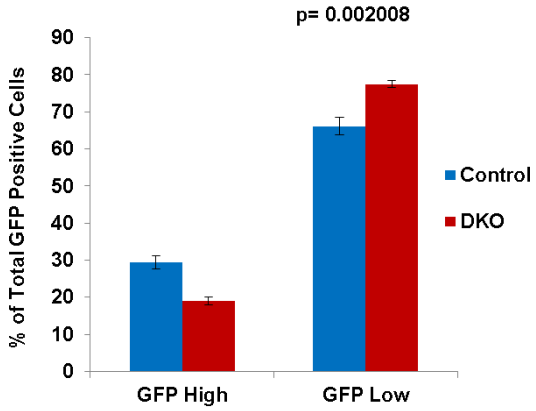

10d Time Point

Total GFP positive cells

Figure 3.5m

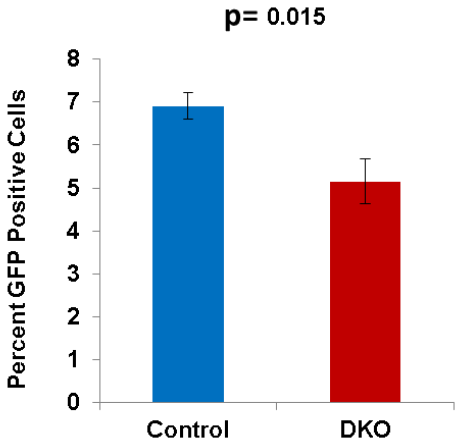

Figure 3.5n

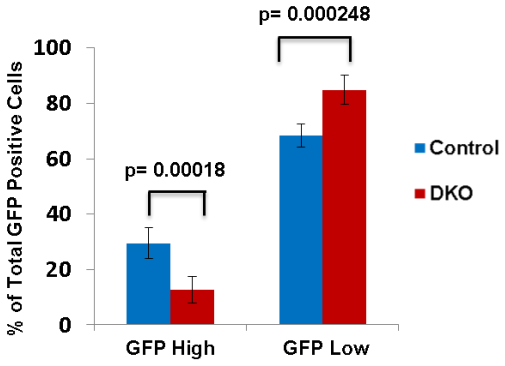

Figure 3.5o

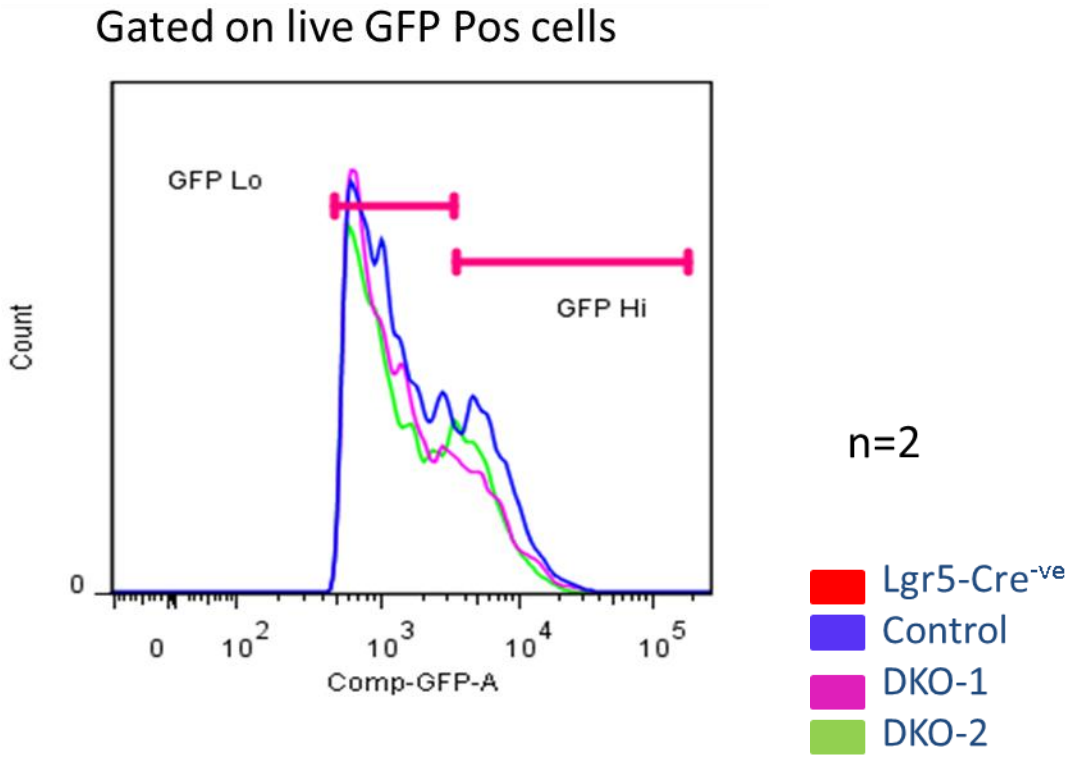
Gated on live GFP Pos cells
GFP Lo
GFP Hi
Count
0
0
10^2
10^3
10^4
10^5
Comp-GFP-A
n=2
Lgr5-Cre-ve
Control
DKO-1
DKO-2

3.6 Loss of Cbl/ Cbl-b promotes commitment to differentiation

Since the GFP analysis revealed that there was an increase in Lgr5-GFP Lo progenitor population and with no change in cleaved caspase 3+ apoptotic cells in the crypt, we suspected that these iDKO progenitors must be moving towards a more committed fate. To probe this further, we performed lineage tracing of iDKO and WT Lgr5+ cells by analyzing the expression pattern of β-galactosidase (LacZ) expressed under ubiquitous Rosa26 promoter. Upon TAM induction, removal of the stop cassette flanked by LoxP sites by Cre-recombinase expressed in the Lgr5+ cells allows transcription and translation of LacZ not only in the recombined stem cells but also in their progeny. Using this strategy we found that at 5 d and 10 d time points there was an increase in blue X-gal (substrate of LacZ) staining in the crypts and villi (**figure3.6 a-d**). Quantitative analysis of these data showed that there was an increase in the partially blue and completely blue crypts but a reduction in the crypts with a single blue cell at 10 d time point (**figure3.6 e-f**). This single stained LacZ+ cell most likely represents the Lgr5+ quiescent secretory progenitor cell (36, 37, 219). This finding was particularly interesting because in the literature, the quiescent secretory progenitor is responsible for repopulating IESC upon damage to the latter (36, 37, 219). However, in the absence of CBL proteins it appeared that these quiescent secretory cells may have also differentiated. Markers for this pool of quiescent progenitor cell are DLL1 (Delta like ligand 1) and Ngn3 (Neurogenin 3) (37, 38, 87). Real-time PCR revealed that there was a reduction in the expression of these markers in the Lgr5-Hi fraction after 5 days of TAM confirming the LacZ findings (**figure3.6g, h**). Percentage of DLL1 expressing GFP+ cells was further assessed after 10d TAM treatment using flow cytometry. Overall, the loss of CBL proteins seemed to have directed stem as well as quiescent progenitor cells towards differentiation.

Figure 3-6 Lineage tracing reveals increased commitment to differentiation in iDKO mice.

X-Gal staining showed increased commitment to differentiation in iDKO mice at 5 (**c**) and 10 (**d**) days post TAM induction as compared to WT mice (**a-b**). Quantitative analysis of the staining showed increase in the percentage of whole and partially blue crypts but a reduction in crypts with single blue cell, representative of the quiescent Lgr5 compartment (**e-f**). To confirm the loss of quiescent progenitor population, real-time PCR showed a reduction in both DLL1 and Neurogenin3 secretory progenitor markers (**g-h**). Flow cytometric analysis of GFP+ DLL1+ cells at 10d after TAM induction showed a precipitous drop in iDKO vs. WT (**i**). Experiments shown in figure 3.6 a-d were repeated 4 times per time-point. Real-time PCR analysis in figure 3.6 was repeated 2 times. Flow analysis for GFP/ DLL1 dual positive cells was repeated twice.

Figure 3.6a

Figure 3.6c

WT

DKO

5 Days Induction

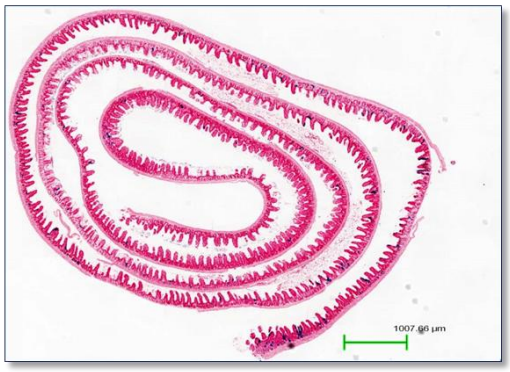

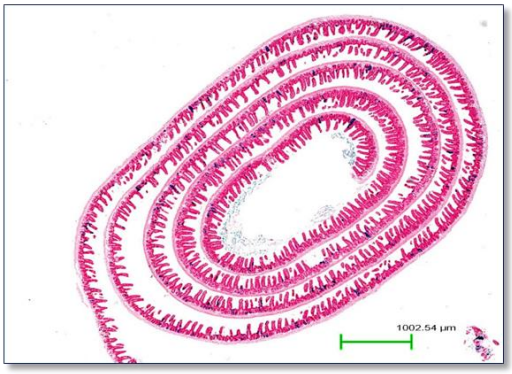

Figure 3.6b

Figure 3.6d

10 Days Induction

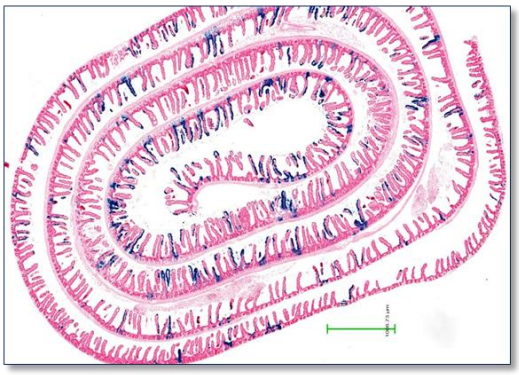

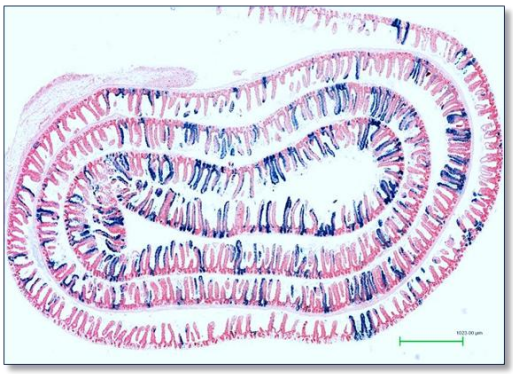

Figure 3.6e

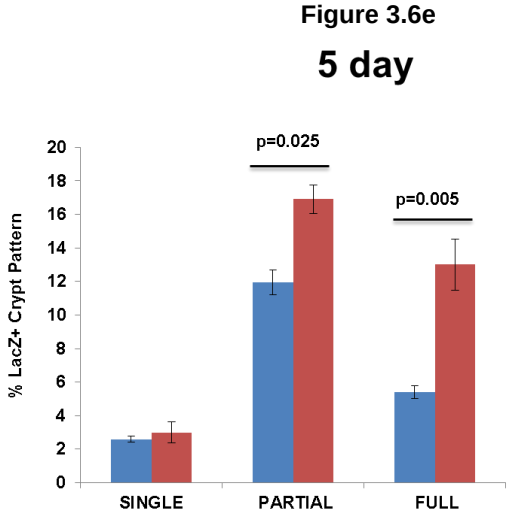

Figure 3.6f

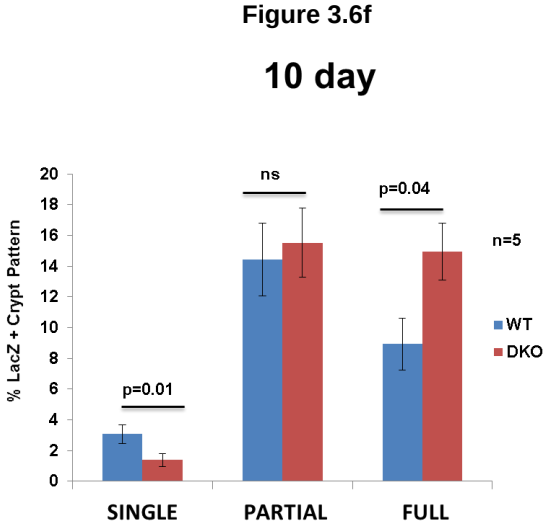

Figure 3.6g

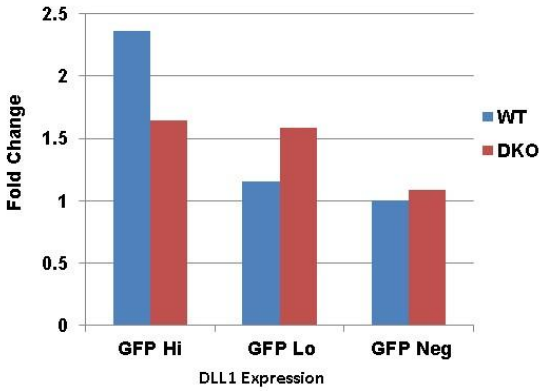

Figure 3.6h

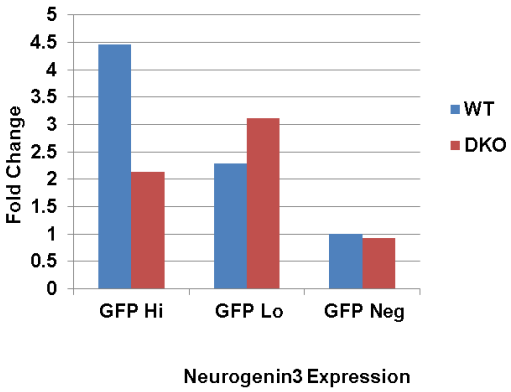

Figure 3.6 i

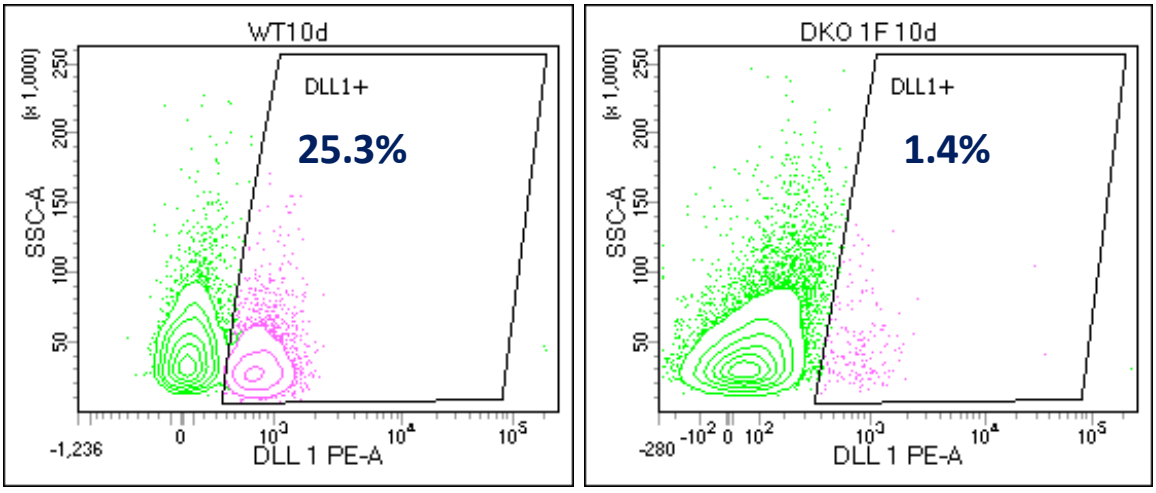

3.7 iDKO mice show goblet cell hyperplasia at the cost of Paneth cells.

Epithelial lining of the intestine is comprised of multiple functional cell types, most abundant of which are enterocytes. Indeed we found an increase in expression of alkaline phosphatase (ALPI) mRNA, a marker of enterocytes (**figure3.7a**).

Of the secretory lineage of cells, iDKO mice showed a significant increase in the number of LacZ-PAS dual+ goblet cells and a concomitant reduction in the number of LacZ-PAS dual + Paneth cells (**figure3.7b-d**). Co-staining of LacZ and ChromograninA revealed no significant difference in the number of enteroendocrine cells (**figure3.7e-g**). Thus, loss of CBL proteins skewed stem cell differentiation towards enterocytic and goblet cell fate.

Figure 3-7 iDKO stem cells show increased commitment towards Enterocyte and Goblet cell fate and a reduction in Paneth cells.

After 10 days of TAM induction, PAS and X-gal co-staining in iDKO mice revealed significant increase in commitment to goblet cells with a reduction in Paneth cell (**b-d**) while q-PCR showed increased expression of ALPI in the progenitor and differentiated cells (**a**). IHC of ChromograninA+ enteroendocrine cells on X-gal stained sections showed no difference in their number (**e-g**). These experiments were repeated four times.

Figure 3.7a

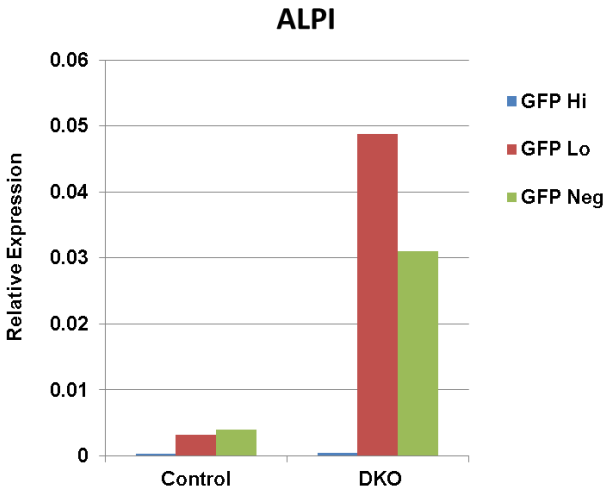

Figure 3.7b

Figure 3.7c

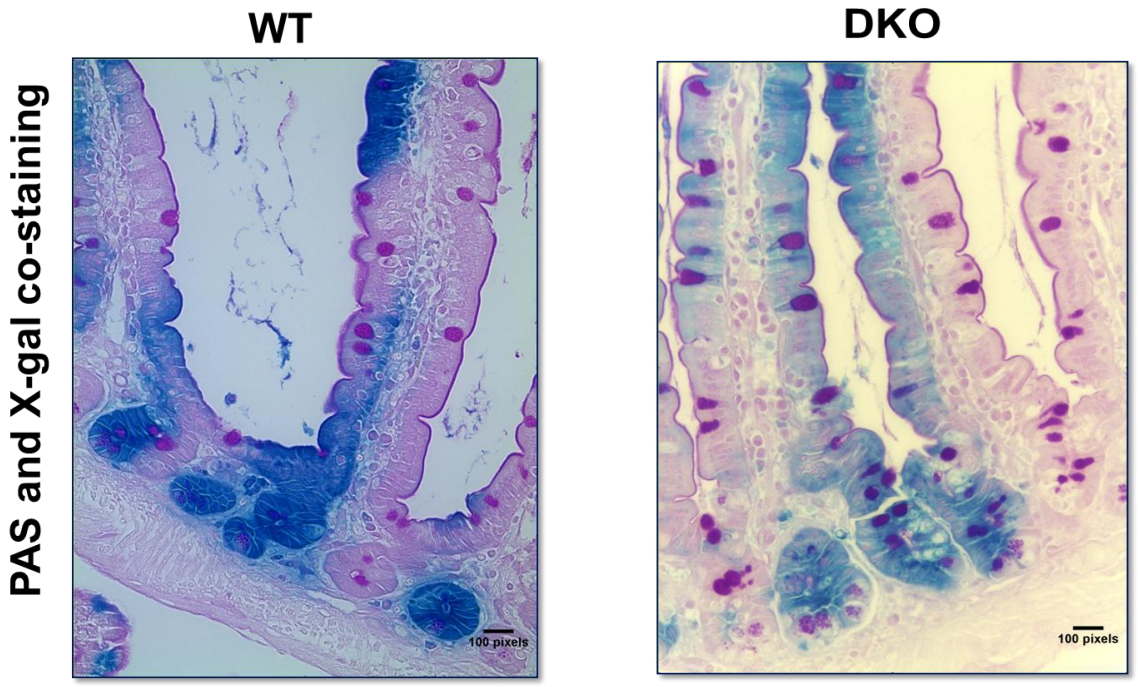

Figure 3.7d

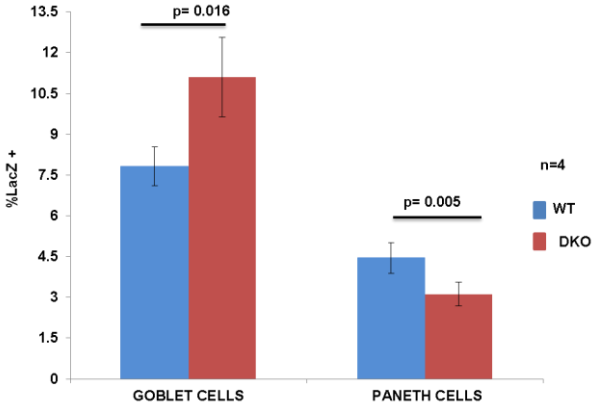

ChromograninA LacZ Co-staining

Figure 3.7e

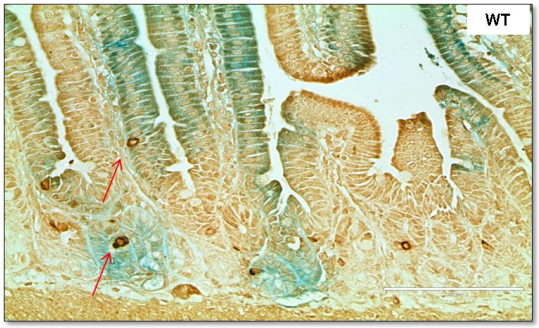

Figure 3.7f

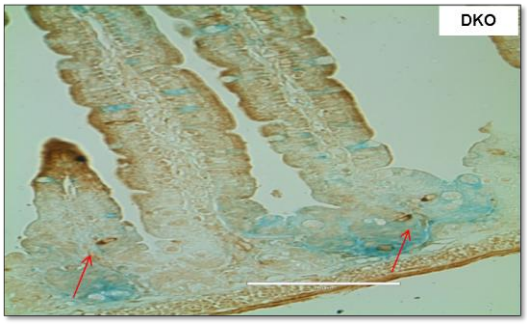

Figure 3.7g

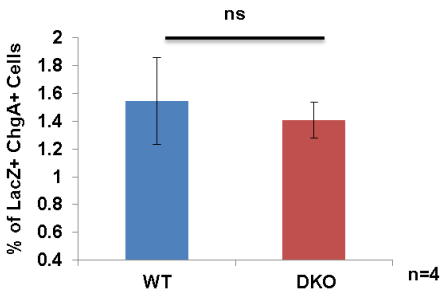

3.8 DKO mice show delayed recovery of injured mucosa in abdominal radiation model

Regeneration of lost cells in the intestinal epithelium under normal homeostasis is extremely important to maintain the epithelial barrier that prevents potential pathogens to infiltrate internal organs of our body. This process becomes even more crucial in case of mucosal insults such as exposure to radiation. Radiation induces cell death of proliferating cells by introducing double stranded breaks into the genetic material of these cells and because stem and absorptive progenitor compartment of the gut are both cycling in nature, it is one of the most severely affected organs by this kind of injury. Under these circumstances, the quiescent secretory progenitor is thought to re-enter the cell cycle and regenerate lost stem cells that can then take over the process of establishing epithelial homeostasis again.

Most studies subject mice to whole-body radiation, however, this treatment severely compromises their bone marrow resident hematopoietic stem cells and they die at moderate to high doses of 10-12Gy because of hematopoietic complications (220). In order to understand the ability of iDKO Lgr5+ stem and progenitor compartment to differentiate and repopulate the epithelia following injury damage, we subjected experimental and control mice to 14 Gy of abdominal radiation to kill a majority of the proliferating Lgr5+ stem cells. Because of the mosaic expression of Lgr5-Cre, we chose a particularly high dose of radiation so that we could reduce regeneration from Cre negative crypts. Abdominal radiation has been used by few researchers to avoid hematopoietic toxicity and effectively target gut epithelium with 100% recovery of the animals due to re-establishment of epithelia by the gut stem cells (221). To perform abdominal radiation, we subjected anesthetized mice to CT scanning using the simulation CT scanner located in the Radiation Oncology Department at the University of

Nebraska Medical Center. The CT images were then used to identify the radiation target (small and large intestine) and organs at risk (stomach, liver and spleen) and treatment was contoured to avoid hitting anything other than the bowel by radiation (**figure3.8 a, b**).

After the planning, mice received conformal radiation at a dose of 14Gy. WT mice were first used to validate this method. In **figure3.8 c**, we can see that as compared to un-irradiated control mice, at 3 d post radiation, crypts are obliterated in all the regions of the intestine. By day 5, the surviving clones begin the process of repopulation and by day 7 the mice are well on their way to recovery. After validating every step of this treatment plan in our hands, we subjected WT and age matched iDKO to radiation and TAM treatment. The latter was continued for another 2 days and mice were analyzed on the 7^{th} day after radiation. Mice were weighed every day as weight loss is good indicator of mucosal health (221). **Figure3.8 d** shows the treatment plan followed and **figure3.8 e** shows weight loss trends of WT, iDKO and Cbl-b-/- mice. At day 7 iDKO mice showed delayed recovery of injured mucosa as evidenced by blunted villi and various bare crypt-less regions shown in **figure3.8f**. Next, tissue sections from these mice were stained with Ki67 proliferation marker and the average number of surviving crypts (defined as a crypt with at least 5 adjacent Ki67+ cells) was determined (35). **Figure3.8 g-i** shows there was a significant reduction in the surviving crypts in the iDKO mice. **Figure3.8 j-n** shows that the same trend that we observed previously of loss of Lgr5-Hi cells and a moderate increment of Lgr5-Lo cells. Sorting of GFP+ cells and analysis by qPCR for differentiation markers revealed that as compared to the WT animals there was a drop in expression ALPI (marker for enterocytes) and lysozyme (marker for Paneth cells) but an increase in the expression of Muc2 (marker for goblet cells) (**figure3.8 o-q**).

Figure 3-8 iDKO mice show delayed recovery abdominal radiation injury.

CT conformal 14Gy abdominal X-ray radiation treatment was standardized using WT mice which quickly recovered from the mucosal damage (**a-c**). iDKO mice on exposure of the same treatment showed significant delay in recovery from the injury as evidenced by the weight loss, H&E and Ki67 staining (**d-i**). This inability to repopulate injured epithelia coincided with precipitous drop in Lgr5-Hi stem cells in iDKO mice (**j-n**). Differentiation to enterocyte and Paneth cell lineages was also reduced but increase in Muc2 showed the trend towards goblet cell fate differentiation in iDKO at 5 days after TAM (**o-q**). Experiments shown in figures 3.8 d-i were repeated three times. Flow cytometric analysis of stem and progenitor cells was repeated four times (j-n). Real-time PCR was performed once (o-q).

Figure 3.8a **Figure 3.8b**

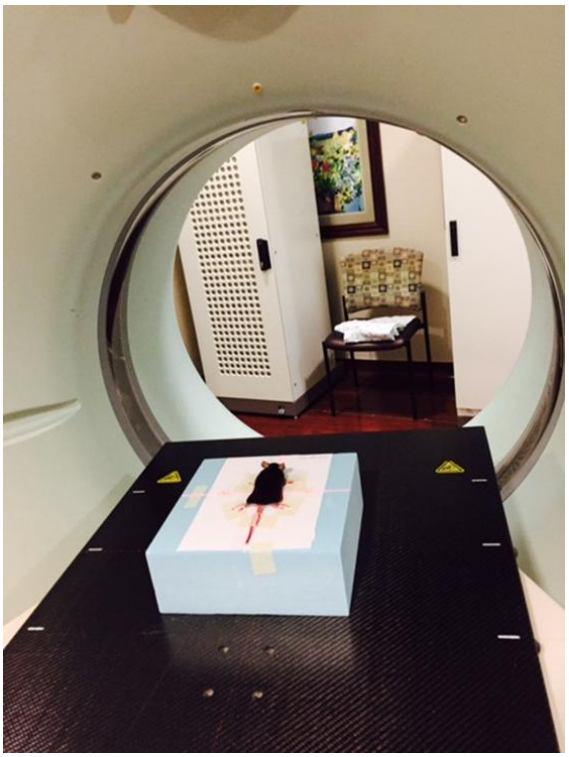

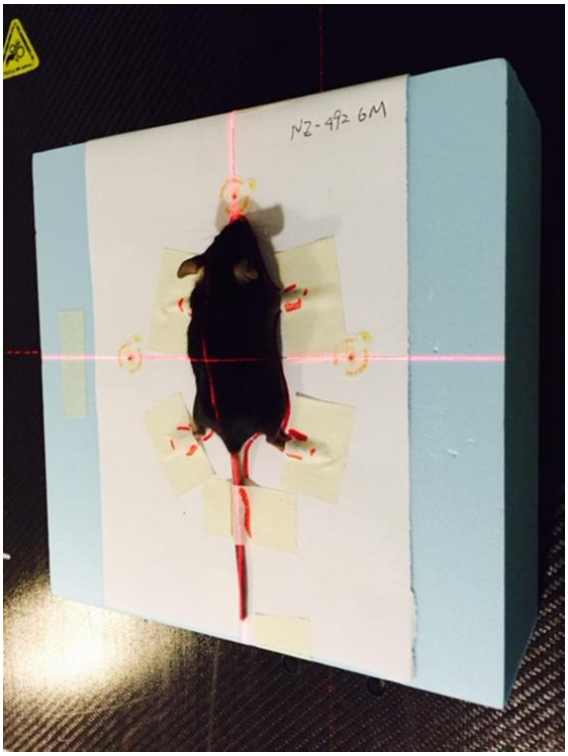

Figure 3.8c

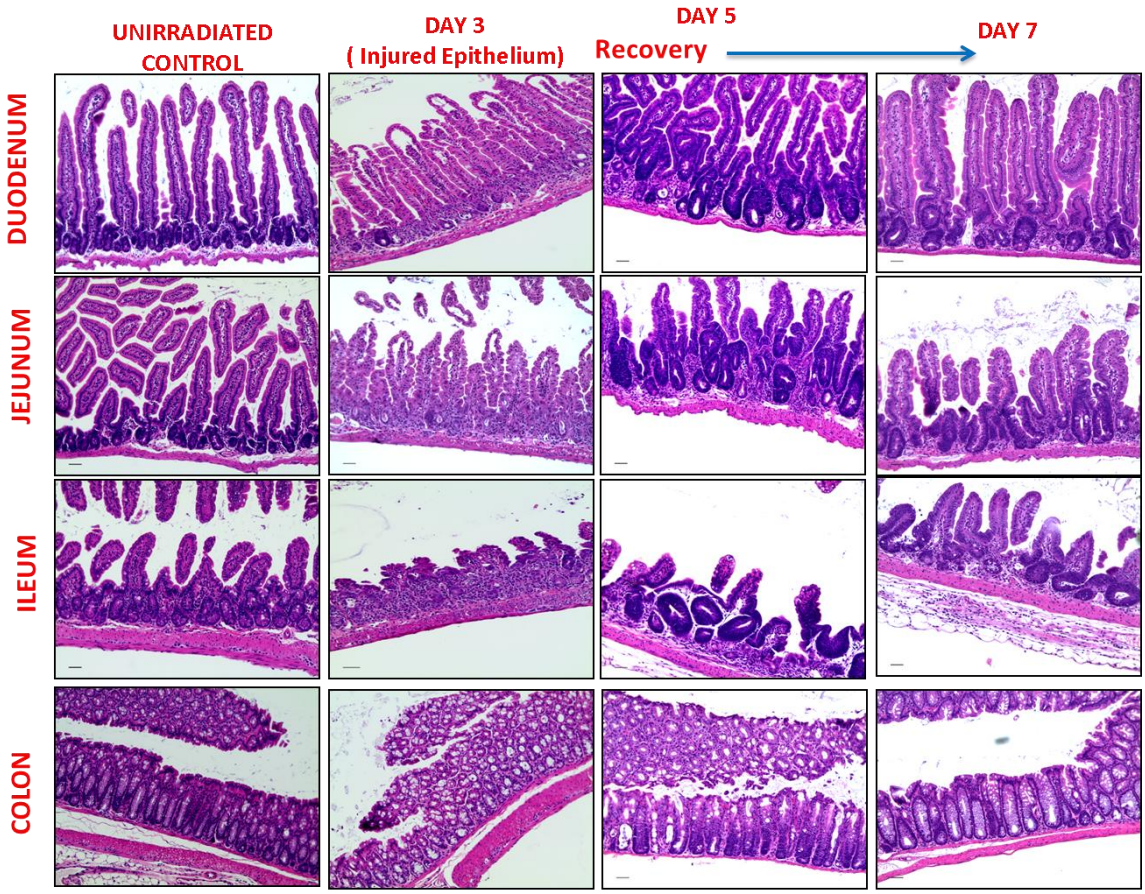
UNIRRADIATED CONTROL
DAY 3 (Injured Epithelium)
DAY 5 Recovery
DAY 7
DUODENUM
JEJUNUM
ILEUM
COLON

Figure 3.8d: Experimental plan

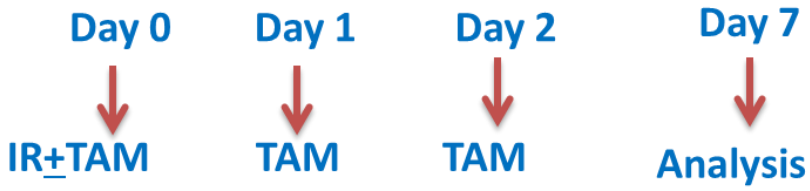

Figure 3.8e

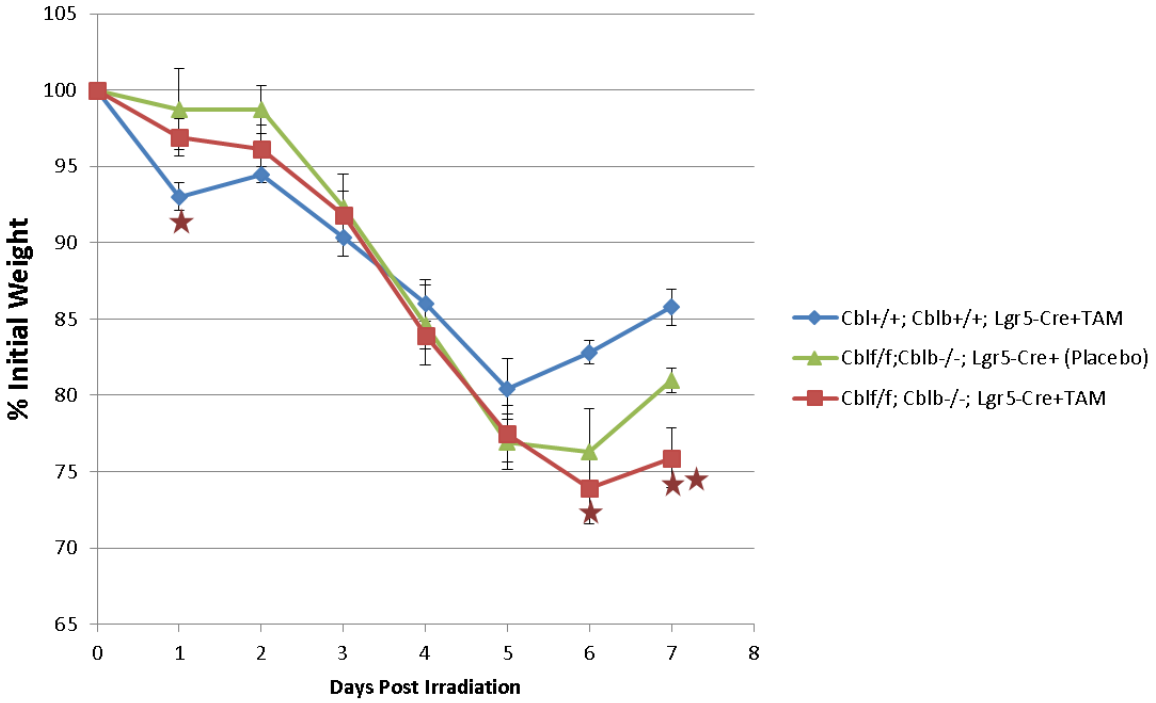

Figure 3.8f

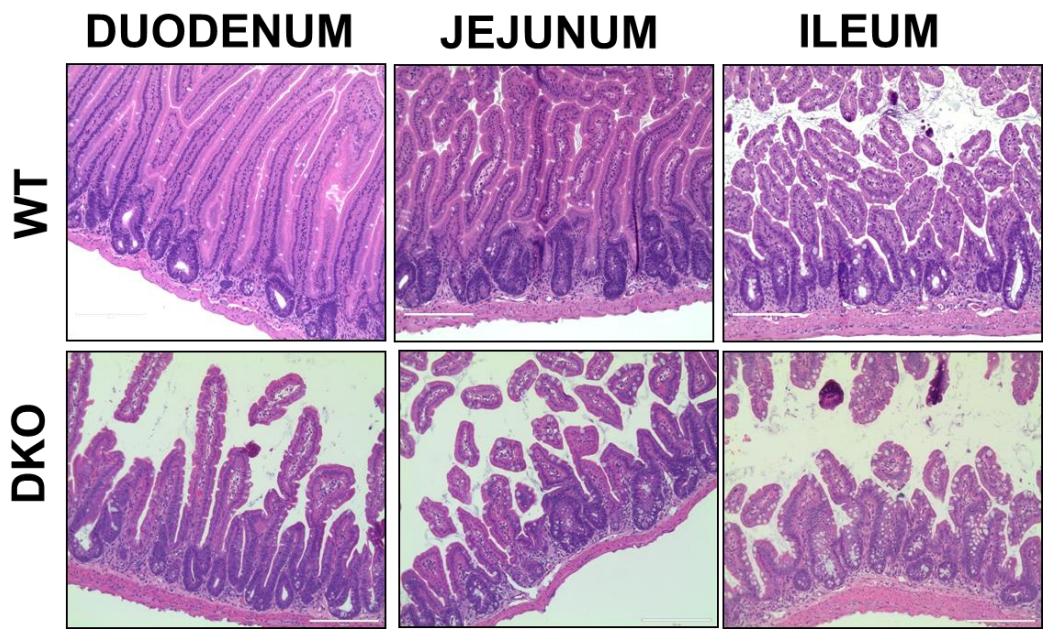

Figure 3.8g

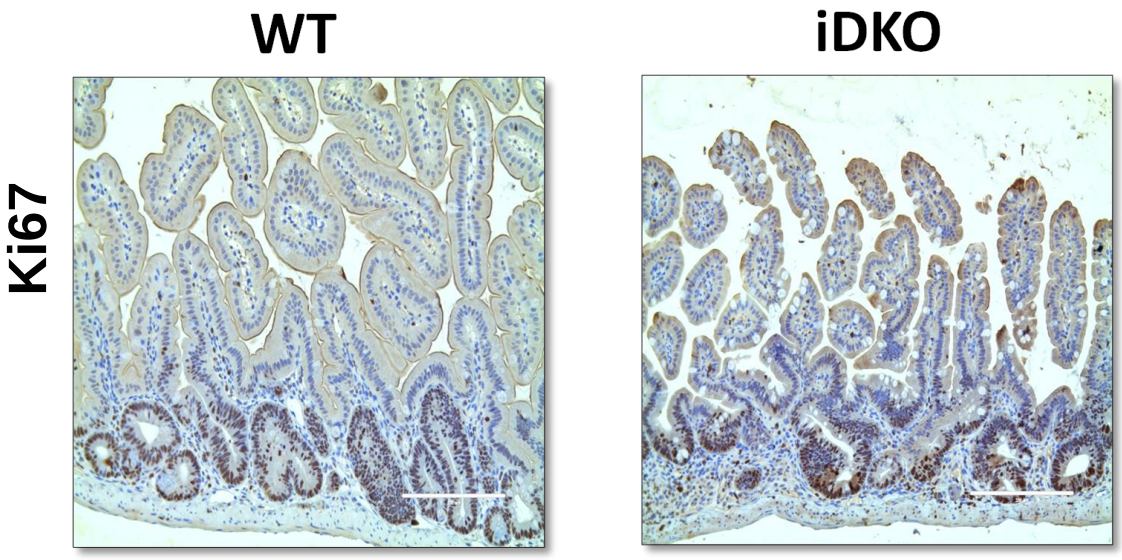

Figure 3.8h

Figure 3.8i

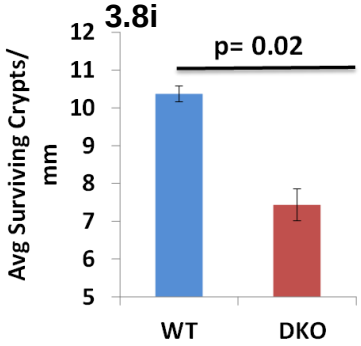

Figure 3.8j

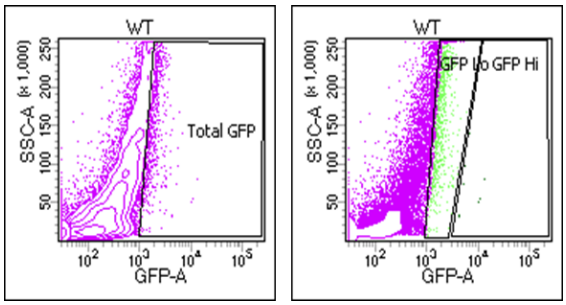

Figure 3.8k

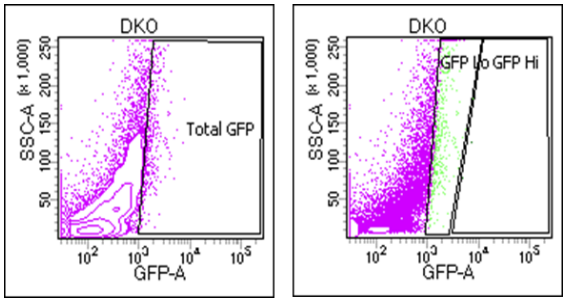

Figure 3.8l

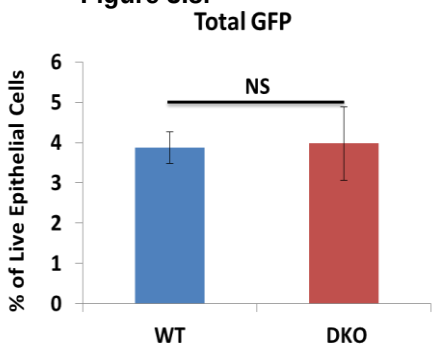

Figure 3.8m

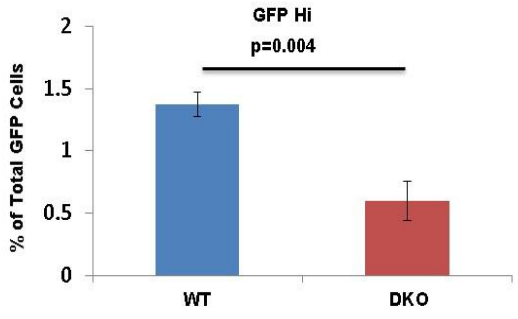

Figure 3.8n

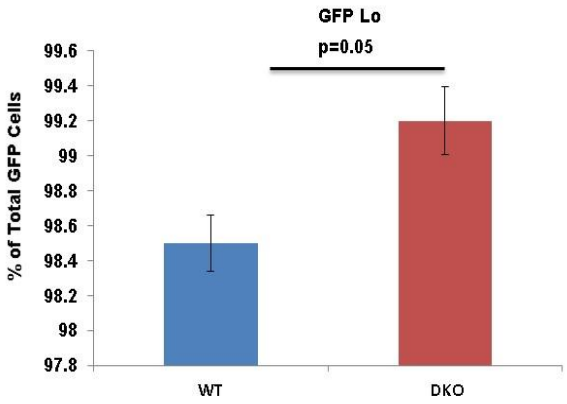

Figure 3.8o

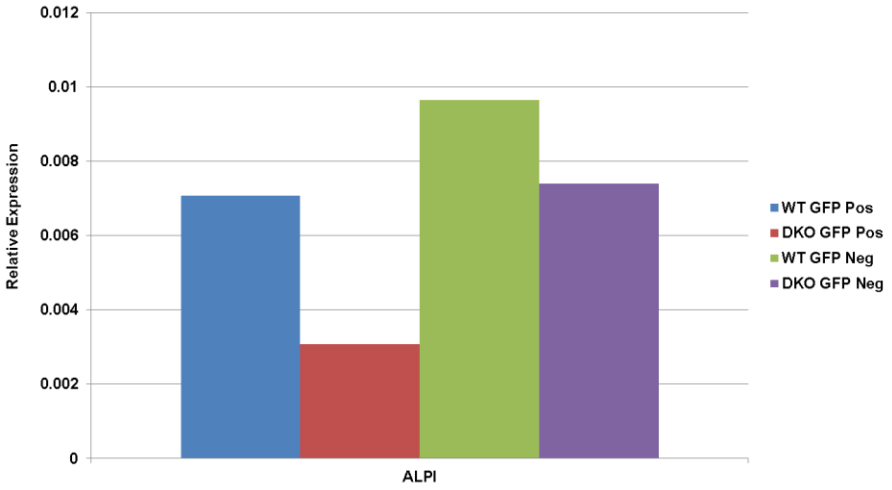

Figure 3.8p

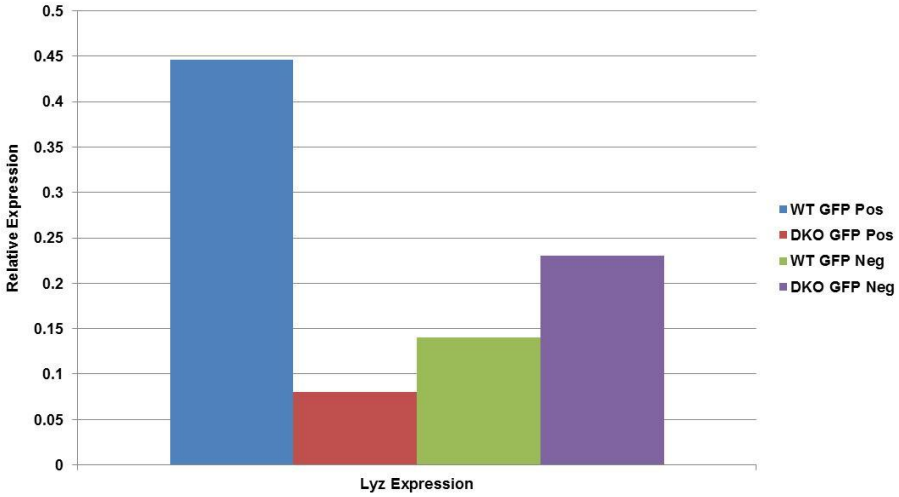

Figure 3.8q

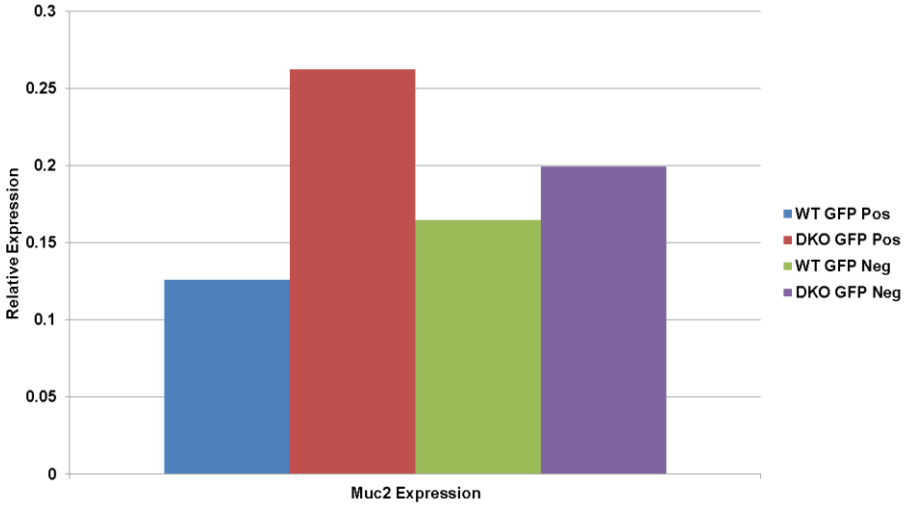

3.9 Inability of iDKO crypts to self-renew prohibits their re-passage in organoid assay

Crypts can be cultured *in vitro* as organoids in the presence of essential growth factors (R-spondin1, EGF and Noggin) and an extracellular matrix material like matrigel (BD Bioscience) (49)(222). Organoids can also be generated from single Lgr5+ stem cells, albeit at a much reduced frequency (222). Because Lgr5-Cre is mosaic in expression, for these experiments we used another mouse model in which both alleles of Cbl and Cbl-b are floxed and they have been bred to TAM inducible Cre expressed under the ubiquitous Rosa26 promoter (**figure3.9a**). We started by isolating the crypts from Cblf/f; Cbl-bf/f (Control) and from Cblf/f; Cbl-bf/f; R26-CreERT+ (Experimental) mice, and embedding them in matrigel with the growth conditions mentioned above. 24 hours after plating we observed that the luminal ends of crypts had sealed off and they looked like tiny balls (**figure3.9b-c**). 3 days after plating, the crypts began budding and after 8 days they had metamorphosed into organoid structures with well-defined crypt regions, connecting villus domains and luminal mass comprising of dying cells (**figure3.9d-i**). After 8 days of initial plating we re-plated these organoids in a split ratio of 1:4 and grew them for another 4 days before introducing 4-hydroxy tamoxifen (4-OH TAM) into the culture to activate the Cre (**figure3.9 j-m**). After 24 and 48 hours of TAM treatment, we found DKO organoids grew more rapidly but by 72 hours after induction they began to deteriorate (**figure3.9 j-m**). Real-time PCR analysis at 72h time point showed reduction in the transcripts of both Cbl and Cbl-b (**figure3.9 n-o**). When the 4-OH TAM treated structures were re-plated for a second passage at a split ratio of 1:4, Control organoids re-created the same 3-dimensional (3-D) structure with intact crypt and villus domain but not a single organoid could be seen in case of DKO (**figure3.9 q-s**). This showed that combined loss of Cbl/Cbl-b coincided with loss of self-renewal in the organoid structures.

Figure 3-9 Loss of CBL proteins reduces the self-renewal potential of iDKO organoids.

We used Cbl; Cbl-b double floxed mice carrying Cre under ubiquitous Rosa26 promoter. For these experiments we cultured Cre negative (Control) and Cre+ (iDKO) mice (**a**). Initial growth kinetics was indistinguishable between both the genotypes (**b-i**). These organoids were re-plated and exposed to 4-OH TAM to induce deletion of Cbl proteins (**j-m**). iDKO mice showed enormous budding of organoids till 48h time point. At 72h after TAM induction, DKO organoids lost their 3D morphology. qPCR analysis confirmed reduction of Cbl proteins at 72h time point (**n-o**). Re-passage of iDKO organoids did not generate any organoids suggesting a loss of self-renewal (**p-s**). These experiments were repeated two times.

Figure 3.9a

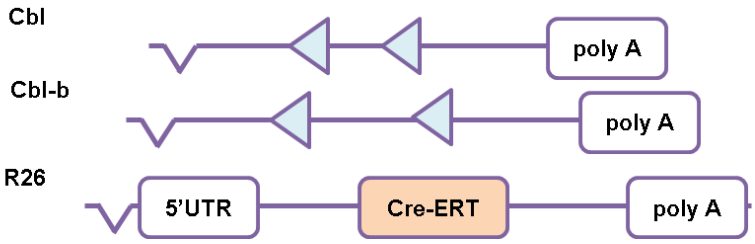

Cblf/f; Cblbf/f; Cre-ve (Control)

Cblf/f; Cblbf/f; Cre+ve (DKO)

Figure 3.9b

Figure 3.9c

24h

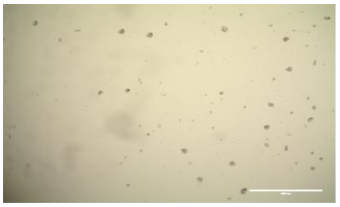

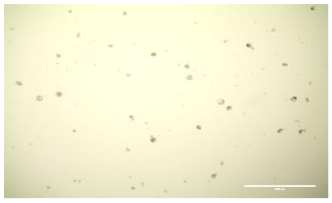

Figure 3.9d

Figure 3.9e

72h

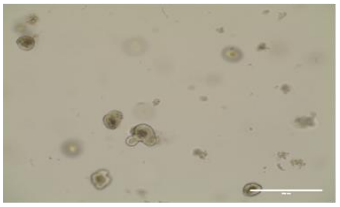

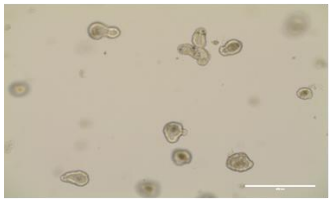

Figure 3.9f

Figure 3.9f

96h

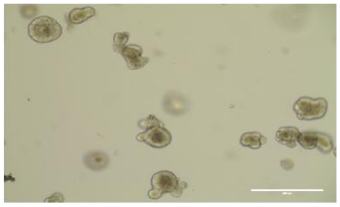

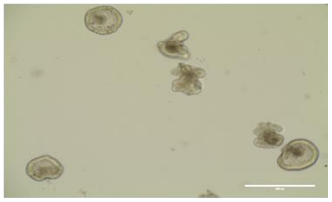

Figure 3.9h

Figure 3.9i

8days

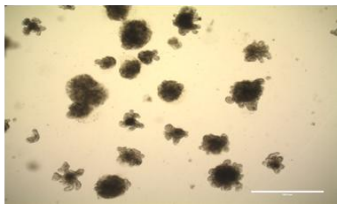

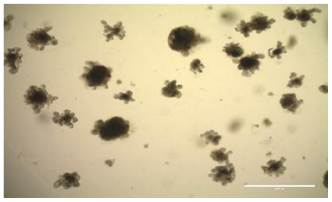

Figure 3.9j Figure 3.9k Figure 3.9l Figure 3.9m

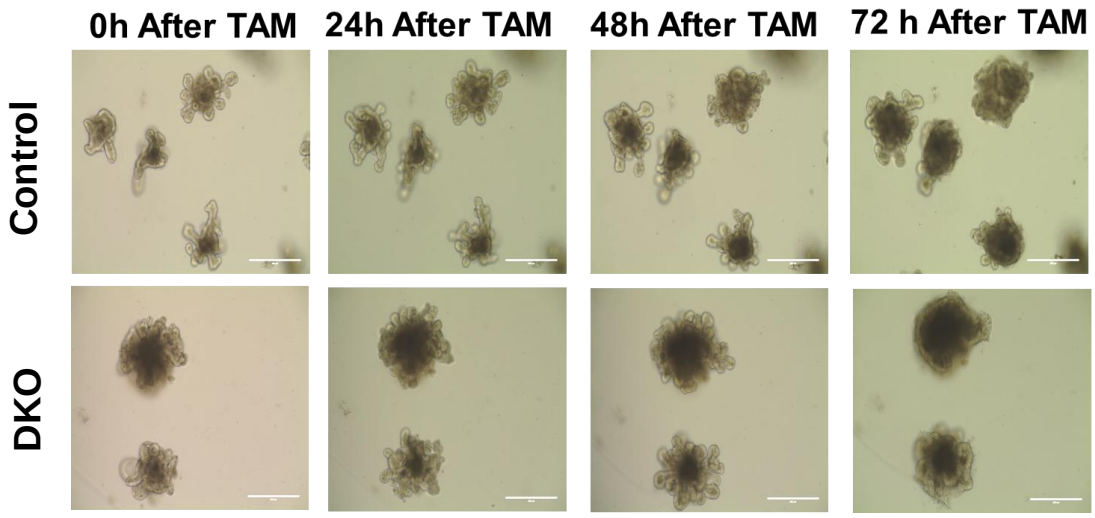

Figure 3.9n

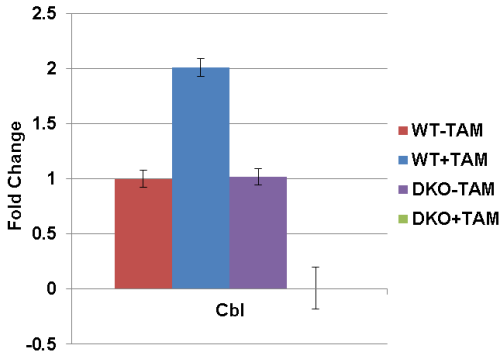

Figure 3.9o

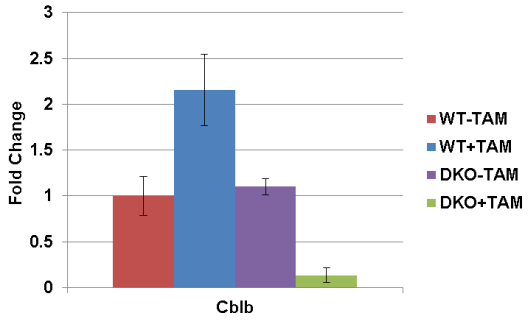

2nd Passage After TAM induction

Figure 3.9p

Cblf/f; Cblbf/f; Cre-ve (Control)

4X

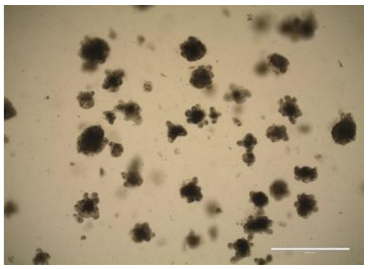

Figure 3.9q

Cblf/f; Cblbf/f; Cre+ve (DKO)

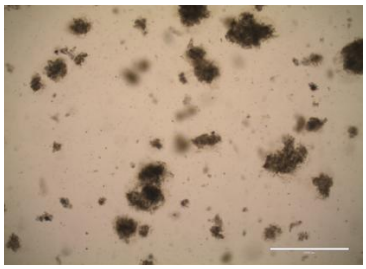

Figure 3.9r

10X

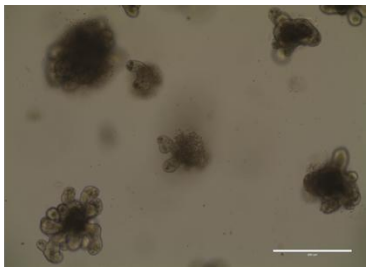

Figure 3.9s

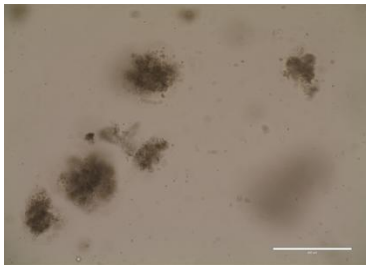

3.10 Hyperactive MAPK pathway in Cbl/Cbl-b DKO in organoids suppresses Wnt pathway

Organoids were collected at 24 hour and 72 hour time points after TAM treatment and lysed to isolate proteins to study cell signaling changes accompanying the phenotypic alterations (**figure3.10a-b**). Upregulation of p-MEK1/2, p-AKT and p-S6 in the DKO organoids at both time points are indicative of hyperactive MAPK pathway. At the same time we analyzed TCF4 expression, which is the transcription factor that activates the transcription of Wnt target genes and is considered to be indispensable for maintenance of stem/progenitor compartment of the intestine (223, 224). In the intestine, the different splice variants of Tcf4 have been identified that have different capacity to bind to DNA and hence carry out transcription of downstream Wnt effector genes (150, 225). While the longer 70 kDa isoform, Tcf4E has a binding site for CtBP (carboxyl terminal binding protein) and an elongated C-terminal domain harboring a C-clamp (a DNA binding domain), the shorter 50 kDa isoforms, Tcf4M and Tcf4S lack both these structures (150, 225). Although the shorter isoforms can bind to Wnt response elements and can be co-immunoprecipitated with β-catenin, they cannot initiate transcription of target genes such as Axin2 (225). Interestingly, MAPK signaling has been shown to regulate the relative abundance of these isoforms at the translational level (150). Indeed, we observed that at the 24h time point, there was an increase in the 70kDa isoform but by 72 hours it decayed drastically. In addition to confirming previous findings of MAPK signaling as a regulator of Wnt activity (150), these data also suggest that fine tuning of MAPK signaling can have very different effects on Wnt pathway output, thereby regulating properties like self-renewal and differentiation.

Figure 3-10 Hyperactivation of MAPK signaling reduced functional TCF4 isoform expression.

Probing cell signaling changes at early (24h, **a**) and late (72h, **b**) time points showed that loss of Cbl proteins was accompanied by increased output through MAPK signaling as seen by upregulation of p-AKT, p-Mek1/2 and p-S6. This hyperactivation of MAPK signaling appeared to have fine-tuned the translation of different isoforms of TCF4, which is the effector of Wnt pathway. This could possibly be responsible for loss of self-renewal seen in iDKO organoids.

Figure 3.10a

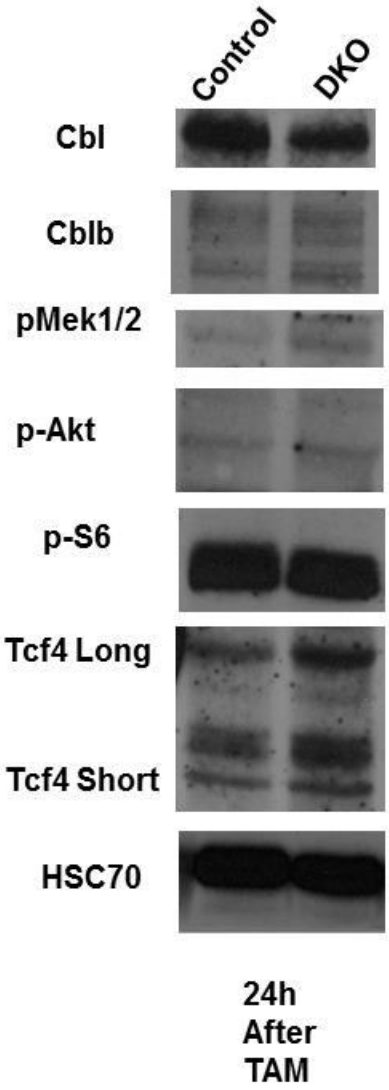

Figure 3.10b

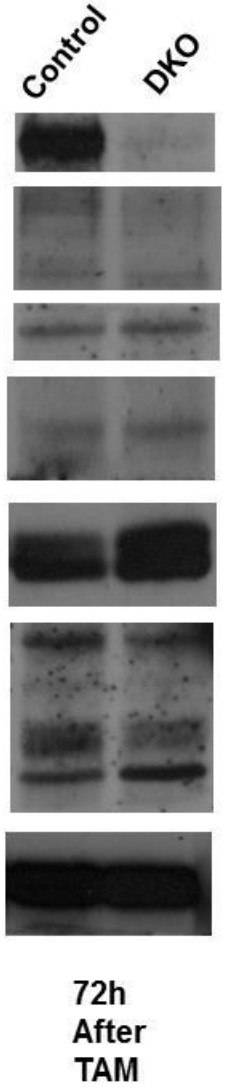

4 Discussion

Multiple biochemical and cell biological studies have established that CBL family of proteins (CBL, CBL-B and CBL-C) function as negative regulators of activated receptor and non-receptor tyrosine kinases by ubiquitinating and targeting them for degradation. While *in vivo* analysis of these proteins has established them as critical regulators of immune function, hematopoietic system and neural progenitors, their function in epithelial organs is not clearly established. Detailed analysis of the mammary gland in our lab, revealed that CBL and CBL-B, the two full length family members of CBL family, are vital to the development of this gland such that in their absence there is reduced ductal branching and defects in mammary stem cell self-renewal (Mohapatra et al., unpublished). This finding was very counterintuitive considering the role of activated protein tyrosine kinases in hyper-proliferative epithelial cancers (141-147, 148-149). In order to tease apart the role of CBL proteins in another epithelial organ we decided to look at the intestinal epithelium not only because it is the fastest self-renewing tissue in mammals, has a well-defined tissue architecture with well characterized stem/progenitor/differentiated cell population but also because RTK signaling plays a crucial role in its normal physiology and pathology.

Since no study thus far had looked at the expression or function of CBL proteins in the intestinal epithelium, we decided to begin by first studying their expression pattern in the tissue. Our analysis using immunohistochemistry, western blotting and quantitative real-time PCR revealed that CBL and CBL-B are both expressed in a gradient from crypt to villus. Crypt enrichment of these family members pointed to their potential role in regulating the proliferative stem/progenitor compartment of intestine that is also localized within the crypts (Fig. 3.1). LacZ expression analysis of Cblc LacZ knock-in mice revealed a reverse expression pattern to the other two family members. Cbl-c was

highest in the villi, which comprise the differentiated cells of the intestinal epithelium (Fig 3.1). Thus, from our expression analysis as well as from our previous analysis of hematopoietic and mammary gland systems we proposed that CBL and CBL-B might play redundant roles in the maintenance of tissue resident stem cells of intestinal epithelium. Since Cbl-c expression was mainly restricted to differentiated epithelial cells and Cbl-c-/- mice have no apparent phenotype we decided to focus our analysis on Cbl and Cbl-b for further studies.

Next, we decided to look at the gut of single Cbl and Cbl-b knockout mice. We found that while Cbl-b-/- mice looked indistinguishable from age matched WT animals, Cbl-/- mice showed goblet cell hyperplasia and increased commitment of stem/progenitor cells towards cell cycle entry (Fig 3.2). This finding showed that even though CBL and CBL-B may regulate certain aspects of tissue maintenance redundantly, some degree of fate determination was controlled solely by CBL. Nonetheless, because of their largely overlapping expression pattern, we decided to study their function together, in the intestinal stem cells. As mentioned before a whole body combined knockout of Cbl and Cbl-b is not conducive for live birth, thus, we generated a novel intestinal stem cell specific DKO of Cbl and Cbl-b by introducing Cblf/f; Cbl-b-/- alleles in Lgr5-eGFP-IRES-CreERT2; R26-LSL-LacZ mice (Fig 3.3). This model allowed us to not only monitor self-renewal based on the GFP expression within the Lgr5+ compartment but also assess their ability to commit to differentiated cell fate in an inducible fashion.

Analysis of proliferation in the iDKO (inducible double knockout) mice revealed increased entry into the cell cycle with no change in apoptosis (Fig. 3.4). This phenotype was similar to the one observed in Cbl-/- mice, although the difference was more significant in iDKO mice. This suggested that even though proliferation within the stem/progenitor compartment was predominantly controlled by CBL, there was an

additive effect on the phenotype with the loss of both family members. Further scrutiny of self-renewal using flow cytometric analysis of GFP+ Lgr5 cells demonstrated a significant drop in the percentage of live Lgr5-Hi stem cells with a concomitant increase in Lgr5-Lo progenitor cells in the iDKO mice (Fig 3.5). These data combined with the previous analysis of proliferation and apoptosis suggested that Lgr5-Hi cells were committing to differentiation over self-renewal in the iDKO mice.

To further probe the differentiation phenotype, we performed lineage tracing experiments of iDKO and WT mice by staining for LacZ (Fig 3.6). These data showed increased blue staining in the villi as well as crypts of iDKO mice suggestive of increased commitment to differentiation. Analysis of crypt filling pattern revealed a significant increase in the percentage of partially and fully blue crypts but a precipitous drop in the crypts with a single blue cell. These blue cells represent Lgr5 expressing cells that did not divide, and hence comprise the Lgr5 expressing quiescent secretory progenitor fraction. It was interesting to note that in the absence of CBL proteins a loss of quiescence did not translate into reverting to stem cell fate (as they are known to interconvert with Lgr5+ stem cells) instead differentiated into progeny as evidenced by the continued depression in the percentage of GFP-Hi cells at the 10d time point. Since GFP+ stem cells do eventually equilibrate their numbers when the effect of TAM has subsided (Fig. 3.4 o), it could mean that the abundant ALPI expressing proliferative absorptive progenitors could potentially be the candidate cells that replace the lost Lgr5-Hi stem cells as has been shown recently by Hans Clevers' group (39).

Identification of differentiation fates taken by iDKO stem cells, revealed a preference towards enterocyte and goblet cell fate (Fig. 3.7) and a loss of Paneth cell compartment. Interestingly, it has previously been shown that signaling downstream of RTKs can tilt the balance amongst different types of secretory cells (150, 137, 139). Loss of Paneth

cells in the iDKO crypts coincided very well with the loss of quiescent secretory progenitor population, whose default fate was shown to be Paneth cells (36). However, at this point it is difficult to ascertain if loss of Cbl/Cbl-b impacts the allocation of Lgr5+ quiescent compartment or promotes their conversion to alternate fates (such as goblet cells or enterocyte).

Nonetheless, loss of quiescent progenitors could have deleterious implications for maintaining homeostasis of intestinal epithelia especially under circumstances that could kill proliferating cells such as exposure to anti-mitotic drugs or exposure to radiation injury. To assess the impact of such an injury on the self-renewal of Cbl/Cbl-b deficient epithelia we subjected mice to radiation injury (Fig. 3.8). As expected, loss of CBL proteins rendered the stem/progenitor compartment incapable of re-establishing epithelial homeostasis. One possibility could be that in the absence of a functional quiescent compartment and because radiation killed the proliferating ALPI+ enterocyte progenitors, the stem cell pool could not be repopulated soon enough to regain epithelial integrity.

A potential limitation of our mouse model was the constitutive knockout of Cbl-b in all the cell types of the intestine. As Cbl-b -/- mice have been reported to have a hyperactive immune system when challenged with antigens (169, 197, 198), to overcome this constraint we made use of our newly generated mouse model carrying both Cbl and Cbl-b alleles as floxed with TAM inducible Cre being expressed from the R26 promoter to study the effect of loss of CBL proteins in *in vitro* culture of crypts (Fig. 3.9). Not only did this model recapitulate the loss of self-renewal phenotype of DKO mice, but it also allowed us to assess cell signaling changes that accompanied the said phenotype, which was difficult to perform in the mosaic Lgr5-Cre model. In keeping with the expected role of CBL proteins as negative regulators of PTK signaling, loss of Cbl

proteins increased the downstream effector MAPK signaling through both AKT and MEK pathways. This hyperactivation of the MAPK pathway interestingly also accompanied changes in TCF4 isoforms confirming the observations of Heuberger et al., 2014 (150) who showed that reduction in MAPK signaling through knockout of its positive regulator SHP2 caused degradation of the lower defective TCF4 isoform. In contrast, we saw that hyperactivation of MAPK signaling through loss of Cbl/Cbl-b stabilized the lower TCF4 isoforms but reduced the longer functional isoform. Since this longer isoform is responsible for activation of Wnt targets, we believe that loss of self-renewal observed upon knockout of CBL proteins could possibly be due to the effects of dysregulated MAPK signaling on Wnt pathway, which is a well-known preserver of self-renewal in the intestine.

5 Conclusion

The work presented within this thesis describes the role of CBL family of proteins as essential regulators of epithelial homeostasis under normal physiology and injury conditions. Due to their E3 Ubiquitin ligase function, CBL proteins are well known negative regulators of activated protein tyrosine kinases. However, their *in vivo* function in the context of epithelial tissues is still not known, even though their targets such as EGFR, FGFR and PDGFR play crucial roles during development as well as pathogenesis of epithelial tissues. Since the intestinal epithelium is the fastest self-renewing epithelial tissue, we chose to focus on it to delve into the question of CBL proteins' purpose in the maintenance of this tissue.

As this was the first work done to decipher the role of CBL proteins in the gut, we first determined their expression pattern. We found that while CBL/CBL-B are expressed predominantly within the crypts, Cbl-c is restricted to the villi. Germline deletion of Cbl led to increased proliferation within the crypts and commitment to goblet cells. We further designed a novel mouse genetic model (Cbl-flox/flox; Cbl-b-null; Lgr5-CreERT2-IRES-EGFP; R26-LacZ) to examine the combined role of CBL and CBL-B in the epithelial stem cells of the intestinal epithelium. Tamoxifen injection in this inducible CBL/CBL-B double knockout (iDKO) mouse model resulted in a rapid and significant reduction in the Lgr5-High intestinal epithelial stem cell (IESC) pool with a concomitant increase in the Lgr5-Lo transit amplifying cells. Lineage tracing using LacZ-staining revealed an increase in the number of blue progeny in the iDKOs, suggesting an increased IESC commitment to differentiation. Of the progeny, iDKO animals showed a propensity towards enterocyte and goblet cell fate at the expense of Paneth cells. Loss of IESCs in iDKO mice led to slower recovery from intestinal epithelial injury due to X-ray radiation of the abdomen. *In vitro* culture of crypts of Cblf/f; Cblbf/f; R26CreERT mice

reiterated the loss of self-renewal phenotype seen in the iDKO mice. Analysis of cell signaling revealed hyperactivation of MAPK pathways which was accompanied by changes in the relative abundance of TCF4 variants. These results demonstrate a novel requirement of Cbl/Cbl-b in the maintenance of a well-studied epithelial stem cell compartment, the IESC, and suggest that CBL proteins by regulating MAPK signaling to protect IESCs from exhaustion by balancing commitment to differentiation vs. self-renewal.

Thus, our study showcases this novel role of Cbl proteins as regulators of stem cell fate in the intestinal epithelium. These results could have possible implications in the field of regenerative medicine as well as cancer. For example, inhibition of CBL proteins using small molecule inhibitors could result in pro- as well as anti-proliferative effects depending on the dose and extent of inhibition.

6 Future Directions

Our study has for the first time elucidated the expression and function of CBL and CBL-B proteins in the context intestinal epithelium. However, there have been some limitations of our model system as well as some questions that remain unanswered.

To study the combined role of redundantly functioning CBL/CBL-B we crossed floxed Cbl with Cbl-b-/- mice to obtain a DKO in the intestinal stem cells using Lgr5-Cre. However, Cbl-b-/- mice have a hyperactive immune phenotype when challenged with an allergen. Although in the context of normal homeostasis, Cbl-b-/- intestinal epithelium did not show a phenotype but a much more detailed investigation is required especially in case of radiation or other kinds of epithelial injury (such as dextran sodium sulfate induced colitis) which are thought to instigate immune cells. To overcome this challenge to some extent and study purely epithelial contributions of CBL-B, we used Cblf/f; Cbl-bf/f crypts in vitro to corroborate the *in vivo* findings. Nonetheless, combining the floxed alleles with an intestinal epithelium specific Cre that deletes in a less mosaic fashion such as Villin-CreERT could further confirm our findings.

Secondly, the effects of intraperitoneal TAM injection induced deletion in our model system were transient and stem cells are able to re-establish their numbers at a later time point examined due to extensive plasticity within the crypt cells. A long term effect of abolishing CBL proteins could, thus, not be assessed. An alternative to this drawback could be a continuous pulse of TAM given in chow. However, effectiveness of this strategy to induce deletion of CBL proteins would need to be assessed. If this strategy would be effective in knocking out CBL for an extended period of time, it would be interesting to see if complete exhaustion of stem cells under these circumstances would be incompatible with life or would neighboring Cre negative crypts undergo increased

rates of fission to generate the epithelium that would potentially have no GFP positive crypts.

Part of the reason for the reduced ability of iDKO epithelium to recover from radiation damage could have been the loss of quiescent Lgr5+ progenitor pool. From the literature, these cells under normal homeostasis have been shown to be precursors of Paneth cells and under injury conditions have been demonstrated to de-differentiate into Lgr5+ stem cells to re-establish recovery of the epithelial lining. Thus, the effects seen in iDKO mice with respect to reduced Paneth cells and delayed recovery from injury could be ascribed to the loss of quiescent Lgr5+ fraction. However, to look at the role of CBL proteins more directly within the quiescent progenitors, it would be interesting to directly delete CBL proteins in this compartments using DLL1 or Ngn3 directed Cre. If CBL proteins are indeed essential for maintenance of quiescence, it could have therapeutic implications in case of cancer where relapse has been associated with dormant clones of cancer stem cell population.

Since CBL and CBL-B in this study have been shown to maintain self-renewal within the normal intestinal stem cell compartment, it would be of immediate interest to see if this finding translates to cancer stem cells since they are thought to be derivatives of normal stem/ progenitor compartment (58, 159-165). However, because of increased ability of CBL-B-/- mice to reject spontaneous tumors (203), it would be necessary to use Cbl-bf/f alleles along with floxed Cbl alleles in these experiments. Because loss of CBL proteins accompanies hyperactivation of MAPK signaling and downregulation of Wnt pathway activator TCF4, it would be interesting to see the effect of their absence on the tumorogenic potential in both Wnt hyperactivation cancer model of Apc and MAPK hyperactivation model of $Kras^{G12D}$ mutations. An easier approach would be to stably transfect colon cancer cell lines with inducible shRNAs against Cbl and Cbl-b and

perform subcutaneous transplants in immune compromised mice and monitor tumor development.

Heuberger et al., showed that downregulation of MAPK signaling resulted in hyperactivation of Wnt pathway in the intestine and that this regulation was proteosome mediated (150). Our data showed that the converse of this regulation was also true, i.e., hyperactivation of MAPK by knockout of Cbl and Cbl-b resulted in downregulation functional TCF4 isoform. Although TCF4 is the main TCF/LEF family member in the adult intestinal epithelium, it will be imperative to also assess the transcription of its target genes in iDKO animals as well as in iDKO organoids.

Lastly, the exact mechanism of interaction between MAPK and Wnt pathway would be important to tease apart especially since it has been reported in the endothelial cell system that CBL proteins degrade nuclear β-catenin, thereby downregulating Wnt pathway (227). It could be possible that such a regulation may not take place in the epithelial cells. On the other hand, β-catenin can interact with both the isoforms of TCF4, hence it could be possible that in the epithelial cells CBL proteins' could preferentially be targeting the β-catenin pool complexed with shorter isoforms? Or the interaction of CBL and TCF4 could be independent of β-catenin. Nonetheless, it would be important to understand the nature of interaction between the two pathways.

Overall, using novel genetic mouse models we have demonstrate that by regulating MAPK signaling CBL/CBL-B maintain IESCs, balancing commitment to differentiation vs. self-renewal and hence preventing exhaustion of stem cells.

References

1. Gordon JI, Hermiston ML. Differentiation and self-renewal in the mouse gastrointestinal epithelium. Curr Opin Cell Biol 1994;6(6):795-803.

2. de Santa Barbara P, van den Brink GR, Roberts DJ. Development and differentiation of the intestinal epithelium. Cell Mol Life Sci 2003;60(7):1322-32.

3. Rubin DC. Intestinal morphogenesis. Curr Opin Gastroenterol 2007;23(2):111-4.

4. Noah TK, Donahue B, Shroyer NF. Intestinal development and differentiation. Exp Cell Res 2011;317(19):2702-10.

5. Rao JN, Wang JY. 2010.

6. van der Flier LG, Clevers H. Stem cells, self-renewal, and differentiation in the intestinal epithelium. Annu Rev Physiol 2009;71:241-60.

7. Barker N. Adult intestinal stem cells: Critical drivers of epithelial homeostasis and regeneration. Nat Rev Mol Cell Biol 2014;15(1):19-33.

8. Potten CS. Stem cells in gastrointestinal epithelium: Numbers, characteristics and death. Philos Trans R Soc Lond B Biol Sci 1998;353(1370):821-30.

9. Mabbott NA, Donaldson DS, Ohno H, Williams IR, Mahajan A. Microfold (M) cells: Important immunosurveillance posts in the intestinal epithelium. Mucosal Immunol 2013;6(4):666-77.

10. Cheng H, Leblond CP. Origin, differentiation and renewal of the four main epithelial cell types in the mouse small intestine. V. unitarian theory of the origin of the four epithelial cell types. Am J Anat 1974;141(4):537-61.

11. Cheng H, Leblond CP. Origin, differentiation and renewal of the four main epithelial cell types in the mouse small intestine. I. columnar cell. Am J Anat 1974;141(4):461-79.

12. Cheng H, Leblond CP. Origin, differentiation and renewal of the four main epithelial cell types in the mouse small intestine. III. entero-endocrine cells. Am J Anat 1974;141(4):503-19.

13. Barker N, van Es JH, Kuipers J, et al. Identification of stem cells in small intestine and colon by marker gene Lgr5. Nature 2007;449(7165):1003-7.

14. Snippert HJ, van der Flier LG, Sato T, et al. Intestinal crypt homeostasis results from neutral competition between symmetrically dividing Lgr5 stem cells. Cell 2010;143(1):134-44.

15. Snippert HJ, Haegebarth A, Kasper M, et al. Lgr6 marks stem cells in the hair follicle that generate all cell lineages of the skin. Science 2010;327(5971):1385-9.

16. Jaks V, Barker N, Kasper M, et al. Lgr5 marks cycling, yet long-lived, hair follicle stem cells. Nat Genet 2008;40(11):1291-9.

17. de Visser KE, Ciampricotti M, Michalak EM, et al. Developmental stage-specific contribution of LGR5(+) cells to basal and luminal epithelial lineages in the postnatal mammary gland. J Pathol 2012;228(3):300-9.

18. Plaks V, Brenot A, Lawson DA, et al. Lgr5-expressing cells are sufficient and necessary for postnatal mammary gland organogenesis. Cell Rep 2013;3(1):70-8.

19. Barker N, Huch M, Kujala P, et al. Lgr5(+ve) stem cells drive self-renewal in the stomach and build long-lived gastric units in vitro. Cell Stem Cell 2010;6(1):25-36.

20. Barker N, Rookmaaker MB, Kujala P, et al. Lgr5(+ve) stem/progenitor cells contribute to nephron formation during kidney development. Cell Rep 2012;2(3):540-52.

21. Shi F, Kempfle JS, Edge AS. Wnt-responsive Lgr5-expressing stem cells are hair cell progenitors in the cochlea. J Neurosci 2012;32(28):9639-48.

22. Huch M, Bonfanti P, Boj SF, et al. Unlimited in vitro expansion of adult bi-potent pancreas progenitors through the Lgr5/R-spondin axis. EMBO J 2013;32(20):2708-21.

23. Huch M, Dorrell C, Boj SF, et al. In vitro expansion of single Lgr5+ liver stem cells induced by wnt-driven regeneration. Nature 2013;494(7436):247-50.

24. Potten CS, Booth C, Pritchard DM. The intestinal epithelial stem cell: The mucosal governor. Int J Exp Pathol 1997;78(4):219-43.

25. Potten CS, Hume WJ, Reid P, Cairns J. The segregation of DNA in epithelial stem cells. Cell 1978;15(3):899-906.

26. Yan KS, Chia LA, Li X, et al. The intestinal stem cell markers Bmi1 and Lgr5 identify two functionally distinct populations. Proc Natl Acad Sci U S A 2012;109(2):466-71.

27. Sangiorgi E, Capecchi MR. Bmi1 is expressed in vivo in intestinal stem cells. Nat Genet 2008;40(7):915-20.

29. Xian CJ, Couper R, Howarth GS, Read LC, Kallincos NC. Increased expression of HGF and c-met in rat small intestine during recovery from methotrexate-induced mucositis. Br J Cancer 2000;82(4):945-52.

30. Powell AE, Wang Y, Li Y, et al. The pan-ErbB negative regulator Lrig1 is an intestinal stem cell marker that functions as a tumor suppressor. Cell 2012;149(1):146-58.

31. Takeda N, Jain R, LeBoeuf MR, Wang Q, Lu MM, Epstein JA. Interconversion between intestinal stem cell populations in distinct niches. Science 2011;334(6061):1420-4.

32. Montgomery RK, Carlone DL, Richmond CA, et al. Mouse telomerase reverse transcriptase (mTert) expression marks slowly cycling intestinal stem cells. Proc Natl Acad Sci U S A 2011;108(1):179-84.

33. He XC, Yin T, Grindley JC, et al. PTEN-deficient intestinal stem cells initiate intestinal polyposis. Nat Genet 2007;39(2):189-98.

34. He XC, Zhang J, Tong WG, et al. BMP signaling inhibits intestinal stem cell self-renewal through suppression of wnt-beta-catenin signaling. Nat Genet 2004;36(10):1117-21.

35. Metcalfe C, Kljavin NM, Ybarra R, de Sauvage FJ. Lgr5+ stem cells are indispensable for radiation-induced intestinal regeneration. Cell Stem Cell 2014;14(2):149-59.

36. Buczacki SJ, Zecchini HI, Nicholson AM, et al. Intestinal label-retaining cells are secretory precursors expressing Lgr5. Nature 2013;495(7439):65-9.

37. van Es JH, Sato T, van de Wetering M, et al. Dll1+ secretory progenitor cells revert to stem cells upon crypt damage. Nat Cell Biol 2012;14(10):1099-104.

38. Stamataki D, Holder M, Hodgetts C, et al. Delta1 expression, cell cycle exit, and commitment to a specific secretory fate coincide within a few hours in the mouse intestinal stem cell system. PLoS One 2011;6(9):e24484.

39. Tetteh PW, Basak O, Farin HF, et al. Replacement of lost Lgr5-positive stem cells through plasticity of their enterocyte-lineage daughters. Cell Stem Cell 2016;18(2):203-13.

40. Carulli AJ, Samuelson LC, Schnell S. Unraveling intestinal stem cell behavior with models of crypt dynamics. Integr Biol (Camb) 2014;6(3):243-57.

41. Carulli AJ, Keeley TM, Demitrack ES, Chung J, Maillard I, Samuelson LC. Notch receptor regulation of intestinal stem cell homeostasis and crypt regeneration. Dev Biol 2015;402(1):98-108.

42. Kim TH, Escudero S, Shivdasani RA. Intact function of Lgr5 receptor-expressing intestinal stem cells in the absence of paneth cells. Proc Natl Acad Sci U S A 2012;109(10):3932-7.

43. Farin HF, Van Es JH, Clevers H. Redundant sources of wnt regulate intestinal stem cells and promote formation of paneth cells. Gastroenterology 2012;143(6):1518,1529.e7.

44. Durand A, Donahue B, Peignon G, et al. Functional intestinal stem cells after paneth cell ablation induced by the loss of transcription factor Math1 (Atoh1). Proc Natl Acad Sci U S A 2012;109(23):8965-70.

45. Shroyer NF, Wallis D, Venken KJ, Bellen HJ, Zoghbi HY. Gfi1 functions downstream of Math1 to control intestinal secretory cell subtype allocation and differentiation. Genes Dev 2005;19(20):2412-7.

46. Bastide P, Darido C, Pannequin J, et al. Sox9 regulates cell proliferation and is required for paneth cell differentiation in the intestinal epithelium. J Cell Biol 2007;178(4):635-48.

47. Mori-Akiyama Y, van den Born M, van Es JH, et al. SOX9 is required for the differentiation of paneth cells in the intestinal epithelium. Gastroenterology 2007;133(2):539-46.

48. Kabiri Z, Greicius G, Madan B, et al. Stroma provides an intestinal stem cell niche in the absence of epithelial wnts. Development 2014;141(11):2206-15.

49. Sato T, van Es JH, Snippert HJ, et al. Paneth cells constitute the niche for Lgr5 stem cells in intestinal crypts. Nature 2011;469(7330):415-8.

50. Carmon KS, Gong X, Lin Q, Thomas A, Liu Q. R-spondins function as ligands of the orphan receptors LGR4 and LGR5 to regulate Wnt/beta-catenin signaling. Proc Natl Acad Sci U S A 2011;108(28):11452-7.

51. Carmon KS, Lin Q, Gong X, Thomas A, Liu Q. LGR5 interacts and cointernalizes with wnt receptors to modulate Wnt/beta-catenin signaling. Mol Cell Biol 2012;32(11):2054-64.

52. Koo BK, Spit M, Jordens I, et al. Tumour suppressor RNF43 is a stem-cell E3 ligase that induces endocytosis of wnt receptors. Nature 2012;488(7413):665-9.

53. Hao HX, Xie Y, Zhang Y, et al. ZNRF3 promotes wnt receptor turnover in an R-spondin-sensitive manner. Nature 2012;485(7397):195-200.

54. Morita H, Mazerbourg S, Bouley DM, et al. Neonatal lethality of LGR5 null mice is associated with ankyloglossia and gastrointestinal distension. Mol Cell Biol 2004;24(22):9736-43.

55. de Lau W, Barker N, Low TY, et al. Lgr5 homologues associate with wnt receptors and mediate R-spondin signalling. Nature 2011;476(7360):293-7.

56. Barker N, Clevers H. Leucine-rich repeat-containing G-protein-coupled receptors as markers of adult stem cells. Gastroenterology 2010;138(5):1681-96.

57. Schuijers J, Clevers H. Adult mammalian stem cells: The role of wnt, Lgr5 and R-spondins. EMBO J 2012;31(12):2685-96.

58. Barker N, Ridgway RA, van Es JH, et al. Crypt stem cells as the cells-of-origin of intestinal cancer. Nature 2009;457(7229):608-11.

59. Lopez-Garcia C, Klein AM, Simons BD, Winton DJ. Intestinal stem cell replacement follows a pattern of neutral drift. Science 2010;330(6005):822-5.

60. Gutierrez-Gonzalez L, Deheragoda M, Elia G, et al. Analysis of the clonal architecture of the human small intestinal epithelium establishes a common stem cell for all lineages and reveals a mechanism for the fixation and spread of mutations. J Pathol 2009;217(4):489-96.

61. Novelli MR, Williamson JA, Tomlinson IP, et al. Polyclonal origin of colonic adenomas in an XO/XY patient with FAP. Science 1996;272(5265):1187-90.

62. Greaves LC, Preston SL, Tadrous PJ, et al. Mitochondrial DNA mutations are established in human colonic stem cells, and mutated clones expand by crypt fission. Proc Natl Acad Sci U S A 2006;103(3):714-9.

63. Taylor RW, Barron MJ, Borthwick GM, et al. Mitochondrial DNA mutations in human colonic crypt stem cells. J Clin Invest 2003;112(9):1351-60.

64. Ritsma L, Ellenbroek SI, Zomer A, et al. Intestinal crypt homeostasis revealed at single-stem-cell level by in vivo live imaging. Nature 2014;507(7492):362-5.

66. Tetteh PW, Farin HF, Clevers H. Plasticity within stem cell hierarchies in mammalian epithelia. Trends Cell Biol 2015;25(2):100-8.

67. Clevers H, Loh KM, Nusse R. Stem cell signaling. an integral program for tissue renewal and regeneration: Wnt signaling and stem cell control. Science 2014;346(6205):1248012.

68. Flanagan DJ, Phesse TJ, Barker N, et al. Frizzled7 functions as a wnt receptor in intestinal epithelial Lgr5(+) stem cells. Stem Cell Reports 2015;4(5):759-67.

69. Gregorieff A, Pinto D, Begthel H, Destree O, Kielman M, Clevers H. Expression pattern of wnt signaling components in the adult intestine. Gastroenterology 2005;129(2):626-38.

70. Byun T, Karimi M, Marsh JL, Milovanovic T, Lin F, Holcombe RF. Expression of secreted wnt antagonists in gastrointestinal tissues: Potential role in stem cell homeostasis. J Clin Pathol 2005;58(5):515-9.

71. Koch S, Nava P, Addis C, et al. The wnt antagonist Dkk1 regulates intestinal epithelial homeostasis and wound repair. Gastroenterology 2011;141(1):259,68, 268.e1-8.

72. Leppert M, Dobbs M, Scambler P, et al. The gene for familial polyposis coli maps to the long arm of chromosome 5. Science 1987;238(4832):1411-3.

73. Bodmer WF, Bailey CJ, Bodmer J, et al. Localization of the gene for familial adenomatous polyposis on chromosome 5. Nature 1987;328(6131):614-6.

74. Munemitsu S, Albert I, Souza B, Rubinfeld B, Polakis P. Regulation of intracellular beta-catenin levels by the adenomatous polyposis coli (APC) tumor-suppressor protein. Proc Natl Acad Sci U S A 1995;92(7):3046-50.

75. de Sousa EM, Vermeulen L, Richel D, Medema JP. Targeting wnt signaling in colon cancer stem cells. Clin Cancer Res 2011;17(4):647-53.

76. Segditsas S, Tomlinson I. Colorectal cancer and genetic alterations in the wnt pathway. Oncogene 2006;25(57):7531-7.

77. Sansom OJ, Reed KR, Hayes AJ, et al. Loss of apc in vivo immediately perturbs wnt signaling, differentiation, and migration. Genes Dev 2004;18(12):1385-90.

78. Sansom OJ, Meniel VS, Muncan V, et al. Myc deletion rescues apc deficiency in the small intestine. Nature 2007;446(7136):676-9.

79. Andreu P, Colnot S, Godard C, et al. Crypt-restricted proliferation and commitment to the paneth cell lineage following apc loss in the mouse intestine. Development 2005;132(6):1443-51.

80. Wong MH, Rubinfeld B, Gordon JI. Effects of forced expression of an NH2-terminal truncated beta-catenin on mouse intestinal epithelial homeostasis. J Cell Biol 1998;141(3):765-77.

81. Korinek V, Barker N, Moerer P, et al. Depletion of epithelial stem-cell compartments in the small intestine of mice lacking tcf-4. Nat Genet 1998;19(4):379-83.

82. Kuhnert F, Davis CR, Wang HT, et al. Essential requirement for wnt signaling in proliferation of adult small intestine and colon revealed by adenoviral expression of dickkopf-1. Proc Natl Acad Sci U S A 2004;101(1):266-71.

83. Muncan V, Sansom OJ, Tertoolen L, et al. Rapid loss of intestinal crypts upon conditional deletion of the Wnt/Tcf-4 target gene c-myc. Mol Cell Biol 2006;26(22):8418-26.

84. Andreu P, Peignon G, Slomianny C, et al. A genetic study of the role of the Wnt/beta-catenin signalling in paneth cell differentiation. Dev Biol 2008;324(2):288-96.

85. Finch AJ, Soucek L, Junttila MR, Swigart LB, Evan GI. Acute overexpression of myc in intestinal epithelium recapitulates some but not all the changes elicited by Wnt/beta-catenin pathway activation. Mol Cell Biol 2009;29(19):5306-15.

86. Gracz AD, Magness ST. Sry-box (sox) transcription factors in gastrointestinal physiology and disease. Am J Physiol Gastrointest Liver Physiol 2011;300(4):G503-15.

87. Schonhoff SE, Giel-Moloney M, Leiter AB. Neurogenin 3-expressing progenitor cells in the gastrointestinal tract differentiate into both endocrine and non-endocrine cell types. Dev Biol 2004;270(2):443-54.

88. Batlle E, Henderson JT, Beghtel H, et al. Beta-catenin and TCF mediate cell positioning in the intestinal epithelium by controlling the expression of EphB/ephrinB. Cell 2002;111(2):251-63.

89. Kullander K, Klein R. Mechanisms and functions of eph and ephrin signalling. Nat Rev Mol Cell Biol 2002;3(7):475-86.

90. Solanas G, Batlle E. Control of cell adhesion and compartmentalization in the intestinal epithelium. Exp Cell Res 2011;317(19):2695-701.

91. Holmberg J, Genander M, Halford MM, et al. EphB receptors coordinate migration and proliferation in the intestinal stem cell niche. Cell 2006;125(6):1151-63.

92. Pinto D, Gregorieff A, Begthel H, Clevers H. Canonical wnt signals are essential for homeostasis of the intestinal epithelium. Genes Dev 2003;17(14):1709-13.

94. van de Wetering M, Sancho E, Verweij C, et al. The beta-catenin/TCF-4 complex imposes a crypt progenitor phenotype on colorectal cancer cells. Cell 2002;111(2):241-50.

95. van Es JH, Jay P, Gregorieff A, et al. Wnt signalling induces maturation of paneth cells in intestinal crypts. Nat Cell Biol 2005;7(4):381-6.

97. Pellegrinet L, Rodilla V, Liu Z, et al. Dll1- and dll4-mediated notch signaling are required for homeostasis of intestinal stem cells. Gastroenterology 2011;140(4):1230,1240.e1-7.

98. Fre S, Huyghe M, Mourikis P, Robine S, Louvard D, Artavanis-Tsakonas S. Notch signals control the fate of immature progenitor cells in the intestine. Nature 2005;435(7044):964-8.

99. Stanger BZ, Datar R, Murtaugh LC, Melton DA. Direct regulation of intestinal fate by notch. Proc Natl Acad Sci U S A 2005;102(35):12443-8.

100. Gerbe F, van Es JH, Makrini L, et al. Distinct ATOH1 and Neurog3 requirements define tuft cells as a new secretory cell type in the intestinal epithelium. J Cell Biol 2011;192(5):767-80.

101. VanDussen KL, Carulli AJ, Keeley TM, et al. Notch signaling modulates proliferation and differentiation of intestinal crypt base columnar stem cells. Development 2012;139(3):488-97.

102. van Es JH, van Gijn ME, Riccio O, et al. Notch/gamma-secretase inhibition turns proliferative cells in intestinal crypts and adenomas into goblet cells. Nature 2005;435(7044):959-63.

103. Riccio O, van Gijn ME, Bezdek AC, et al. Loss of intestinal crypt progenitor cells owing to inactivation of both Notch1 and Notch2 is accompanied by derepression of CDK inhibitors p27Kip1 and p57Kip2. EMBO Rep 2008;9(4):377-83.

104. Sander GR, Powell BC. Expression of notch receptors and ligands in the adult gut. J Histochem Cytochem 2004;52(4):509-16.

105. Crosnier C, Vargesson N, Gschmeissner S, Ariza-McNaughton L, Morrison A, Lewis J. Delta-notch signalling controls commitment to a secretory fate in the zebrafish intestine. Development 2005;132(5):1093-104.

106. Benedito R, Duarte A. Expression of Dll4 during mouse embryogenesis suggests multiple developmental roles. Gene Expr Patterns 2005;5(6):750-5.

107. Kopan R, Ilagan MX. The canonical notch signaling pathway: Unfolding the activation mechanism. Cell 2009;137(2):216-33.

108. Jensen J, Pedersen EE, Galante P, et al. Control of endodermal endocrine development by hes-1. Nat Genet 2000;24(1):36-44.

109. Suzuki K, Fukui H, Kayahara T, et al. Hes1-deficient mice show precocious differentiation of paneth cells in the small intestine. Biochem Biophys Res Commun 2005;328(1):348-52.

110. van Es JH, de Geest N, van de Born M, Clevers H, Hassan BA. Intestinal stem cells lacking the Math1 tumour suppressor are refractory to notch inhibitors. Nat Commun 2010;1:18.

111. Ueo T, Imayoshi I, Kobayashi T, et al. The role of hes genes in intestinal development, homeostasis and tumor formation. Development 2012;139(6):1071-82.

112. Li HJ, Kapoor A, Giel-Moloney M, Rindi G, Leiter AB. Notch signaling differentially regulates the cell fate of early endocrine precursor cells and their maturing descendants in the mouse pancreas and intestine. Dev Biol 2012;371(2):156-69.

113. Vanuytsel T, Senger S, Fasano A, Shea-Donohue T. Major signaling pathways in intestinal stem cells. Biochim Biophys Acta 2013;1830(2):2410-26.

114. Haramis AP, Begthel H, van den Born M, et al. De novo crypt formation and juvenile polyposis on BMP inhibition in mouse intestine. Science 2004;303(5664):1684-6.

115. He XC, Yin T, Grindley JC, et al. PTEN-deficient intestinal stem cells initiate intestinal polyposis. Nat Genet 2007;39(2):189-98.

116. Auclair BA, Benoit YD, Rivard N, Mishina Y, Perreault N. Bone morphogenetic protein signaling is essential for terminal differentiation of the intestinal secretory cell lineage. Gastroenterology 2007;133(3):887-96.

117. Beck SE, Jung BH, Del Rosario E, Gomez J, Carethers JM. BMP-induced growth suppression in colon cancer cells is mediated by p21WAF1 stabilization and modulated by RAS/ERK. Cell Signal 2007;19(7):1465-72.

119. Kosinski C, Li VS, Chan AS, et al. Gene expression patterns of human colon tops and basal crypts and BMP antagonists as intestinal stem cell niche factors. Proc Natl Acad Sci U S A 2007;104(39):15418-23.

120. Avraham R, Yarden Y. Feedback regulation of EGFR signalling: Decision making by early and delayed loops. Nat Rev Mol Cell Biol 2011;12(2):104-17.

121. Lemmon MA, Schlessinger J. Cell signaling by receptor tyrosine kinases. Cell 2010;141(7):1117-34.

122. Bird AR, Croom WJ,Jr, Fan YK, et al. Jejunal glucose absorption is enhanced by epidermal growth factor in mice. J Nutr 1994;124(2):231-40.

123. Calvert R, Beaulieu JF, Menard D. Epidermal growth factor (EGF) accelerates the maturation of fetal mouse intestinal mucosa in utero. Experientia 1982;38(9):1096-7.

124. Goodlad RA, Raja KB, Peters TJ, Wright NA. Effects of urogastrone-epidermal growth factor on intestinal brush border enzymes and mitotic activity. Gut 1991;32(9):994-8.

125. O'Loughlin EV, Chung M, Hollenberg M, Hayden J, Zahavi I, Gall DG. Effect of epidermal growth factor on ontogeny of the gastrointestinal tract. Am J Physiol 1985;249(6 Pt 1):G674-8.

126. Dembinski A, Gregory H, Konturek SJ, Polanski M. Trophic action of epidermal growth factor on the pancreas and gastroduodenal mucosa in rats. J Physiol 1982;325:35-42.

127. Scheving LA, Yeh YC, Tsai TH, Scheving LE. Circadian phase-dependent stimulatory effects of epidermal growth factor on deoxyribonucleic acid synthesis in the duodenum, jejunum, ileum, caecum, colon, and rectum of the adult male mouse. Endocrinology 1980;106(5):1498-503.

128. Troyer KL, Luetteke NC, Saxon ML, Qiu TH, Xian CJ, Lee DC. Growth retardation, duodenal lesions, and aberrant ileum architecture in triple null mice lacking EGF, amphiregulin, and TGF-alpha. Gastroenterology 2001;121(1):68-78.

129. Frey MR, Golovin A, Polk DB. Epidermal growth factor-stimulated intestinal epithelial cell migration requires src family kinase-dependent p38 MAPK signaling. J Biol Chem 2004;279(43):44513-21.

130. Dise RS, Frey MR, Whitehead RH, Polk DB. Epidermal growth factor stimulates rac activation through src and phosphatidylinositol 3-kinase to promote colonic epithelial cell migration. Am J Physiol Gastrointest Liver Physiol 2008;294(1):G276-85.

131. Jones MK, Tomikawa M, Mohajer B, Tarnawski AS. Gastrointestinal mucosal regeneration: Role of growth factors. Front Biosci 1999;4:D303-9.

132. Miettinen PJ, Berger JE, Meneses J, et al. Epithelial immaturity and multiorgan failure in mice lacking epidermal growth factor receptor. Nature 1995;376(6538):337-41.

133. Sibilia M, Wagner EF. Strain-dependent epithelial defects in mice lacking the EGF receptor. Science 1995;269(5221):234-8.

134. Islam S, Loizides AM, Fialkovich JJ, Grand RJ, Montgomery RK. Developmental expression of eph and ephrin family genes in mammalian small intestine. Dig Dis Sci 2010;55(9):2478-88.

136. Miao H, Strebhardt K, Pasquale EB, Shen TL, Guan JL, Wang B. Inhibition of integrin-mediated cell adhesion but not directional cell migration requires catalytic activity of EphB3 receptor tyrosine kinase. role of rho family small GTPases. J Biol Chem 2005;280(2):923-32.

137. Vidrich A, Buzan JM, Brodrick B, et al. Fibroblast growth factor receptor-3 regulates paneth cell lineage allocation and accrual of epithelial stem cells during murine intestinal development. Am J Physiol Gastrointest Liver Physiol 2009;297(1):G168-78.

138. Freier S, Eran M, Reinus C, et al. Relative expression and localization of the insulin-like growth factor system components in the fetal, child and adult intestine. J Pediatr Gastroenterol Nutr 2005;40(2):202-9.

139. Al Alam D, Danopoulos S, Schall K, et al. Fibroblast growth factor 10 alters the balance between goblet and paneth cells in the adult mouse small intestine. Am J Physiol Gastrointest Liver Physiol 2015;308(8):G678-90.

140. Wong VW, Stange DE, Page ME, et al. Lrig1 controls intestinal stem-cell homeostasis by negative regulation of ErbB signalling. Nat Cell Biol 2012;14(4):401-8.

141. Radinsky R, Risin S, Fan D, et al. Level and function of epidermal growth factor receptor predict the metastatic potential of human colon carcinoma cells. Clin Cancer Res 1995;1(1):19-31.

142. Hayashi Y, Widjono YW, Ohta K, et al. Expression of EGF, EGF-receptor, p53, v-erb B and ras p21 in colorectal neoplasms by immunostaining paraffin-embedded tissues. Pathol Int 1994;44(2):124-30.

143. Yasui W, Sumiyoshi H, Hata J, et al. Expression of epidermal growth factor receptor in human gastric and colonic carcinomas. Cancer Res 1988;48(1):137-41.

144. Malecka-Panas E, Kordek R, Biernat W, Tureaud J, Liberski PP, Majumdar AP. Differential activation of total and EGF receptor (EGF-R) tyrosine kinase (tyr-k) in the rectal mucosa in patients with adenomatous polyps, ulcerative colitis and colon cancer. Hepatogastroenterology 1997;44(14):435-40.

145. Roberts RB, Min L, Washington MK, et al. Importance of epidermal growth factor receptor signaling in establishment of adenomas and maintenance of carcinomas during intestinal tumorigenesis. Proc Natl Acad Sci U S A 2002;99(3):1521-6.

146. Guo DL, Zhang J, Yuen ST, et al. Reduced expression of EphB2 that parallels invasion and metastasis in colorectal tumours. Carcinogenesis 2006;27(3):454-64.

147. Lugli A, Spichtin H, Maurer R, et al. EphB2 expression across 138 human tumor types in a tissue microarray: High levels of expression in gastrointestinal cancers. Clin Cancer Res 2005;11(18):6450-8.

148. Kaneda A, Feinberg AP. Loss of imprinting of IGF2: A common epigenetic modifier of intestinal tumor risk. Cancer Res 2005;65(24):11236-40.

149. Martinelli E, De Palma R, Orditura M, De Vita F, Ciardiello F. Anti-epidermal growth factor receptor monoclonal antibodies in cancer therapy. Clin Exp Immunol 2009;158(1):1-9.

150. Heuberger J, Kosel F, Qi J, Grossmann KS, Rajewsky K, Birchmeier W. Shp2/MAPK signaling controls goblet/paneth cell fate decisions in the intestine. Proc Natl Acad Sci U S A 2014;111(9):3472-7.

151. Cully M, You H, Levine AJ, Mak TW. Beyond PTEN mutations: The PI3K pathway as an integrator of multiple inputs during tumorigenesis. Nat Rev Cancer 2006;6(3):184-92.

152. Vivanco I, Sawyers CL. The phosphatidylinositol 3-kinase AKT pathway in human cancer. Nat Rev Cancer 2002;2(7):489-501.

154. Liaw D, Marsh DJ, Li J, et al. Germline mutations of the PTEN gene in cowden disease, an inherited breast and thyroid cancer syndrome. Nat Genet 1997;16(1):64-7.

155. Tan S, Barker N. Epithelial stem cells and intestinal cancer. Semin Cancer Biol 2015;32:40-53.

156. Kreso A, van Galen P, Pedley NM, et al. Self-renewal as a therapeutic target in human colorectal cancer. Nat Med 2014;20(1):29-36.

157. Fearon ER, Vogelstein B. A genetic model for colorectal tumorigenesis. Cell 1990;61(5):759-67.

159. Vermeulen L, Morrissey E, van der Heijden M, et al. Defining stem cell dynamics in models of intestinal tumor initiation. Science 2013;342(6161):995-8.

160. Snippert HJ, Schepers AG, van Es JH, Simons BD, Clevers H. Biased competition between Lgr5 intestinal stem cells driven by oncogenic mutation induces clonal expansion. EMBO Rep 2014;15(1):62-9.

161. Ricci-Vitiani L, Lombardi DG, Pilozzi E, et al. Identification and expansion of human colon-cancer-initiating cells. Nature 2007;445(7123):111-5.

162. O'Brien CA, Kreso A, Ryan P, et al. ID1 and ID3 regulate the self-renewal capacity of human colon cancer-initiating cells through p21. Cancer Cell 2012;21(6):777-92.

163. O'Brien CA, Pollett A, Gallinger S, Dick JE. A human colon cancer cell capable of initiating tumour growth in immunodeficient mice. Nature 2007;445(7123):106-10.

164. Todaro M, Alea MP, Di Stefano AB, et al. Colon cancer stem cells dictate tumor growth and resist cell death by production of interleukin-4. Cell Stem Cell 2007;1(4):389-402.

165. Dalerba P, Dylla SJ, Park IK, et al. Phenotypic characterization of human colorectal cancer stem cells. Proc Natl Acad Sci U S A 2007;104(24):10158-63.

166. Pinto D, Clevers H. Wnt, stem cells and cancer in the intestine. Biol Cell 2005;97(3):185-96.

167. Langdon WY, Hartley JW, Klinken SP, Ruscetti SK, Morse HC,3rd. v-cbl, an oncogene from a dual-recombinant murine retrovirus that induces early B-lineage lymphomas. Proc Natl Acad Sci U S A 1989;86(4):1168-72.

168. Blake TJ, Shapiro M, Morse HC,3rd, Langdon WY. The sequences of the human and mouse c-cbl proto-oncogenes show v-cbl was generated by a large truncation encompassing a proline-rich domain and a leucine zipper-like motif. Oncogene 1991;6(4):653-7.

169. Mohapatra B, Ahmad G, Nadeau S, et al. Protein tyrosine kinase regulation by ubiquitination: Critical roles of cbl-family ubiquitin ligases. Biochim Biophys Acta 2013;1833(1):122-39.

170. Meng W, Sawasdikosol S, Burakoff SJ, Eck MJ. Structure of the amino-terminal domain of cbl complexed to its binding site on ZAP-70 kinase. Nature 1999;398(6722):84-90.

171. Zheng N, Wang P, Jeffrey PD, Pavletich NP. Structure of a c-cbl-UbcH7 complex: RING domain function in ubiquitin-protein ligases. Cell 2000;102(4):533-9.

172. Langenick J, Araki T, Yamada Y, Williams JG. A dictyostelium homologue of the metazoan cbl proteins regulates STAT signalling. J Cell Sci 2008;121(Pt 21):3524-30.

173. Lupher ML,Jr, Songyang Z, Shoelson SE, Cantley LC, Band H. The cbl phosphotyrosine-binding domain selects a D(N/D)XpY motif and binds to the Tyr292 negative regulatory phosphorylation site of ZAP-70. J Biol Chem 1997;272(52):33140-4.

174. Bonita DP, Miyake S, Lupher ML,Jr, Langdon WY, Band H. Phosphotyrosine binding domain-dependent upregulation of the platelet-derived growth factor receptor alpha signaling cascade by transforming mutants of cbl: Implications for cbl's function and oncogenicity. Mol Cell Biol 1997;17(8):4597-610.

175. Miyake S, Mullane-Robinson KP, Lill NL, Douillard P, Band H. Cbl-mediated negative regulation of platelet-derived growth factor receptor-dependent cell proliferation. A critical role for cbl tyrosine kinase-binding domain. J Biol Chem 1999;274(23):16619-28.

176. Thien CB, Langdon WY. Tyrosine kinase activity of the EGF receptor is enhanced by the expression of oncogenic 70Z-cbl. Oncogene 1997;15(24):2909-19.

177. Miyake S, Lupher ML,Jr, Druker B, Band H. The tyrosine kinase regulator cbl enhances the ubiquitination and degradation of the platelet-derived growth factor receptor alpha. Proc Natl Acad Sci U S A 1998;95(14):7927-32.

178. Joazeiro CA, Wing SS, Huang H, Leverson JD, Hunter T, Liu YC. The tyrosine kinase negative regulator c-cbl as a RING-type, E2-dependent ubiquitin-protein ligase. Science 1999;286(5438):309-12.

179. Abella JV, Peschard P, Naujokas MA, et al. Met/Hepatocyte growth factor receptor ubiquitination suppresses transformation and is required for hrs phosphorylation. Mol Cell Biol 2005;25(21):9632-45.

180. Lee PS, Wang Y, Dominguez MG, et al. The cbl protooncoprotein stimulates CSF-1 receptor multiubiquitination and endocytosis, and attenuates macrophage proliferation. EMBO J 1999;18(13):3616-28.

181. Peschard P, Fournier TM, Lamorte L, et al. Mutation of the c-cbl TKB domain binding site on the met receptor tyrosine kinase converts it into a transforming protein. Mol Cell 2001;8(5):995-1004.

182. Rao N, Dodge I, Band H. The cbl family of ubiquitin ligases: Critical negative regulators of tyrosine kinase signaling in the immune system. J Leukoc Biol 2002;71(5):753-63.

183. Rao N, Ghosh AK, Douillard P, Andoniou CE, Zhou P, Band H. An essential role of ubiquitination in cbl-mediated negative regulation of the src-family kinase fyn. Signal Transduct 2002;2(1-2):29-39.

184. Rao N, Ghosh AK, Ota S, et al. The non-receptor tyrosine kinase syk is a target of cbl-mediated ubiquitylation upon B-cell receptor stimulation. EMBO J 2001;20(24):7085-95.

185. Rao N, Lupher ML,Jr, Ota S, Reedquist KA, Druker BJ, Band H. The linker phosphorylation site Tyr292 mediates the negative regulatory effect of cbl on ZAP-70 in T cells. J Immunol 2000;164(9):4616-26.

186. Kassenbrock CK, Anderson SM. Regulation of ubiquitin protein ligase activity in c-cbl by phosphorylation-induced conformational change and constitutive activation by tyrosine to glutamate point mutations. J Biol Chem 2004;279(27):28017-27.

187. Swaminathan G, Tsygankov AY. The cbl family proteins: Ring leaders in regulation of cell signaling. J Cell Physiol 2006;209(1):21-43.

188. Duan L, Raja SM, Chen G, et al. Negative regulation of EGFR-Vav2 signaling axis by cbl ubiquitin ligase controls EGF receptor-mediated epithelial cell adherens junction dynamics and cell migration. J Biol Chem 2011;286(1):620-33.

189. Naramura M, Nandwani N, Gu H, Band V, Band H. Rapidly fatal myeloproliferative disorders in mice with deletion of casitas B-cell lymphoma (cbl) and cbl-b in hematopoietic stem cells. Proc Natl Acad Sci U S A 2010;107(37):16274-9.

190. Rathinam C, Thien CB, Langdon WY, Gu H, Flavell RA. The E3 ubiquitin ligase c-cbl restricts development and functions of hematopoietic stem cells. Genes Dev 2008;22(8):992-7.

191. Rathinam C, Thien CB, Flavell RA, Langdon WY. Myeloid leukemia development in c-cbl RING finger mutant mice is dependent on FLT3 signaling. Cancer Cell 2010;18(4):341-52.

192. Griffiths EK, Sanchez O, Mill P, et al. Cbl-3-deficient mice exhibit normal epithelial development. Mol Cell Biol 2003;23(21):7708-18.

193. Murphy MA, Schnall RG, Venter DJ, et al. Tissue hyperplasia and enhanced T-cell signalling via ZAP-70 in c-cbl-deficient mice. Mol Cell Biol 1998;18(8):4872-82.

194. Naramura M, Kole HK, Hu RJ, Gu H. Altered thymic positive selection and intracellular signals in cbl-deficient mice. Proc Natl Acad Sci U S A 1998;95(26):15547-52.

195. Molero JC, Jensen TE, Withers PC, et al. c-cbl-deficient mice have reduced adiposity, higher energy expenditure, and improved peripheral insulin action. J Clin Invest 2004;114(9):1326-33.

196. El Chami N, Ikhlef F, Kaszas K, et al. Androgen-dependent apoptosis in male germ cells is regulated through the proto-oncoprotein cbl. J Cell Biol 2005;171(4):651-61.

197. Bachmaier K, Krawczyk C, Kozieradzki I, et al. Negative regulation of lymphocyte activation and autoimmunity by the molecular adaptor cbl-b. Nature 2000;403(6766):211-6.

198. Chiang YJ, Kole HK, Brown K, et al. Cbl-b regulates the CD28 dependence of T-cell activation. Nature 2000;403(6766):216-20.

199. Nikawa T, Ishidoh K, Hirasaka K, et al. Skeletal muscle gene expression in space-flown rats. FASEB J 2004;18(3):522-4.

200. Nakao R, Hirasaka K, Goto J, et al. Ubiquitin ligase cbl-b is a negative regulator for insulin-like growth factor 1 signaling during muscle atrophy caused by unloading. Mol Cell Biol 2009;29(17):4798-811.

201. Rafiq K, Kolpakov MA, Seqqat R, et al. c-cbl inhibition improves cardiac function and survival in response to myocardial ischemia. Circulation 2014;129(20):2031-43.

202. Bonala S, Lokireddy S, McFarlane C, Patnam S, Sharma M, Kambadur R. Myostatin induces insulin resistance via casitas B-lineage lymphoma b (cblb)-mediated degradation of insulin receptor substrate 1 (IRS1) protein in response to high calorie diet intake. J Biol Chem 2014;289(11):7654-70.

203. Naramura M, Jang IK, Kole H, Huang F, Haines D, Gu H. c-cbl and cbl-b regulate T cell responsiveness by promoting ligand-induced TCR down-modulation. Nat Immunol 2002;3(12):1192-9.

205. Kitaura Y, Jang IK, Wang Y, et al. Control of the B cell-intrinsic tolerance programs by ubiquitin ligases cbl and cbl-b. Immunity 2007;26(5):567-78.

206. Caligiuri MA, Briesewitz R, Yu J, et al. Novel c-CBL and CBL-b ubiquitin ligase mutations in human acute myeloid leukemia. Blood 2007;110(3):1022-4.

207. Makishima H, Cazzolli H, Szpurka H, et al. Mutations of e3 ubiquitin ligase cbl family members constitute a novel common pathogenic lesion in myeloid malignancies. J Clin Oncol 2009;27(36):6109-16.

208. Kao HW, Sanada M, Liang DC, et al. A high occurrence of acquisition and/or expansion of C-CBL mutant clones in the progression of high-risk myelodysplastic syndrome to acute myeloid leukemia. Neoplasia 2011;13(11):1035-42.

209. Nicholson L, Knight T, Matheson E, et al. Casitas B lymphoma mutations in childhood acute lymphoblastic leukemia. Genes Chromosomes Cancer 2012;51(3):250-6.

210. Schnittger S, Bacher U, Alpermann T, et al. Use of CBL exon 8 and 9 mutations in diagnosis of myeloproliferative neoplasms and myelodysplastic/myeloproliferative disorders: An analysis of 636 cases. Haematologica 2012;97(12):1890-4.

211. Martinelli S, De Luca A, Stellacci E, et al. Heterozygous germline mutations in the CBL tumor-suppressor gene cause a noonan syndrome-like phenotype. Am J Hum Genet 2010;87(2):250-7.

212. An W, Nadeau SA, Mohapatra BC, et al. Loss of cbl and cbl-b ubiquitin ligases abrogates hematopoietic stem cell quiescence and sensitizes leukemic disease to chemotherapy. Oncotarget 2015;6(12):10498-509.

213. Li Z, Dong T, Proschel C, Noble M. Chemically diverse toxicants converge on fyn and c-cbl to disrupt precursor cell function. PLoS Biol 2007;5(2):e35.

214. Ferron SR, Pozo N, Laguna A, et al. Regulated segregation of kinase Dyrk1A during asymmetric neural stem cell division is critical for EGFR-mediated biased signaling. Cell Stem Cell 2010;7(3):367-79.

215. Dieudonne FX, Severe N, Biosse-Duplan M, Weng JJ, Su Y, Marie PJ. Promotion of osteoblast differentiation in mesenchymal cells through cbl-mediated control of STAT5 activity. Stem Cells 2013;31(7):1340-9.

216. Barker N, Clevers H. Lineage tracing in the intestinal epithelium. Curr Protoc Stem Cell Biol 2010;Chapter 5:Unit5A.4.

217. Wang F, Scoville D, He XC, et al. Isolation and characterization of intestinal stem cells based on surface marker combinations and colony-formation assay. Gastroenterology 2013;145(2):383,95.e1-21.

219. Tian H, Biehs B, Warming S, et al. A reserve stem cell population in small intestine renders Lgr5-positive cells dispensable. Nature 2011;478(7368):255-9.

220. Hua G, Thin TH, Feldman R, et al. Crypt base columnar stem cells in small intestines of mice are radioresistant. Gastroenterology 2012;143(5):1266-76.

221. Van Landeghem L, Santoro MA, Krebs AE, et al. Activation of two distinct Sox9-EGFP-expressing intestinal stem cell populations during crypt regeneration after irradiation. Am J Physiol Gastrointest Liver Physiol 2012;302(10):G1111-32.

222. Sato T, Vries RG, Snippert HJ, et al. Single Lgr5 stem cells build crypt-villus structures in vitro without a mesenchymal niche. Nature 2009;459(7244):262-5.

223. Korinek V, Barker N, Moerer P, et al. Depletion of epithelial stem-cell compartments in the small intestine of mice lacking tcf-4. Nat Genet 1998;19(4):379-83.

224. van Es JH, Haegebarth A, Kujala P, et al. A critical role for the wnt effector Tcf4 in adult intestinal homeostatic self-renewal. Mol Cell Biol 2012;32(10):1918-27.

225. Weise A, Bruser K, Elfert S, et al. Alternative splicing of Tcf7l2 transcripts generates protein variants with differential promoter-binding and transcriptional activation properties at Wnt/beta-catenin targets. Nucleic Acids Res 2010;38(6):1964-81.

227. Chitalia V, Shivanna S, Martorell J, Meyer R, Edelman E, Rahimi N. c-cbl, a ubiquitin E3 ligase that targets active beta-catenin: A novel layer of wnt signaling regulation. J Biol Chem 2013;288(32):23505-17.